
Electronic Thesis and Dissertation Repository

6-18-2020 4:00 PM

Comparing Motion Outcomes in Salvage Procedures for Wrist Arthritis

Stacy Fan, *The University of Western Ontario*

Supervisor: Suh, Nina, *The University of Western Ontario*

Co-Supervisor: Ross, Douglas, *The University of Western Ontario*

A thesis submitted in partial fulfillment of the requirements for the Master of Science degree in Surgery

© Stacy Fan 2020

Follow this and additional works at: <https://ir.lib.uwo.ca/etd>



Part of the [Plastic Surgery Commons](#)

Recommended Citation

Fan, Stacy, "Comparing Motion Outcomes in Salvage Procedures for Wrist Arthritis" (2020). *Electronic Thesis and Dissertation Repository*. 7093.

<https://ir.lib.uwo.ca/etd/7093>

This Dissertation/Thesis is brought to you for free and open access by Scholarship@Western. It has been accepted for inclusion in Electronic Thesis and Dissertation Repository by an authorized administrator of Scholarship@Western. For more information, please contact wlsadmin@uwo.ca.

ABSTRACT

Scaphoidectomy and four corner fusion (4CF), and proximal row carpectomy (PRC) are salvage procedures that may be offered in advanced wrist arthritis. The optimal clinical treatment remains unclear. Biomechanical studies comparing outcomes of these procedures often only report uniplanar motion, rather than multiplanar motion which is more representative of functional wrist motion. Further, the impact of altering the relationship of the proximal and distal carpal rows in the coronal plane during 4CF has not been well-studied.

The purpose of this *in-vitro* biomechanical study was to quantify changes in wrist kinematics during wrist flexion-extension, radial-ulnar deviation, and circumduction in “anatomic 4CF”, “radial 4CF”, and PRC conditions using an active motion simulator. Three important findings are reported: 1) Radial-aligned 4CF resulted in reduced wrist extension and total circumduction compared to the native state, 2) Anatomic 4CF was more restricted in wrist extension than PRC, while PRC was more restricted in radial deviation compared to 4CF, and 3) Total circumduction area was similar between anatomic 4CF and PRC.

These results suggest that 4CF and PRC have comparable motion outcomes. When patients are candidates for either operation, the advantages and disadvantages of each must be considered. If the decision to perform 4CF has been made, anatomic 4CF may provide a better motion profile, provided there is adequate bone stock between the capitate and lunate. In certain situations, adjusting the alignment of the proximal and distal carpal rows is required, making radial 4CF more appropriate. Further clinical investigation comparing these procedures is warranted.

Key words: wrist arthritis, four corner fusion, proximal row carpectomy, biomechanics

SUMMARY FOR LAY AUDIENCE

Wrist arthritis is a common condition. As arthritis progresses, it involves different areas of the wrist; consequently, treatment methods must be adjusted accordingly. Two commonly performed operations are “scaphoidectomy and four corner fusion”, where one wrist bone is removed and four others are connected together, and “proximal row carpectomy”, where three wrist bones are removed. There are specific indications for each, but some patients may be candidates for both operations. In this group of patients, there are no clinical or biomechanical studies demonstrating the superiority of either procedure, so the operative intervention is largely determined by surgeon experience rather than scientific evidence. Further, within four corner fusion, there is no consensus on the optimal position to connect the four bones.

A comprehensive overview of the current literature is reported in this thesis. The body of this work employs cadaveric wrists and an active motion simulator (whereby motors apply a force on tendons to control wrist motion) to evaluate how motion compares in a native wrist, two positions of four corner fusion, and proximal row carpectomy.

The primary objective of this work is to assist clinicians with decision-making by providing information as to which procedure best retains functional wrist motion in this patient population.

CO-AUTHORSHIP STATEMENT

Chapter 1: Introduction

Authorship: Stacy Fan

Chapter Review: Nina Suh, Douglas Ross, Graham King, Daniel Langohr

Chapter 2: A Biomechanical Study Comparing Uniplanar and Multiplanar Wrist Motion in Two Positions of Four Corner Fusion

Study Design: Stacy Fan, Clare Padmore, Assaf Kadar, Nina Suh

Specimen Preparation: Stacy Fan, Assaf Kadar, Clare Padmore, Nina Suh

Data Collection: Stacy Fan, Assaf Kadar, Clare Padmore

Data Analysis: Stacy Fan

Statistical Analysis: Clare Padmore

Manuscript Preparation: Stacy Fan

Manuscript Review: Nina Suh, Douglas Ross, Graham King, Daniel Langohr

Chapter 3: A Biomechanical Study Comparing Uniplanar and Multiplanar Wrist Motion After Four Corner Fusion and Proximal Row Carpectomy

Study Design: Stacy Fan, Clare Padmore, Assaf Kadar, Nina Suh

Specimen Preparation: Stacy Fan, Assaf Kadar, Clare Padmore, Nina Suh

Data Collection: Stacy Fan, Assaf Kadar, Clare Padmore

Data Analysis: Stacy Fan

Statistical Analysis: Clare Padmore

Manuscript Preparation: Stacy Fan

Manuscript Review: Nina Suh, Douglas Ross, Graham King, Daniel Langohr

Chapter 4: General Discussion and Conclusions

Authorship: Stacy Fan

Chapter Review: Nina Suh, Douglas Ross, Graham King, Daniel Langohr

ACKNOWLEDGEMENTS

This thesis was completed with the kind and generous support of several individuals.

Firstly, I express my gratitude to Dr. Nina Suh and Dr. Douglas Ross for being kind enough to accept me as a Master's student and for their support and guidance as research supervisors. Their mentorship, encouragement, and expertise were critical to the completion of this project.

Many thanks to Dr. Suh for her commitment to this study and investing her time into specimen preparation and long testing days on weekends and during her academic time. Your dedication to research and to learners is appreciated. It was very enjoyable working with such a skilled surgeon.

I would also like to express my thanks to the members of the Roth|McFarlane Hand and Upper Limb Centre research laboratory. In particular, I would like to thank Clare Padmore and Dr. Assaf Kadar for their assistance and guidance during the study. Clare and Assaf both played an integral role and dedicated numerous hours in the lab. Additionally, thanks to Dr. Dan Langhor who was available and receptive to providing advice when we ran into technical difficulties with the simulator. Thank you to Dr. Graham King for his recommendations on improving study design.

I am fortunate to have had this opportunity to complete the Master's of Science in Surgery program during Plastic Surgery residency training. The division was supportive of my goal and provided ample research time in order to complete my project.

Finally, I would like to thank my mother, father and sister for their unconditional love, encouragement and support for all these years.

In loving memory of my mother.

TABLE OF CONTENTS

| | |
|---|----------|
| Abstract..... | ii |
| Summary for Lay Audience..... | iii |
| Co-authorship Statement..... | iv |
| Acknowledgements..... | v |
| Table of Contents..... | vi |
| List of Tables..... | ix |
| List of Figures..... | x |
| List of Abbreviations..... | xiv |
| 1 Introduction..... | 1 |
| 1.1 HAND AND WRIST ANATOMY..... | 2 |
| 1.1.1 <i>Structure of Bones</i> | 3 |
| 1.1.2 <i>Forearm Bone Anatomy</i> | 4 |
| 1.1.3 <i>Carpal Bone Anatomy</i> | 6 |
| 1.1.4 <i>Soft Tissue Anatomy</i> | 14 |
| 1.2 BIOMECHANICS OF THE WRIST..... | 21 |
| 1.2.1 <i>Kinematic models of carpal motion</i> | 23 |
| 1.2.2 <i>Laboratory-based analysis of wrist kinematics</i> | 25 |
| 1.3 CLINICAL DISORDERS OF THE WRIST: SCAPHOID FRACTURES..... | 31 |
| 1.3.1 <i>Scaphoid fractures</i> | 31 |
| 1.3.2 <i>Scaphoid fracture classification</i> | 32 |
| 1.3.3 <i>Epidemiology of scaphoid fractures</i> | 34 |
| 1.3.4 <i>Clinical diagnosis</i> | 35 |
| 1.3.5 <i>Treatment</i> | 39 |
| 1.4 CLINICAL DISORDERS OF THE WRIST: SCAPHOID NONUNION ADVANCED COLLAPSE..... | 40 |
| 1.4.1 <i>Epidemiology of scaphoid nonunion</i> | 40 |
| 1.4.2 <i>Pathophysiology of scaphoid nonunion advanced collapse</i> | 40 |
| 1.4.3 <i>Clinical presentation of SNAC</i> | 41 |
| 1.5 CLINICAL DISORDERS OF THE WRIST: SCAPHOLUNATE LIGAMENT INJURY..... | 42 |
| 1.5.1 <i>Scapholunate ligament disruption</i> | 42 |
| 1.5.2 <i>Epidemiology of scapholunate ligament disruption</i> | 42 |
| 1.5.3 <i>Clinical diagnosis</i> | 43 |

| | | |
|-------|--|----|
| 1.5.4 | <i>Treatment</i> | 44 |
| 1.6 | CLINICAL DISORDERS OF THE WRIST: SCAPHOLUNATE ADVANCED COLLAPSE | 45 |
| 1.6.1 | <i>Epidemiology of scapholunate advanced collapse</i> | 45 |
| 1.6.2 | <i>Pathophysiology of scapholunate advanced collapse</i> | 45 |
| 1.6.3 | <i>Clinical presentation of SLAC</i> | 46 |
| 1.7 | TREATMENT OF SCAPHOID NONUNION ADVANCED COLLAPSE AND SCAPHOLUNATE ADVANCED COLLAPSE 47 | |
| 1.7.1 | <i>Radial styloidectomy</i> | 48 |
| 1.7.2 | <i>Wrist denervation</i> | 48 |
| 1.7.3 | <i>Distal scaphoid excision</i> | 49 |
| 1.7.4 | <i>Scaphoidectomy and four corner fusion</i> | 50 |
| 1.7.5 | <i>Proximal row carpectomy</i> | 53 |
| 1.7.6 | <i>Total wrist arthrodesis</i> | 54 |
| 1.7.7 | <i>Total wrist arthroplasty</i> | 55 |
| 1.8 | FOUR CORNER FUSION VERSUS PROXIMAL ROW CARPECTOMY | 56 |
| 1.8.1 | <i>Clinical outcomes of 4CF versus PRC</i> | 56 |
| 1.8.2 | <i>Cost-analysis of 4CF versus PRC</i> | 58 |
| 1.9 | RATIONALE FOR THESIS | 59 |
| 1.9.1 | <i>Objective</i> | 59 |
| 1.9.2 | <i>Hypothesis</i> | 60 |
| 1.9.3 | <i>Thesis overview</i> | 60 |
| 2 | A Biomechanical Study Comparing Uniplanar and Multiplanar Wrist Motion in Two Positions of Four Corner Fusion | 72 |
| 2.1 | INTRODUCTION | 72 |
| 2.2 | METHODS | 75 |
| 2.2.1 | <i>Specimen preparation</i> | 75 |
| 2.2.2 | <i>Testing protocol</i> | 80 |
| 2.2.3 | <i>Statistical analysis</i> | 82 |
| 2.3 | RESULTS | 82 |
| 2.3.1 | <i>Specimen demographics</i> | 82 |
| 2.3.2 | <i>Uniplanar wrist motion</i> | 82 |
| 2.3.3 | <i>Circumduction</i> | 83 |
| 2.4 | DISCUSSION | 85 |
| 2.5 | CONCLUSION | 88 |
| 3 | A Biomechanical Study Comparing Uniplanar and Multiplanar Wrist Motion After Four Corner Fusion and Proximal Row Carpectomy | 92 |

| | | |
|-------|--|-----|
| 3.1 | INTRODUCTION | 92 |
| 3.2 | METHODS | 93 |
| 3.2.1 | <i>Specimen preparation</i> | 93 |
| 3.2.2 | <i>Proximal row carpectomy</i> | 93 |
| 3.2.3 | <i>Testing protocol</i> | 93 |
| 3.2.4 | <i>Statistical analysis</i> | 95 |
| 3.3 | RESULTS | 96 |
| 3.3.1 | <i>Specimen demographics</i> | 96 |
| 3.3.2 | <i>Uniplanar wrist motion</i> | 96 |
| 3.3.3 | <i>Circumduction</i> | 97 |
| 3.4 | DISCUSSION | 100 |
| 3.5 | CONCLUSIONS..... | 104 |
| 4 | General Discussion and Conclusions..... | 107 |
| 4.1 | SUMMARY..... | 107 |
| 4.2 | CHAPTER 2: A BIOMECHANICAL STUDY COMPARING UNIPLANAR AND MULTIPLANAR WRIST MOTION IN TWO POSITIONS OF FOUR CORNER FUSION..... | 108 |
| 4.2.1 | <i>Overview</i> | 108 |
| 4.3 | CHAPTER 3: A BIOMECHANICAL STUDY COMPARING UNIPLANAR AND MULTIPLANAR WRIST MOTION AFTER FOUR CORNER FUSION AND PROXIMAL ROW CARPECTOMY | 110 |
| 4.3.1 | <i>Overview</i> | 110 |
| 4.4 | STRENGTHS AND LIMITATIONS | 112 |
| 4.5 | OVERALL CONCLUSION..... | 114 |
| 4.6 | FUTURE DIRECTIONS..... | 115 |

LIST OF TABLES

| | |
|---|----|
| Table 1.1. Dynamic stabilizers of the wrist within anterior forearm. (Modified with permission from: Chambers et al. Thesis Dissertation 2019)..... | 19 |
| Table 1.2. Dynamic stabilizers of the wrist within posterior forearm. (Modified with permission from: Chambers et al. Thesis Dissertation 2019)..... | 20 |
| Table 1.3. Normative wrist range of motion values. | 22 |
| Table 1.4. Specificity and sensitivity of physical exam findings to diagnose scaphoid fractures. Table modified from Parvizi et al. (35)..... | 36 |
| Table 1.5. Vender et al. classification of scaphoid nonunion advanced collapse. | 41 |
| Table 1.6. Watson & Ballet classification of scapholunate advanced collapse. | 45 |
| Table 1.7. Summary of studies comparing fixation methods in 4CF. | 52 |

LIST OF FIGURES

Figure 1.1. Hand and wrist anatomy. Volar and dorsal views of the left hand showing phalanges, metacarpals, carpal bones, radius, and ulna. (Reprinted with permission from: OpenStax, Anatomy & Physiology. OpenStax CNX. Feb 26, 2016 <http://cnx.org/contents/14fb4ad7-39a1-4eee-ab6e-3ef2482e3e22@8.24>.)..... 2

Figure 1.2. Illustration of different bone types with examples. (Reprinted with permission from: Umadevi N, Geethalakshmi SN. A brief study n human bone anatomy and bone fractures. Int J Comp Eng Sci. 2011;1(3);93-104. <https://pdfs.semanticscholar.org/f2c4/56f6e7f108472c62292893f27f0954a1f923.pdf>) 3

Figure 1.3. Anatomy of the radius (A) Lateral view (B) Anterior view (C) Distal articular surface (D) Proximal articular surface. 4

Figure 1.4. Anatomy of the ulna (A) Lateral view (B) Anterior view (C) Distal articular surface (D) Proximal articular surface. 5

Figure 1.5. Hand and wrist anatomy. Volar and dorsal views of the right hand showing carpal bones, distal radius and ulna. (a) radial styloid, (b) ulnar styloid, (c) scaphoid tubercle, (d) scaphoid waist, (e) proximal pole of scaphoid, (f) lunate, (g) triquetrum, (h) pisiform, (i) hook of hamate, (j) hamate, (k) capitate, (l) trapezoid, (m) tubercle of trapezium, (n) trapezium. (Reprinted with permission from Srinivas Reddy, R., & Compson, J. (2005). Examination of the wrist—surface anatomy of the carpal bones. Current Orthopaedics, 19(3), 171–179)..... 6

Figure 1.6. Anatomy of the left scaphoid (A) Medial view (B) Dorsal view (C) Distal articular surface (D) Proximal articular surface..... 7

Figure 1.7. Anatomy of the left lunate (A) Distal articular surface (B) Proximal articular surface (C) Medial view (D) Lateral view. 8

Figure 1.8. Anatomy of the triquetrum. (A) Dorsal view (B) Volar view. 9

Figure 1.9. Anatomy of the trapezium (A) Volar view (B) Lateral view (C) Proximal articular surface..... 10

Figure 1.10. Anatomy of the trapezoid. (A) Volar view (B) Lateral view (C) Proximal articular surface..... 11

Figure 1.11. Anatomy of the capitate (A) Lateral view (B) Volar view (C) Distal articular surface (D) Proximal articular surface. 12

Figure 1.12. Anatomy of the hamate. (A) Radial view (B) Volar view (C) Lateral view..... 13

Figure 1.13. Volar radiocarpal and ulnocarpal ligaments of the wrist. LRL- long radiolunate ligament, RSL- radioscapholunate ligament, SRL- short radiolunate ligament, UL- ulnolunate ligament, UT- ulnotriquetral ligament, LT- lunotriquetral ligament. (Reprinted with permission from: Lichtman, D. M., & Wroten, E. S. (2006). Understanding Midcarpal Instability. The Journal of Hand Surgery, 31(3), 491–498)..... 16

Figure 1.14. Dorsal ligaments of the wrist. RS- radioscaphoid ligament, RT- radiotriquetral ligament, DIC- dorsal intercarpal ligament. (Reprinted with permission from: Lichtman, D. M., & Wroten, E. S. (2006). Understanding Midcarpal Instability. The Journal of Hand Surgery, 31(3), 491–498) 17

Figure 1.15. Muscles of the forearm. (A) Superficial layer of anterior and posterior forearm (B) Deep layer of anterior and posterior forearm. (Reprinted with permission from: OpenStax, Anatomy & Physiology. OpenStax CNX. Feb 26, 2016 <http://cnx.org/contents/14fb4ad7-39a1-4eee-ab6e-3ef2482e3e22@8.24>)..... 18

Figure 1.16. Wrist range of motion. (A) Wrist flexion and extension (B) Wrist radial and ulnar deviation (C) Wrist pronation and supination..... 21

Figure 1.17. Passive motion wrist simulator by Gammon and Nishiwaki (A) Ulna fixed with the elbow at 90° flexion, (B) Radius securing the forearm in neutral rotation, (C) Rigidly fixed humerus, (D) Flexion-extension motion arc, (E) Passive motion guide (Steinmann pin inserted into third metacarpal), (F) Optical tracking markers, (G) Pneumatic actuators, and (H) Cables connecting actuators and corresponding muscle sutures. (Reprinted with permission from: Stoesser H, et al. Biomechanical Evaluation of Carpal Kinematics during Simulated Wrist Motion. J Wrist Surg. 2017;6(2):113-9) 26

Figure 1.18. Active motion wrist simulator by Werner et al. This simulator is capable of producing reproducible planar and combined motions. (Reprinted with permission from: Werner FW, Palmer AK, Somerset JH, Tong JJ, Gillison DB, Fortino MD, et al. Wrist joint motion simulator. J Orthop Res. 1996;14(4):639-46)..... 28

Figure 1.19. Active motion wrist simulator by Dunning et al. Developed to test stability of external fixation in distal radius fractures. (Reprinted with permission from: Dunning CE, Lindsay CS, Bicknell RT, Patterson SD, Johnson JA, King GJ. Supplemental pinning improves the stability

of external fixation in distal radius fractures during simulated finger and forearm motion. J Hand Surg Am. 1999;24(5):992-1000) 29

Figure 1.20. Active motion wrist simulator by Iglesias et al. This active motion simulator utilized closed-loop optical control and tests in several gravity-loaded positions. (Reprinted with permission from: Iglesias et al. Thesis Dissertation 2015: Development of an in-vitro passive and active motion simulator for the investigation of wrist function and kinematics). 30

Figure 1.21. Cleared specimen showing internal vascularity of scaphoid. 1- dorsal scaphoid branch of radial artery, 2- volar scaphoid branch of radial artery. (Reprinted with permission from: Gelberman, R. H., & Menon, J. (1980). The vascularity of the scaphoid bone. The Journal of Hand Surgery, 5(5), 508–513)..... 31

Figure 1.22. Illustration of Herbert Classification of scaphoid fractures. (Reprinted with permission from: Sendher, R., & Ladd, A. L. (2013). The Scaphoid. Orthopedic Clinics of North America, 44(1), 107–120)..... 32

Figure 1.23. Illustration of Mayo Classification of scaphoid fractures. (Reprinted with permission from: Rhemrev, S.J., Ootes, D., Beeres, F.J. et al. (2011) Current methods of diagnosis and treatment of scaphoid fractures. Int J Emerg Med 4(4)) 33

Figure 1.24. Illustration of Russe classification of scaphoid fractures. (Reprinted with permission from: Rhemrev, S.J., Ootes, D., Beeres, F.J. et al. (2011) Current methods of diagnosis and treatment of scaphoid fractures. Int J Emerg Med 4(4)) 34

Figure 1.25. Radiographs of right wrist and scaphoid tubercle fracture. A) Posteroanterior B) Lateral, C) Oblique, D) Scaphoid views. 37

Figure 1.26. Sagittal CT of scaphoid with humpback deformity. 38

Figure 2.1. Plain radiographs of right wrist. (A) Pre-operative with native "capitate overhang" (B) Post-operative after scaphoidectomy and radial-aligned 4CF. (Right image reprinted with permission from: Ozyurekoglu T, Turker T. Results of a method of 4-corner arthrodesis using headless compression screws. The Journal of hand surgery. 2012 Mar 1;37(3):486-92)..... 74

Figure 2.2. Fluoroscopic confirmation of midcarpal fusion. (A) Posteroanterior view (B) Lateral view. 76

Figure 2.3. Flexor tendons with running locking Krakow stitches for motion actuation (from radial to ulnar: FCR, FCU). 77

| | |
|---|----|
| Figure 2.4. Extensor tendons with running locking Krakow stitches for motion actuation (from radial to ulnar: ECRL, ECRB, ECU)..... | 78 |
| Figure 2.5. Schematic illustrating epicondyle block and cable stabilization guides. After tendons of interest are tagged, sutures are passed through epicondyle blocks to maintain physiologic line of pull. | 78 |
| Figure 2.6. Active motion simulator. (A) Schematic of specimen mounted onto simulator using a humeral clamp and ulnar support tower. (B) Cadaveric specimen mounted onto simulator. | 79 |
| Figure 2.7. Cadaveric specimen illustrating scaphoidectomy and four corner fusion. (A) Anatomic 4CF position with capitate overhang (B) Radial-aligned 4CF position. | 81 |
| Figure 2.8. Absolute change (°) in wrist flexion, extension, ulnar and radial deviation compared to native state. Asterisk indicates statistical significance (p<0.05). Asterisk at base illustrates significance compared to native state. | 82 |
| Figure 2.9 Total circumduction area (mm²) in native, anatomic 4CF and radial 4CF conditions. Significant differences (p<0.05) are noted with an asterisk. | 83 |
| Figure 2.10. Circumduction pattern superimposed on native circumduction pattern. (A) Anatomic 4CF (B) Radial 4CF. | 84 |
| Figure 3.1. Absolute change (°) in wrist flexion, extension, ulnar and radial deviation compared to native state. Asterisk indicates statistical significance (p<0.05). Asterisk at base illustrates significance compared to native state. | 96 |
| Figure 3.2 Total circumduction area (mm²) in native, anatomic 4CF and radial 4CF conditions. | 97 |
| Figure 3.3. Circumduction pattern superimposed on native circumduction pattern. (A) 4CF (B) PRC..... | 98 |
| Figure 3.4. Percent of maintained motion within each quadrant compared to native state. | 99 |

LIST OF ABBREVIATIONS

| | |
|------|--|
| 4CF | Four corner fusion |
| ADLs | Activities of daily living |
| AIN | Anterior interosseous nerve |
| APL | Abductor pollicis longus |
| AVN | Avascular necrosis |
| BB | Biceps brachii |
| CH | Capitohamate |
| CMC | Carpometacarpal |
| CT | Computed tomography |
| DASH | Disabilities of the Arm, Shoulder and Hand |
| DIC | Dorsal intercarpal ligament |
| DIPJ | Distal interphalangeal joint |
| DISI | Dorsal intercalated segment instability |
| DRC | Dorsal radiocarpal ligament |
| DRT | Dorsal radiotriquetral ligament |
| DRUJ | Distal radioulnar joint |
| DTM | Dart-throw motion |
| ECRB | Extensor carpi radialis brevis |
| ECRL | Extensor carpi radialis longus |
| ECU | Extensor carpi ulnaris |
| EDC | Extensor digitorum communis |
| EDQ | Extensor digiti quinti |
| EIP | Extensor indicis proprius |
| EPB | Extensor pollicis brevis |
| EPL | Extensor pollicis longus |
| FCR | Flexor carpi radialis |
| FCU | Flexor carpi ulnaris |
| FDP | Flexor digitorum profundus |
| FDS | Flexor digitorum superficialis |

| | |
|---------|---------------------------------------|
| FOOSH | Fall on outstretched hand |
| FPL | Flexor pollicis longus |
| Gd | Gadolinium |
| IPJ | Interphalangeal joint |
| K-wires | Kirshner wires |
| LRL | Long radiolunate ligament |
| LT | Lunotriquetral |
| MC | Metacarpal |
| MRI | Magnetic resonance imaging |
| N | Newtons |
| NSAIDs | Non-steroidal anti-inflammatory drugs |
| OA | Osteoarthritis |
| PA | Posteroanterior |
| PIN | Posterior interosseous nerve |
| PIPJ | Proximal interphalangeal joint |
| PL | Palmaris longus |
| PQ | Pronator quadratus |
| PRC | Proximal row carpectomy |
| PT | Pronator teres |
| RCT | Randomized control trial |
| ROM | Range of motion |
| RS | Radioscaphoid |
| RSC | Radioscaphocapitate |
| RSL | Radioscapholunate |
| RT | Radiotriquetral |
| SC | Scaphocapitate |
| SLAC | Scapholunate advanced collapse |
| SNAC | Scaphoid non-union advanced collapse |
| SNU | Scaphoid non-union |
| SRL | Short radiolunate ligament |
| STT | Scaphotrapeziotrapezoid |

| | |
|------|--|
| TFCC | Triangular fibrocartilage complex |
| TWA | Total wrist arthroplasty |
| UC | Ulnocapitate |
| UL | Ulnolunate |
| UT | Ulnotriquetral |
| VISI | Volar intercalated segmental instability |
| XR | X-ray |

CHAPTER 1

1 INTRODUCTION

This chapter discusses basic hand and wrist anatomy, and wrist kinematics. The pathophysiology of two common conditions leading to wrist arthritis and current treatment options are reviewed. Additionally, management options for wrist arthritis are considered. The rationale, objective, and hypothesis of this thesis are noted.

1.1 HAND AND WRIST ANATOMY

The hand and wrist are anatomically one of the most complex regions in the human body. The hand alone is comprised of 27 bones (14 phalanges, 5 metacarpals, and 8 carpal bones) (**Figure 1.1**). The surrounding soft tissue elements, including muscles, tendons, ligaments and fascia, all contribute to normal function and biomechanics of the joints.

The wrist joint is comprised of articulations between the radius, ulna, carpal bones, and metacarpals. Six tendons insert directly onto the carpal bones or cross at the wrist joint to allow for basic movements of the wrist including flexion, extension, radial deviation, and ulnar deviation(1).

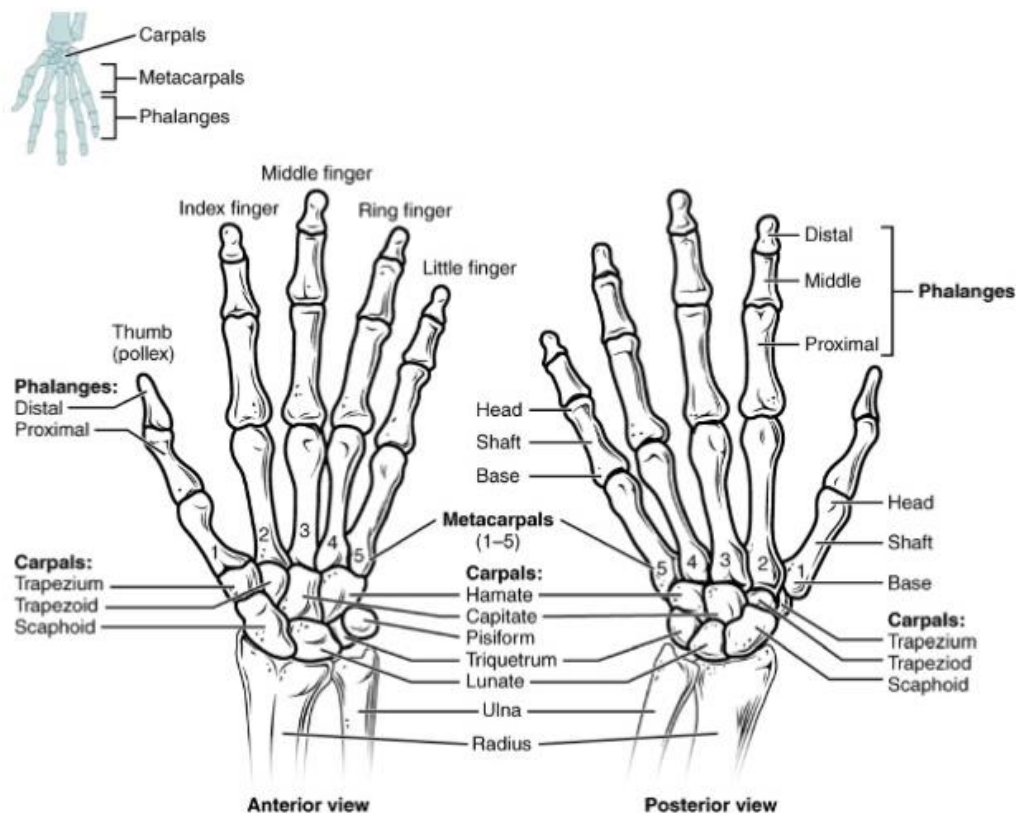


Figure 1.1. Hand and wrist anatomy. Volar and dorsal views of the left hand showing phalanges, metacarpals, carpal bones, radius, and ulna. (Reprinted with permission from: OpenStax, Anatomy & Physiology. OpenStax CNX. Feb 26, 2016 <http://cnx.org/contents/14fb4ad7-39a1-4eee-ab6e-3ef2482e3e22@8.24>)

1.1.1 Structure of Bones

Structurally, bones consist of an outer shell of cortical bone and inner portion which is composed of cancellous bone. In childhood, bone is laid down at the physis, or growth plate, and during development to adulthood is constantly remodeled through the breakdown of bone by osteoclasts and synthesis of bone by osteoblasts.

Bones can be classified into 5 categories: long, short, irregular, flat, or sesamoid (**Figure 1.2**). The hand is comprised of long and short bones. A long bone can be divided into 3 anatomical parts, with the epiphysis at the end, adjacent to the metaphysis, and at the central aspect of the bone lies the diaphysis.

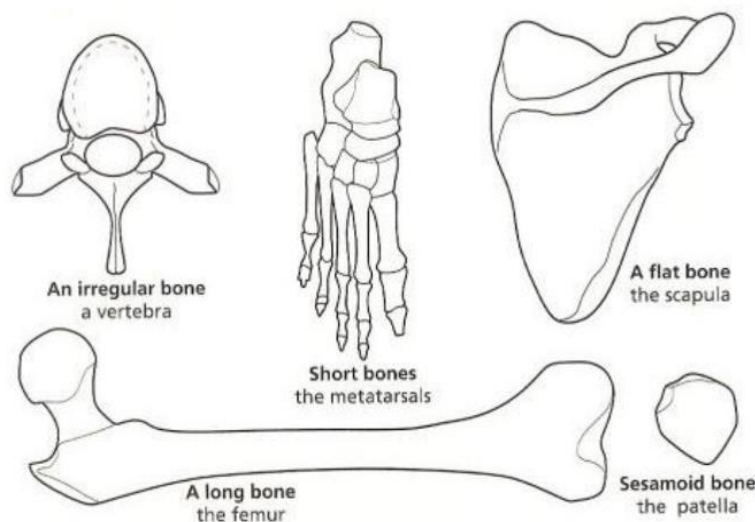


Figure 1.2. Illustration of different bone types with examples. (Reprinted with permission from: Umadevi N, Geethalakshmi SN. A brief study n human bone anatomy and bone fractures. Int J Comp Eng Sci. 2011;1(3);93-104.

<https://pdfs.semanticscholar.org/f2c4/56f6e7f108472c62292893f27f0954a1f923.pdf>)

1.1.2 Forearm Bone Anatomy

The radius and ulna are bones of the forearm. In the anatomic position, the radius is located laterally while the ulna resides medially. The radius and ulna, along with the carpal bones and metacarpals constitute the wrist joint.

1.1.2.1 Radius Osteology

The radius is a long bone that articulates with the ulna and humerus proximally, and the ulna and carpal bones distally(2) (**Figure 1.3**). Normally, the distal radius articular surface has a volar tilt of 10-15° and inclination of 15-25° in an ulnar to radial direction. The distal extension of the lateral radial edge forms the radial styloid. The scaphoid and lunate fossae are located at its concave surface distally and articulate with the proximal surface of the respective carpal bones. These fossae are separated by a fibrocartilage ridge known as the interfacet prominence.

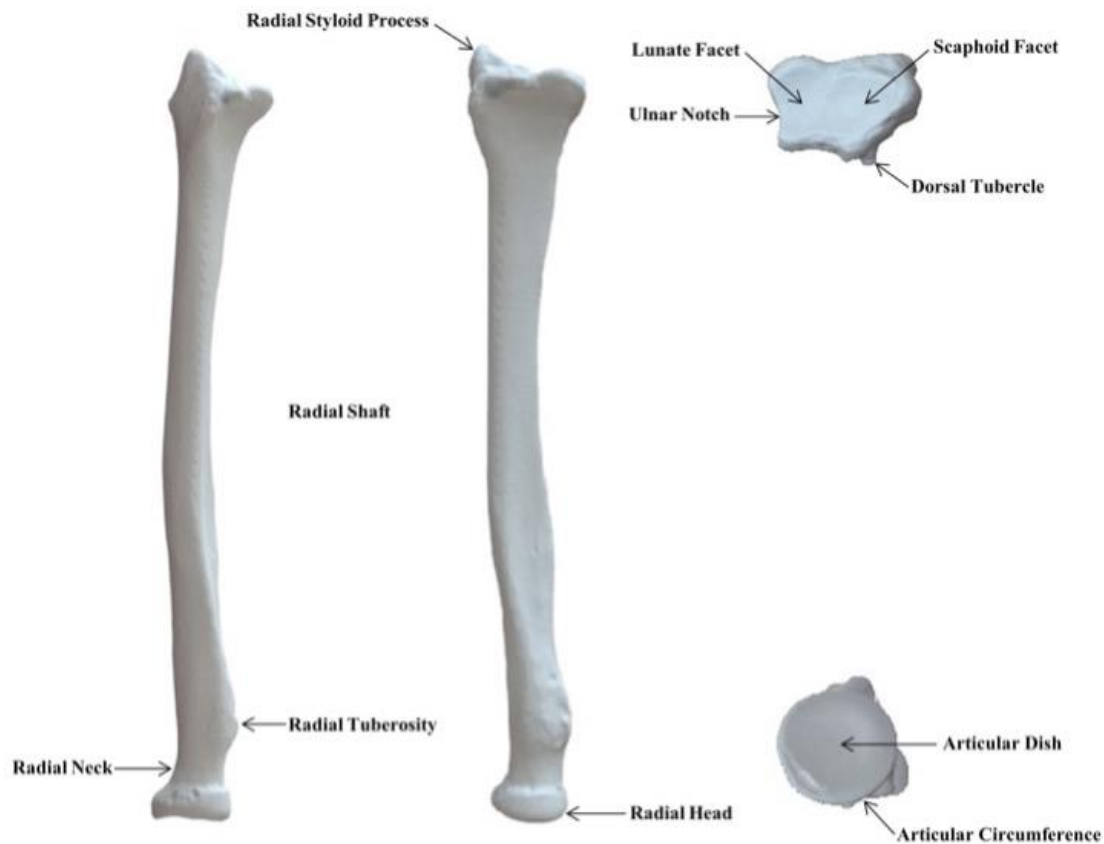


Figure 1.3. Anatomy of the radius (A) Lateral view (B) Anterior view (C) Distal articular surface (D) Proximal articular surface.

1.1.2.2 Ulna Osteology

This section will focus only on the distal ulna. At the distal-most aspect of the ulna is the articular surface named the ulnar head, and medially there is a narrower prominence called the styloid process(3) (**Figure 1.4**). The ulnar head articulates with the triangular fibrocartilage complex (TFCC), which is a cartilaginous load-bearing structure found between the lunate, triquetrum and ulnar head. The ulnar styloid functions as an attachment site for the ulnar collateral ligament, ulnocarpal ligaments and distal radioulnar ligaments of the wrist joint.

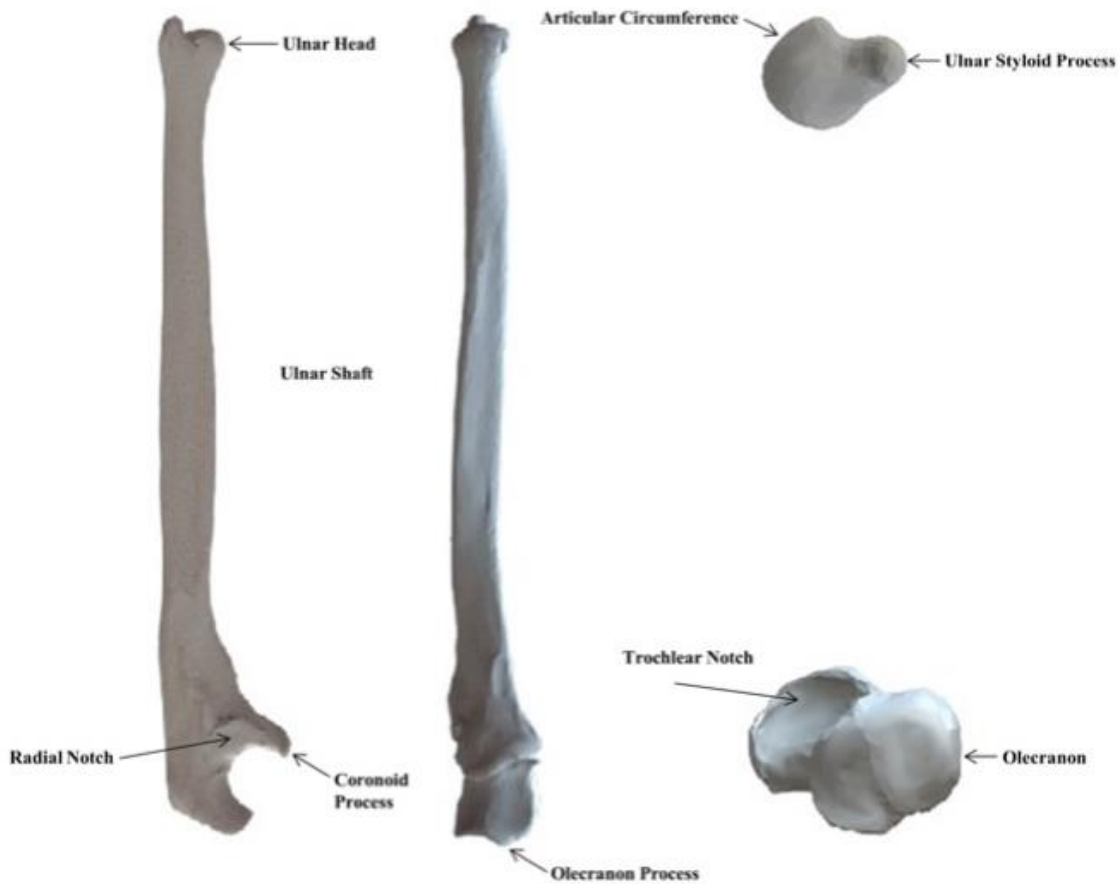


Figure 1.4. Anatomy of the ulna (A) Lateral view (B) Anterior view (C) Distal articular surface (D) Proximal articular surface.

1.1.3 Carpal Bone Anatomy

Carpal bones are unique and classified as irregular bones, with an outer shell of cortical bone and inner cancellous matrix. They are arranged into a proximal and distal row(2) (**Figure 1.5**) with the scaphoid bridging between the two, though typically the scaphoid is considered a member of the proximal row. From radial to ulnar, the proximal row consists of the scaphoid, lunate, and triquetrum, while the distal row consists of the trapezium, trapezoid, capitate, and hamate. The pisiform bone has been traditionally included in the proximal row; however, it functions more as a sesamoid bone within the flexor carpi ulnaris (FCU) tendon rather than a true carpal bone(4).

This work will focus on the carpal bones involved in scaphoid nonunion advanced collapse (SNAC) and scapholunate advanced collapse (SLAC), and four corner fusion surgery (lunate, triquetrum, capitate, and hamate).

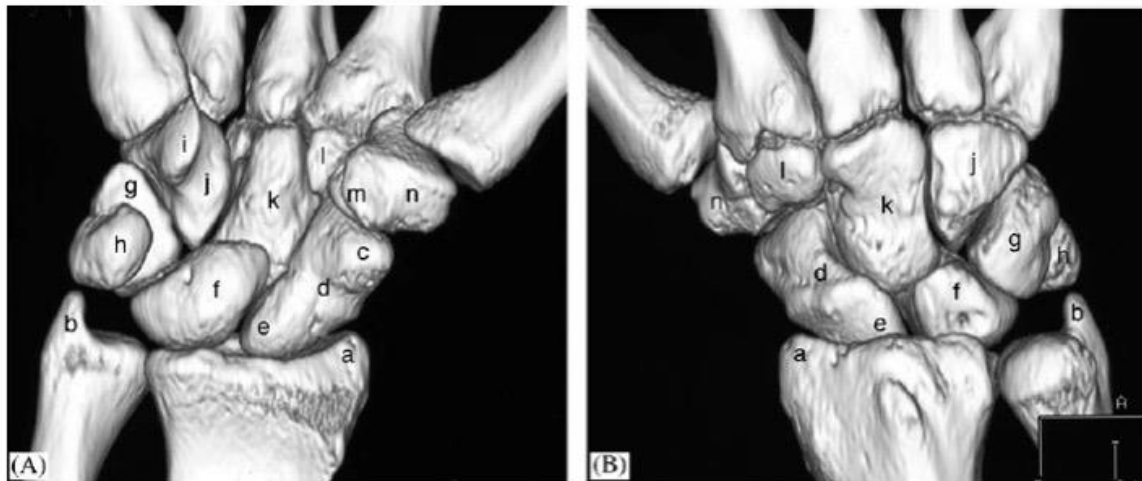


Figure 1.5. Hand and wrist anatomy. Volar and dorsal views of the right hand showing carpal bones, distal radius and ulna. (a) radial styloid, (b) ulnar styloid, (c) scaphoid tubercle, (d) scaphoid waist, (e) proximal pole of scaphoid, (f) lunate, (g) triquetrum, (h) pisiform, (i) hook of hamate, (j) hamate, (k) capitate, (l) trapezoid, (m) tubercle of trapezium, (n) trapezium. (Reprinted with permission from Srinivas Reddy, R., & Compson, J. (2005). Examination of the wrist—surface anatomy of the carpal bones. *Current Orthopaedics*, 19(3), 171–179)

1.1.3.1 Scaphoid Osteology

The scaphoid is named after the latin word, *skaphos*, based on its geometric resemblance to a boat (**Figure 1.6**). It is the second largest carpal bone and is positioned radially within the carpus, providing stability by spanning the proximal and distal carpal rows(2). The scaphoid is oriented obliquely at 45° in the sagittal and coronal planes, resulting in the proximal pole extending relatively more dorsal than the distal pole, where the scaphoid tubercle lies.

The scaphoid can be divided into 3 sections: the proximal pole, scaphoid waist, and distal pole. A dorsal ridge spirals across the waist acting as a capsular attachment and also has multiple foramina for nutrient blood vessels(4, 5).

There are 4 facets that allow for articulation with adjacent carpal bones(2). Proximally, the scaphoid articulates with the lunate via the lunate facet, and with the scaphoid fossa of the radius via the radial facet. Distally there is 1 concave surface that articulates with the capitate head, and 2 convex articulations with the trapezium and trapezoid.

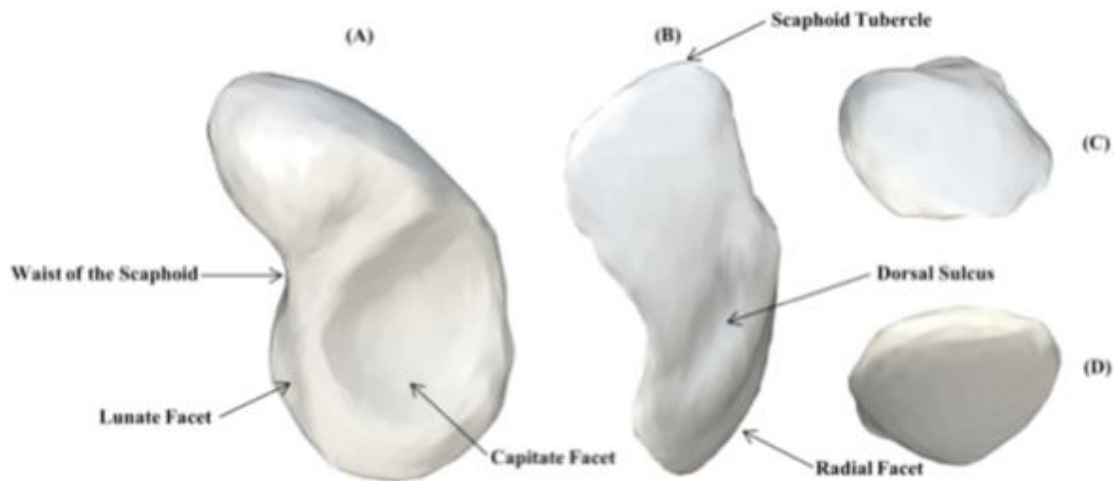


Figure 1.6. Anatomy of the left scaphoid (A) Medial view (B) Dorsal view (C) Distal articular surface (D) Proximal articular surface.

1.1.3.2 Lunate Osteology

The lunate, named after its crescent shape (*luna*, latin for 'moon'), is located centrally between the scaphoid and triquetrum (**Figure 1.7**). In its three-dimensional structure, the lunate is wedge-shaped and can be divided into volar and dorsal poles, with the former being larger than the latter(2).

Two types of lunates were described in the late 1980's(6). Type I lunates have a total of 4 articulations with: the radius proximally, scaphoid radially, and trapezoid and capitate distally. Type II lunates have an additional articulation with the hamate via a medial facet. A ball-in-socket type joint is formed within the midcarpal joint with its articulations to the scaphoid and capitate. There are no articulations at the volar and dorsal surfaces.

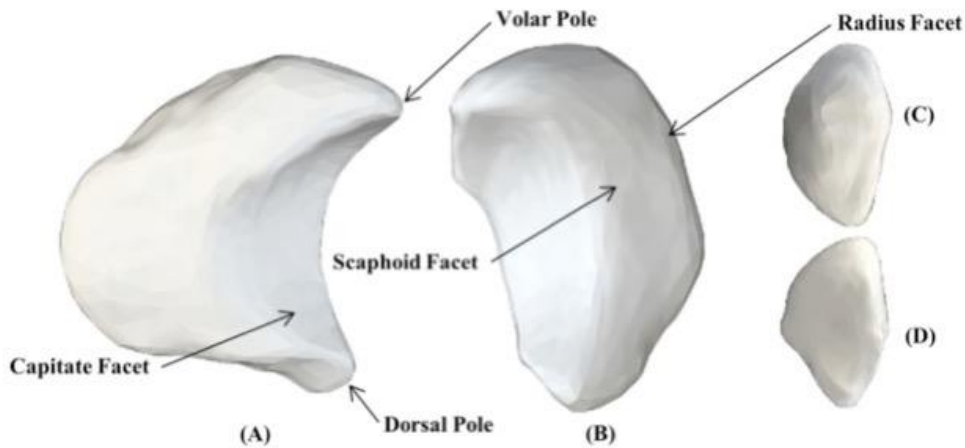


Figure 1.7. Anatomy of the left lunate (A) Distal articular surface (B) Proximal articular surface (C) Medial view (D) Lateral view.

1.1.3.3 Triquetrum Osteology

The triquetrum is pyramidal-shaped bone that resides at the ulnar-most aspect of the proximal carpal row(2) (**Figure 1.8**). It has 3 main articular surfaces, hence its name. At its volar aspect it has a shallow facet for articulation with the pisiform. Distally, it articulates with the hamate and radially with the lunate.

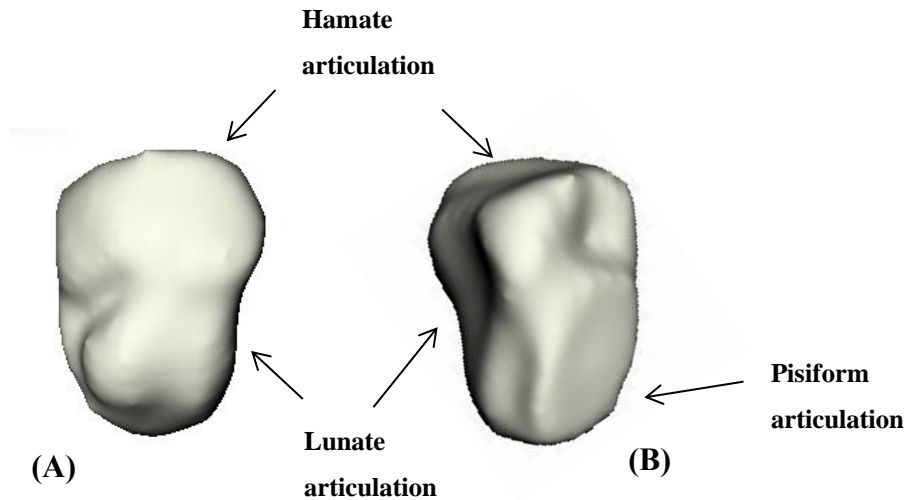


Figure 1.8. Anatomy of the triquetrum. (A) Dorsal view (B) Volar view.

1.1.3.4 Trapezium Osteology

The trapezium, also known as the ‘greater multangular’, is located at the base of the thumb and resides radially within the distal carpal row(2) (**Figure 1.9**). It has a saddle-shaped articular surface for the first (thumb) metacarpal and a small facet for the second (index) metacarpal. Proximally, the trapezium articulates with the scaphoid, and medially with the trapezoid. A prominent ridge is located on its volar surface, where the flexor carpi radialis (FCR) tendon sheath travels.

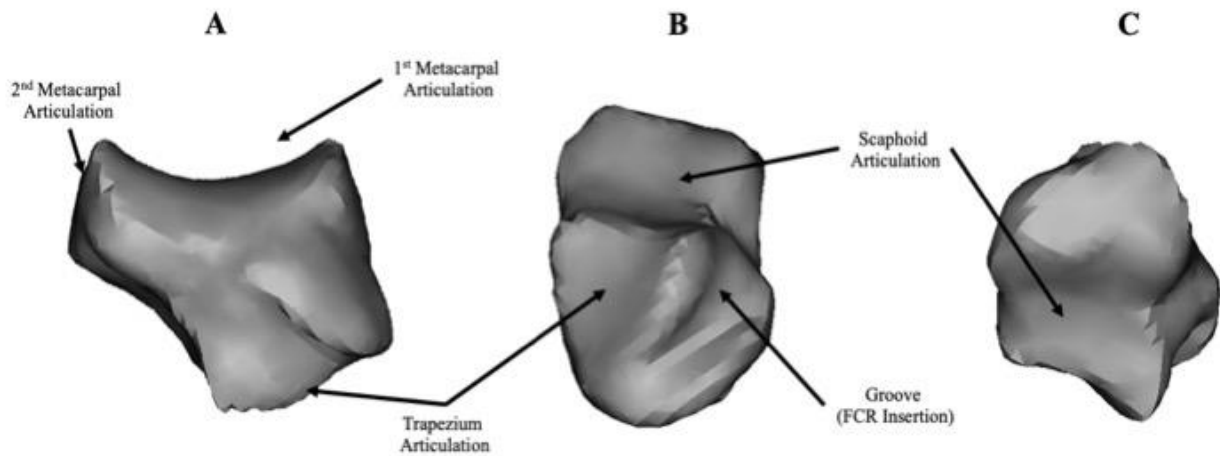


Figure 1.9. Anatomy of the trapezium (A) Volar view (B) Lateral view (C) Proximal articular surface.

1.1.3.5 Trapezoid Osteology

The trapezoid, also known as the ‘lesser multangular’, is found between the trapezium and capitate in the distal carpal row(2) (**Figure 1.10**). It is the second smallest carpal bone, after the pisiform. The volar and dorsal surfaces serve as attachment sites for ligaments and do not have any articulations. Radially, it articulates with the trapezium, proximally with the scaphoid, and ulnarly with the capitate. Distally, two flat surfaces articulate with the base of the second (index) and third (long) metacarpal bases.

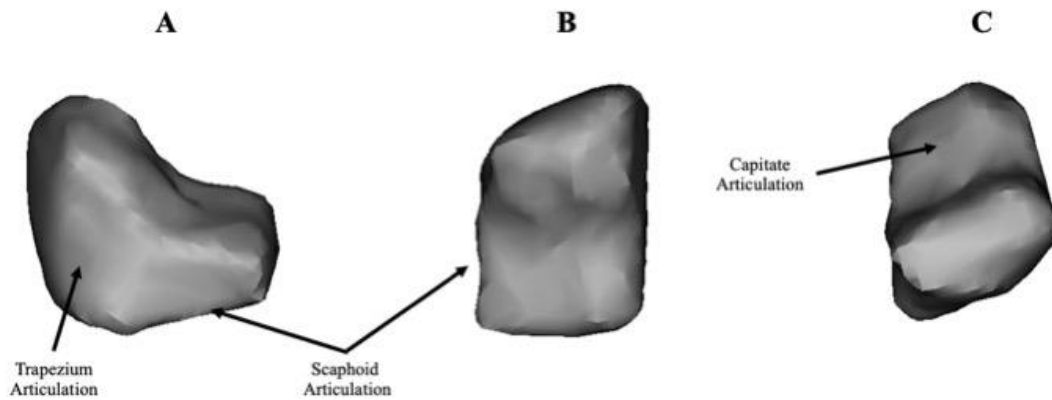


Figure 1.10. Anatomy of the trapezoid. (A) Volar view (B) Lateral view (C) Proximal articular surface.

1.1.3.6 Capitate Osteology

The capitate is the largest of the carpal bones and resides centrally in the distal carpal row(2) (**Figure 1.11**). It can be divided into 3 parts: the head, neck and body. The capitate head refers to the proximal one-third of the bone and its round surface articulates with the scaphoid and lunate. The lunocapitate joint allows for flexion and extension at the midcarpal joint. At its ulnar aspect, the capitate articulates with the hamate. Distally, at its squared-off end, two small concave facets allow for articulation with the second (index), third (long), and occasionally fourth (ring) metacarpals. Its volar and dorsal surfaces are free from articulations.

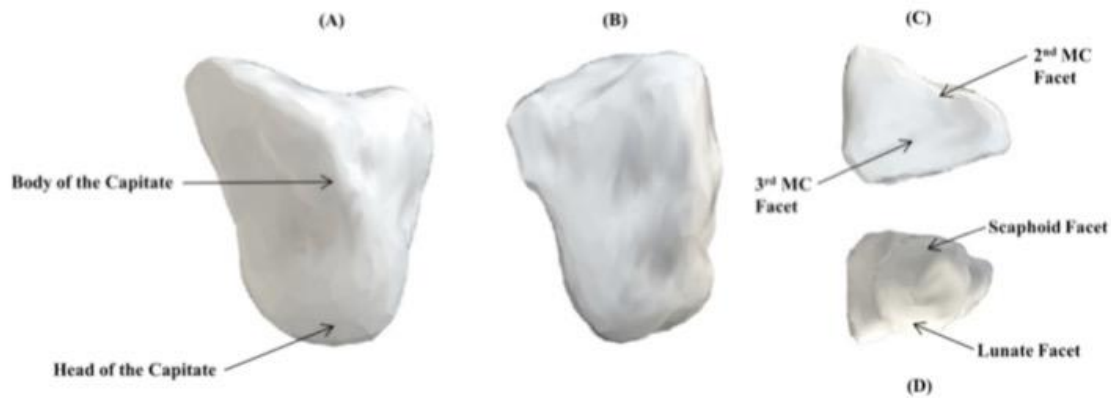


Figure 1.11. Anatomy of the capitate (A) Lateral view (B) Volar view (C) Distal articular surface (D) Proximal articular surface.

1.1.3.7 Hamate Osteology

The hamate, named after the hook at its volar surface (*hamulus*, latin for 'hook'), resides at the ulnar aspect of the distal carpal row(2) (**Figure 1.12**). It can be divided into 3 sections: the proximal pole, hook, and body. At its proximal pole, the hamate articulates with the triquetrum and occasionally with the lunate (as seen in type II lunates). The hamate hook functions as an insertion point for several ligaments. Similar to the capitate, its distal aspect (the body) contains flat articular surfaces for the fourth (ring) and fifth (small) metacarpal bases.

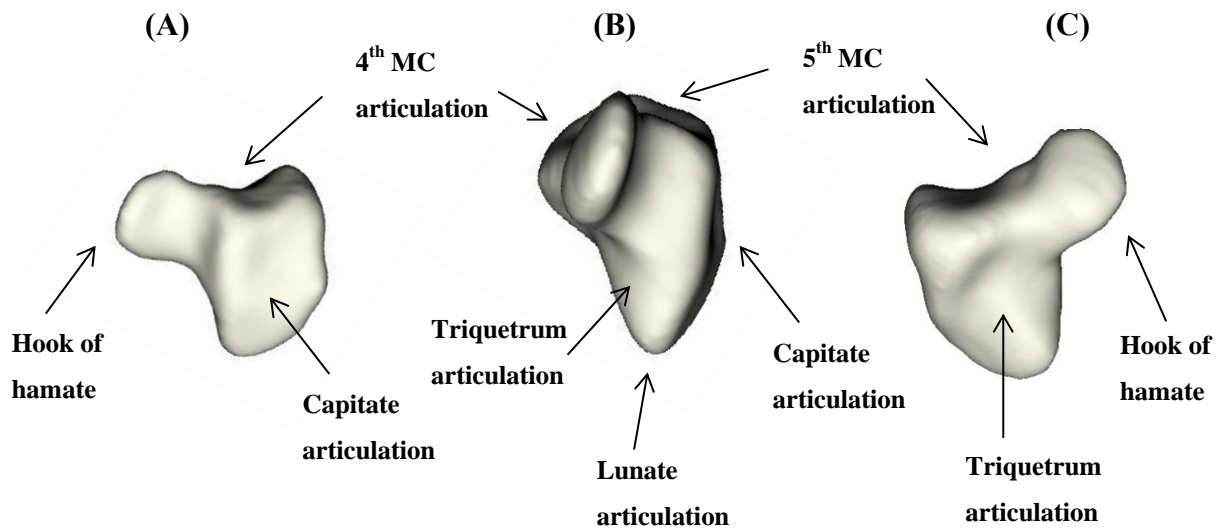


Figure 1.12. Anatomy of the hamate. (A) Radial view (B) Volar view (C) Lateral view.

1.1.4 Soft Tissue Anatomy

The stability of the wrist is maintained primarily by soft tissue structures, which can be classified as static or dynamic.

1.1.4.1 Static wrist stabilizers

Static wrist stabilizers include intrinsic and extrinsic carpal ligaments. Intrinsic carpal ligaments originate and insert within the carpal bones, whereas extrinsic carpal ligaments originate from the distal forearm bones (radius and ulna) and insert into the carpus(3).

1.1.4.1.1 Intrinsic carpal ligaments

Intrinsic carpal ligaments provide critical stabilization through rigid attachments between carpal bones, restricting the motion between them(3). These ligaments exist within each carpal row and between them.

Two interosseous ligaments support the proximal carpal row: the scapholunate (SL) and lunotriquetral (LT) ligaments. Within the midcarpal joint, the dorsal intercarpal ligament (DIL) stabilizes the triquetrum to the scaphoid, lunate and trapezium. Several short ligaments connect various combinations of carpal bones between the proximal and distal carpal rows at the volar midcarpal joint, of which the scaphotrapeziotrapezoid and scaphocapitate ligaments (STT and SC, respectively) are most critical for scaphoid stability.

1.1.4.1.2 Extrinsic carpal ligaments

Extrinsic carpal ligaments provide stabilization while the wrist is in various positions. There are 4 major groups of extrinsic carpal ligaments including the volar radiocarpal, volar ulnocarpal, dorsal radiocarpal, and dorsal ulnocarpal ligaments(5). Collectively, the volar ligaments are thicker and stronger than the dorsal ligaments.

1.1.4.1.2.1 *Volar radiocarpal ligaments*

The volar radiocarpal ligament complex consists of 4 ligaments: the long and short radiolunate ligaments (LRL and SRL ligaments, respectively), radioscapolunate ligament (RSL, also known as the ‘ligament of Testut and Kuentz’), and the radioscapocapitate ligament (RSC)(5) (**Figure 1.13**). These ligaments connect the distal radius to the proximal carpal row, providing stability while the wrist is in extension.

The LRL, RSL and RSC all originate from the lateral distal radius in the region of the radial styloid. The LRL inserts into the lunate and triquetrum and is responsible for lunate stabilization(7), while the RSC travels within a groove of the volar scaphoid before inserting into the capitate. This acts as a fulcrum for scaphoid rotation, and maintains the scaphoid in a flexed position(8). The RSC is the primary stabilizer to prevent ulnar translation of the wrist. Although termed a “ligament”, the RSL functions as a neurovascular conduit for the anterior interosseous nerve and artery and does not add any mechanical strength(9). The SRL ligament originates deeper from the medial distal radius and inserts into the lunate, providing additional stabilization.

1.1.4.1.2.2 *Volar ulnocarpal ligaments*

The volar ulnocarpal ligaments consist of the ulnotriquetral (UT), ulnolunate (UL) and ulnocapitate (UC) ligaments(5) (**Figure 1.13**). The UT ligament originates from the volar radioulnar ligament inserting into the medial triquetrum, while the UL ligament originates from the same and inserts into the lunate. The UC ligament originates from the ulna fovea and inserts into the triquetrum. These ligaments collectively provide support during wrist extension.

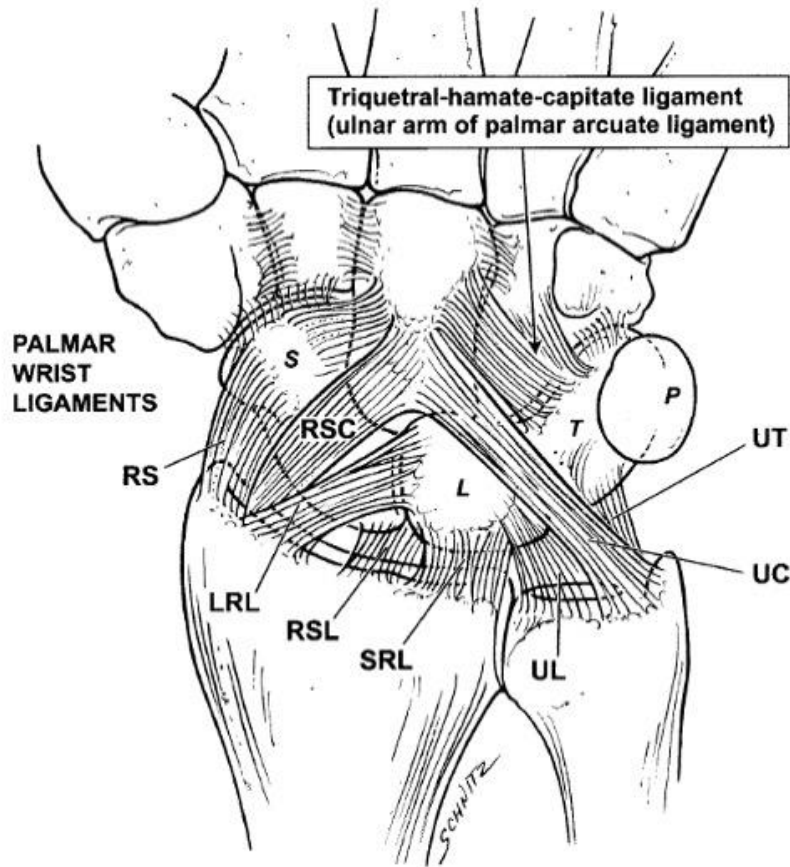


Figure 1.13. Volar radiocarpal and ulnocarpal ligaments of the wrist. LRL- long radiolunate ligament, RSL- radioscapholunate ligament, SRL- short radiolunate ligament, UL- ulnolunate ligament, UT- ulnotriquetral ligament, LT- lunotriquetral ligament. (Reprinted with permission from: Lichtman, D. M., & Wroten, E. S. (2006). Understanding Midcarpal Instability. The Journal of Hand Surgery, 31(3), 491–498)

1.1.4.1.2.3 *Dorsal radiocarpal ligaments*

A single ligament, the dorsal radiocarpal (DRC) ligament or dorsal radiotriquetral (DRT) ligament, originates from the dorsal radial styloid, just ulnar to Lister's tubercle, and attaches to the lunate and triquetrum(5) (**Figure 1.14**). This provides support to the wrist during flexion.

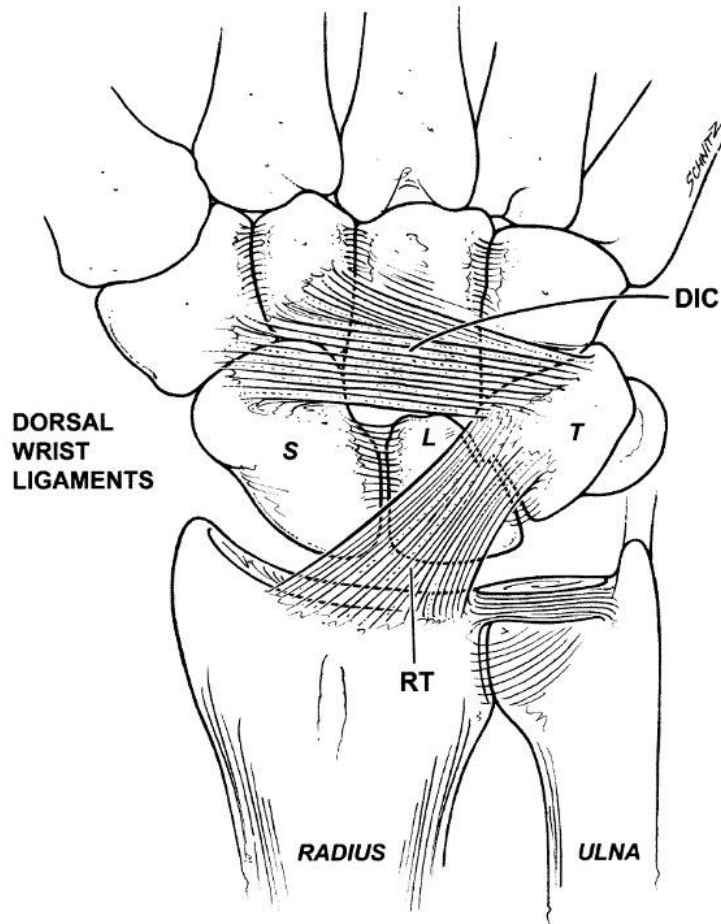


Figure 1.14. Dorsal ligaments of the wrist. RS- radioscapoid ligament, RT- radiotriquetral ligament, DIC- dorsal intercarpal ligament. (Reprinted with permission from: Lichtman, D. M., & Wroten, E. S. (2006). Understanding Midcarpal Instability. *The Journal of Hand Surgery*, 31(3), 491–498)

1.1.4.2 Dynamic wrist stabilizers

Dynamic stabilization of the wrist is maintained by muscles and tendons that cross the wrist joint (**Figure 1.15**). Muscles of the anterior forearm can be divided into 3 layers (superficial, middle, deep) and allow flexion of the wrist and digits(3) (**Table 1.1**). Muscles of the dorsal forearm are divided into 2 layers (superficial, deep) and result in wrist and digit extension(3) (**Table 1.2**).

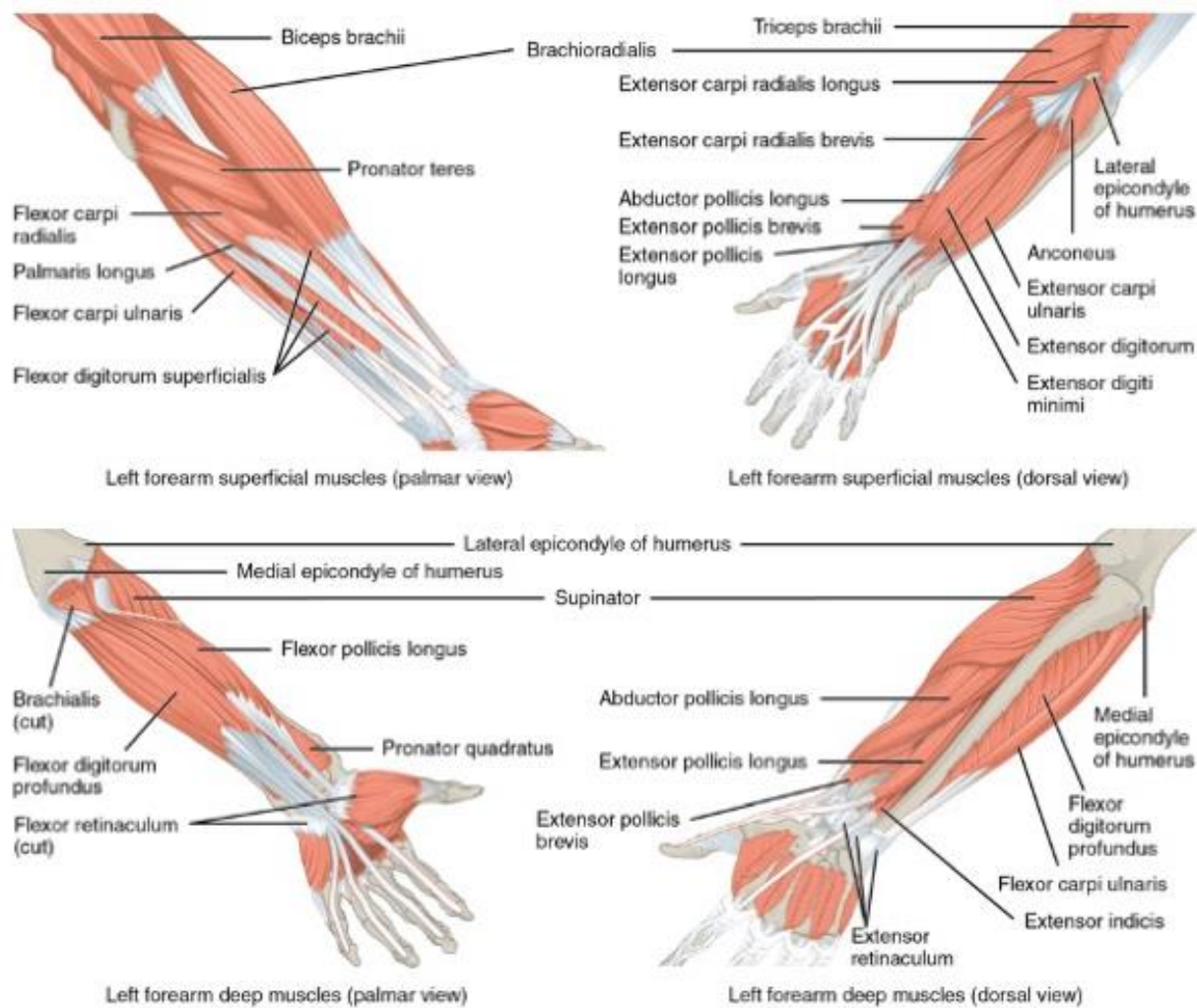


Figure 1.15. Muscles of the forearm. (A) Superficial layer of anterior and posterior forearm (B) Deep layer of anterior and posterior forearm. (Reprinted with permission from: OpenStax, Anatomy & Physiology. OpenStax CNX. Feb 26, 2016 <http://cnx.org/contents/14fb4ad7-39a1-4eee-ab6e-3ef2482e3e22@8.24>)

| | Muscle | Origin | Insertion | Innervation | Action |
|----------------------------------|--------------------------------------|--|--|---|--|
| Superficial | Flexor carpi radialis (FCR) | Medial epicondyle of humerus | Base of 2 nd metacarpal (MC) | Median nerve | Wrist flexion, wrist radial deviation |
| | Palmaris longus (PL) | | Palmar aponeurosis | | Wrist flexion |
| | Flexor carpi ulnaris (FCU) | | Base of 5 th MC, pisiform, hook of hamate | | Wrist flexion, wrist ulnar deviation |
| Middle | Flexor digitorum superficialis (FDS) | | Base of middle phalanx of digits 2-5 | | Digit flexion at proximal interphalangeal joint (PIPJ) |
| | Deep | Flexor pollicis longus (FPL) | Anterior radius and interosseous membrane | Base of thumb distal phalanx | Anterior interosseous nerve (AIN) – branch of median nerve |
| Pronator quadratus (PQ) | | Medial anterior ulna | Lateral anterior radius | | Forearm pronation |
| Flexor digitorum profundus (FDP) | | Anteromedial surface of ulna, interosseous membrane, deep forearm fascia | Base of distal phalanx of digits 2-5 | FDP to index and long – AIN of median nerve FDP to ring and small digits – ulnar nerve | Digit flexion at distal interphalangeal joint (DIPJ) |

Table 1.1. Dynamic stabilizers of the wrist within anterior forearm. (Modified with permission from: Chambers et al. Thesis Dissertation 2019)

| | Muscle | Origin | Insertion | Innervation | Action |
|-------------|---------------------------------------|--|--|---|---|
| Superficial | Extensor carpi radialis brevis (ECRB) | Lateral epicondyle of humerus | Base of 3 rd metacarpal (MC) | Radial nerve | Wrist extension, wrist radial deviation |
| | Extensor carpi radialis longus (ECRL) | | Base of 2 nd MC | | |
| | Extensor digitorum communis (EDC) | | Extensor hood and base of distal phalanx, digits 2-5 | | Wrist extension, digit 2-5 extension |
| | Extensor digiti quinti (EDQ) | | Extensor hood and base of distal phalanx, digit 5 | | Wrist extension, 5 th digit extension |
| | Extensor carpi ulnaris (ECU) | | Base of 5 th MC | | Wrist extension, wrist ulnar deviation |
| Deep | Abductor pollicis longus (APL) | Dorsal radius and ulna, interosseous membrane | Base of 1 st metacarpal, trapezium | Posterior interosseous nerve (PIN) – branch of radial nerve | Thumb abduction and extension |
| | Extensor pollicis brevis (EPB) | Radius and interosseous membrane | Base of thumb proximal phalanx | | Thumb extension at metacarpophalangeal joint |
| | Extensor pollicis longus (EPL) | Middle 1/3 dorsal ulna, interosseous membrane | Base of thumb distal phalanx | | Thumb extension at interphalangeal joint |
| | Extensor indicis proprius (EIP) | Distal 1/3 of dorsal ulna, interosseous membrane | Extensor hood and base of distal phalanx, digit 2 | | Index finger extension (interphalangeal and metacarpophalangeal joints) |

Table 1.2. Dynamic stabilizers of the wrist within posterior forearm. (Modified with permission from: Chambers et al. Thesis Dissertation 2019)

1.2 BIOMECHANICS OF THE WRIST

Complex movements at the wrist joint are possible secondary to multi-planar geometry of the articulations and numerous constraining ligaments(5, 10). There are three main types of motion at the wrist joint including flexion-extension, radial-ulnar deviation, and pronation-supination (rotation about the long axis of the radius) (**Figure 1.16**). Circumduction describes sequential wrist flexion, adduction, extension and abduction motions. These complex movements are defined relative to the wrist in neutral position, where the long axis of the radius is parallel to the long axis of the third metacarpal(11). Neutral forearm rotation is defined with the elbow positioned at 90° of flexion, and volar surface of the hand facing the anatomical midline of the body(12). Normative wrist ROM data in individuals without any previous history of wrist arthritis or trauma is shown in **Table 1.3** (10).

Studies have been conducted to suggest that activities of daily living (ADLs) can be performed with a minimum of 5° of flexion, 30° of extension, 10° of radial deviation, and 15° of ulnar deviation(13), and that all ADLs can be performed with 54° of flexion, 60° of extension, 17° of radial deviation, and 40° of ulnar deviation(14).

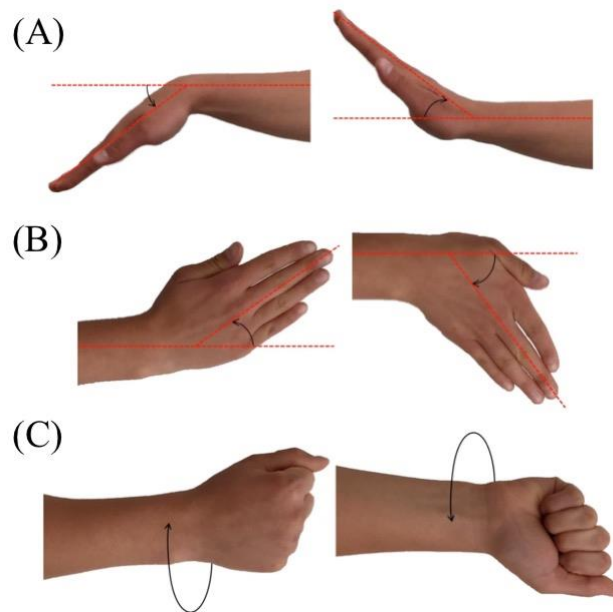


Figure 1.16. Wrist range of motion. (A) Wrist flexion and extension (B) Wrist radial and ulnar deviation (C) Wrist pronation and supination.

| Wrist Motion | Range of Motion (Degrees) |
|---------------------|----------------------------------|
| Flexion | 65-80 |
| Extension | 55-75 |
| Radial Deviation | 15-25 |
| Ulnar Deviation | 30-45 |
| Pronation | 60-80 |
| Supination | 60-85 |

Table 1.3. Normative wrist range of motion values.

Dart-thrower's motion (DTM) describes the transition from a position of wrist extension and radial deviation into wrist flexion and ulnar deviation. This motion is more representative of clinical wrist function compared to uniplanar motion(15). The elliptical pattern formed by wrist circumduction has been shown to fall along the same axis of the DTM pathway(16).

1.2.1 Kinematic models of carpal motion

In general, four main biomechanics concepts of carpal motion have been developed: the row theory, column theory, link theory, and ring theory. These serve as the basis of other theories that have been proposed regarding carpal motion.

1.2.1.1 Row theory

The earliest and most simplistic theory was proposed by Bryce in 1896(17), where he described the kinematic function of the wrist using planar radiographs. He proposed that motion within the proximal carpal row, consisting of the lunate and triquetrum, occurs secondary to signals from the distal carpal row. The distal carpal row, along with its articulations to the metacarpals, move as a single unit. Motion is initiated at the distal carpal row and gets transmitted via the scaphoid, which acts as a bridge, into the proximal carpal row. In this model, flexion and extension at the wrist occurs at the midcarpal joint, while ulnar and radial deviation occurs at the radiocarpal joint.

1.2.1.2 Column theory

Later, in 1921, Navarro (18) proposed an alternative theory where the carpal bones function as radial, central and ulnar columns. The radial column consists of the scaphoid, trapezium and trapezoid. The central column consists of the lunate, capitate and hamate. The ulnar column is comprised solely of the triquetrum. This theory suggests that wrist flexion and extension occur via interactions within the central column, whereas ulnar and radial deviation occur secondary to the ulnar and radial columns, respectively, rotating about the central column.

1.2.1.3 Link theory

In 1943, Gilford et al.(19) promoted a concept originally conceived by Lambrinudi, suggesting the wrist functions in 3 consecutive links. These individual links, each functioning as a unit, were comprised of the radius, proximal carpal row and distal carpal row. Wrist extension occurs mainly at the radiolunate joint, while flexion occurs at the lunocapitate joint. At the ulnar aspect, the triquetrum and TFCC function as a simple hinge, and radially the scaphoid stabilizes the link against collapse. Many criticized this theory as the scaphoid spans both the proximal and distal carpal rows.

1.2.1.4 Ring theory

Again, several years later in 1980, Lichtman et al. developed the “oval-ring” theory(6). This theory views the wrist as 4 segments: the scaphoid, lunate, triquetrum, and distal carpal row. Ligamentous connections join each element to two neighboring segments and normal carpal motion relies on the integrity of ligaments. There is a radial (scaphotrapezium joint) and ulnar (triquetrohamate joint) link. Radial deviation of the wrist results in a greater flexion moment at the radial link causing the proximal carpal row to flex while the capitate and hamate subluxate into a volar intercalated segment instability (VISI) deformity. The converse is also true whereby ulnar deviation of the wrist first causes triquetrum extension relative to the hamate followed by proximal row extension and capitate and hamate dorsal subluxation into a dorsal intercalated segment instability (DISI) deformity. Disruption of the ring at the radial border causes instability of the scaphoid-lunate-capitate, while ulnar disruption results in midcarpal instability.

1.2.2 Laboratory-based analysis of wrist kinematics

In vitro carpal motion simulators assessing cadaveric kinematics can be categorized as passive or active. Passive motion simulators depend on the application of external forces(20), whereas active motion simulators prescribe motion actively using position and/or force feedback to more closely mimic *in vivo* wrist kinematics (21-23).

1.2.2.1 Passive motion simulators

Passive motion simulators rely on the application of an external force, exerted by a mechanical apparatus or an investigator, to a limb resulting in joint motion.

One example of this was developed by Gammon and Nishiwaki(20) (**Figure 1.17**). Upper limb cadaveric specimens were amputated at the mid-humerus level and secured to the base of the simulator. Tendons (FCR, FCU, ECRL, ECU, pronator teres (PT), and biceps brachii (BB)) were tagged and pneumatic actuators were programmed to maintain a specific load on each. Motion was detected using optical trackers inserted into the radius, ulna, scaphoid, lunate, and third metacarpal. Passive motion was initiated by an investigator physically moving a pin that was inserted into the third metacarpal of the specimen.

Another group at the University of Texas developed a passive motion simulator similar to the above design(24). They maintained tone in antagonistic muscles (i.e. flexors and extensors) using a weighted pulley arrangement. Wrist motion was initiated by the investigator moving a third metacarpal pin.

While passive motion simulators often maintain the integrity of muscles and tendons, they require the application of an external force to initiate motion(20, 24). These external forces may generate moment arms that alter normal motion pathways, limiting the reproducibility of wrist motion.

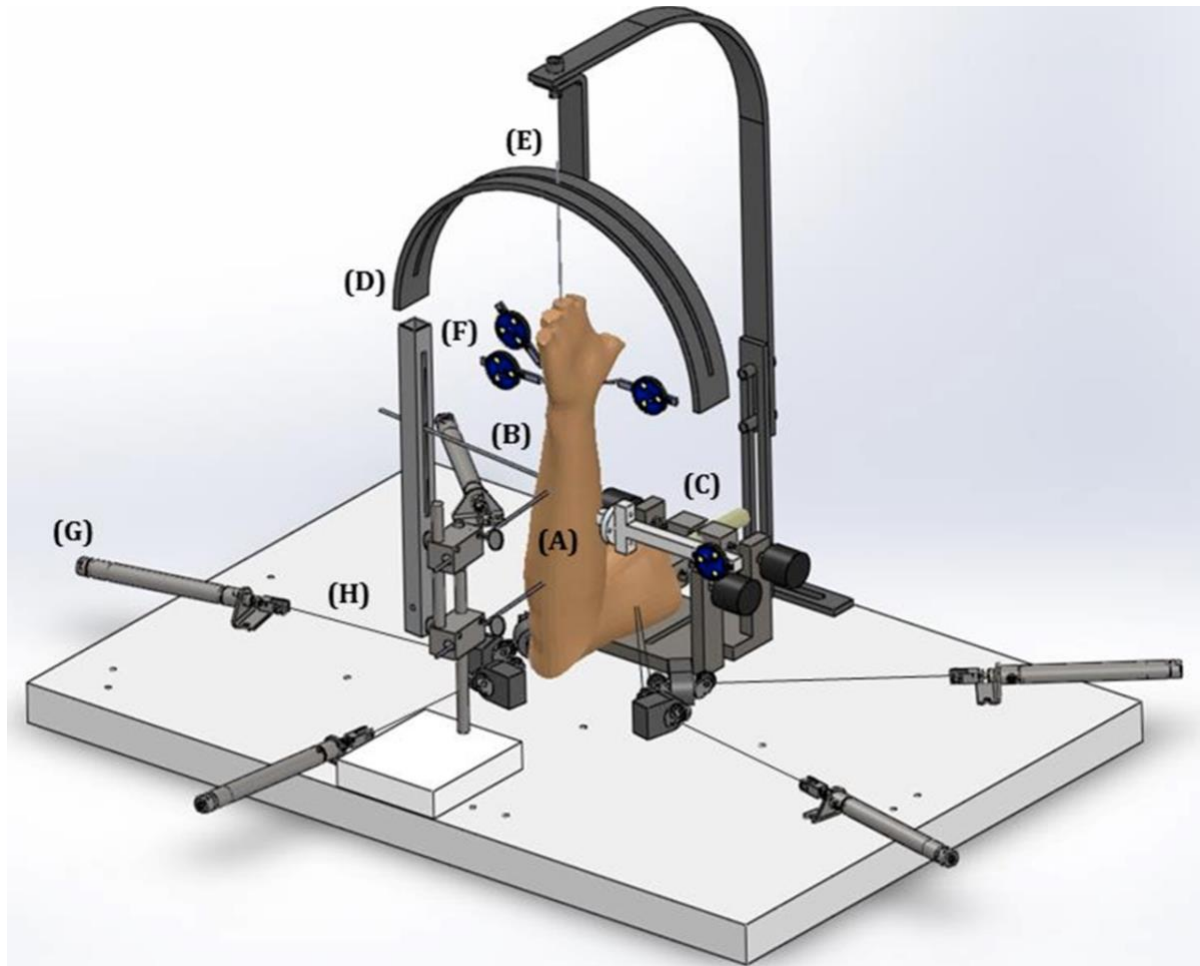


Figure 1.17. Passive motion wrist simulator by Gammon and Nishiwaki (A) Ulna fixed with the elbow at 90° flexion, (B) Radius securing the forearm in neutral rotation, (C) Rigidly fixed humerus, (D) Flexion-extension motion arc, (E) Passive motion guide (Steinmann pin inserted into third metacarpal), (F) Optical tracking markers, (G) Pneumatic actuators, and (H) Cables connecting actuators and corresponding muscle sutures. (Reprinted with permission from: Stoesser H, et al. Biomechanical Evaluation of Carpal Kinematics during Simulated Wrist Motion. *J Wrist Surg.* 2017;6(2):113-9)

1.2.2.2 Active motion simulators

Active motion simulators manipulate joint motion through the application of forces directly to various muscle tendons and rely on positional and/or force feedback (21-23). Forces exerted on antagonistic muscles help maintain tone within their tendons, closely mimicking a physiologic state, while forces applied to synergistic muscles result in angular motions of the wrist.

Werner et al. (21) was first to develop an active motion simulator capable of producing repeatable wrist motions using a closed-loop feedback system (**Figure 1.18**). Cadaveric specimens were transected at the distal humerus level and were cemented into the base of the simulator. All soft tissue structures were excised, except for the muscles and tendons of interest. The remaining structures of FCR, FCU, APL, ECU, and ECRL were connected to a servo-hydraulic system. Wrist position and motion were recorded using electromagnetic spatial trackers inserted into the ulna, lunate, and third metacarpal. These trackers were capable of supplying real-time feedback to adjust tendon loads between trials and specimens. This model also had limitations, primarily that the soft tissue of the specimen was excised and did not replicate a true physiologic state.

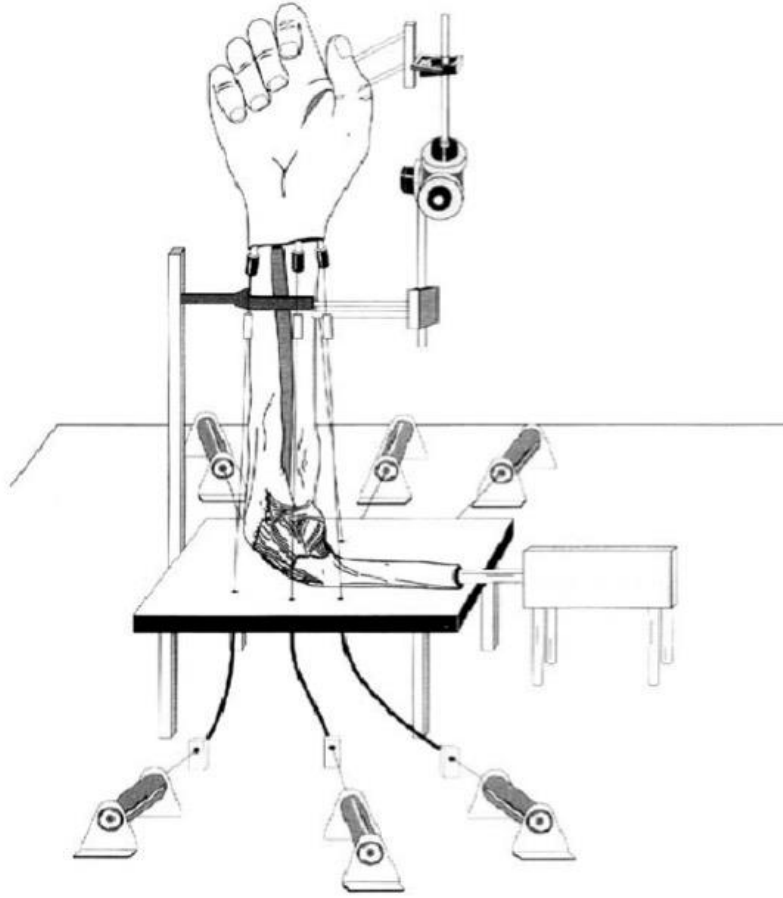


Figure 1.18. Active motion wrist simulator by Werner et al. This simulator is capable of producing reproducible planar and combined motions. (Reprinted with permission from: Werner FW, Palmer AK, Somerset JH, Tong JJ, Gillison DB, Fortino MD, et al. Wrist joint motion simulator. J Orthop Res. 1996;14(4):639-46)

Later, Dunning et al.(22) developed an apparatus whereby computer-controlled pneumatic actuators delivered forces to various muscles resulting in digit and wrist motion (**Figure 1.19**). Again, upper extremity cadaveric specimens were amputated at the mid-humerus level and were mounted at the base of the simulator. Musculotendinous junctions of FCR, FCU, FDP, FPL, ECU, ECRL, ECRB, PT and BB were tagged. Rather than using optical trackers to track motion, this device used electromagnetic receivers that are unable to provide positional feedback. Consequently, investigators had to manually adjust the tendon forces exerted prior to testing, which resulted in inter-specimen variability and limited reproducibility.

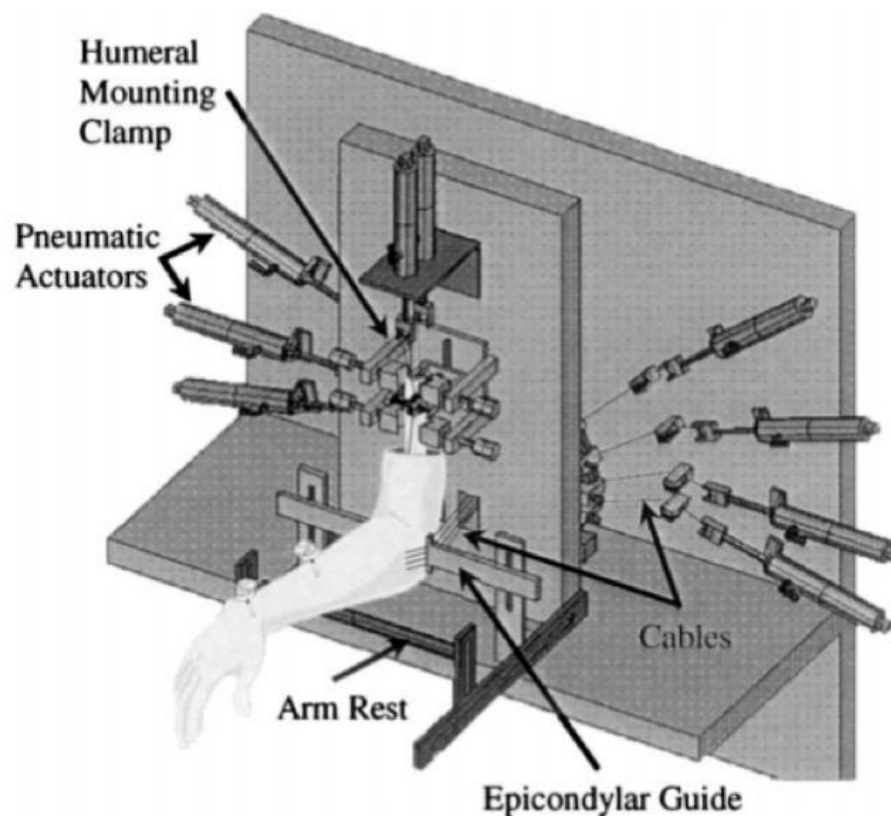


Figure 1.19. Active motion wrist simulator by Dunning et al. Developed to test stability of external fixation in distal radius fractures. (Reprinted with permission from: Dunning CE, Lindsay CS, Bicknell RT, Patterson SD, Johnson JA, King GJ. Supplemental pinning improves the stability of external fixation in distal radius fractures during simulated finger and forearm motion. *J Hand Surg Am.* 1999;24(5):992-1000)

More recently, Iglesias et al.(23) developed a simulator capable of testing passive and active carpal motion in various gravity-loaded positions (**Figure 1.20**). This model required FCR, FCU, ECU, ECRL, ECRB, PT and BB to be connected to electric servomotors. Strain gauges are incorporated into the design to measure and relay muscle force feedback. The simulator was able to maintain a predetermined tone load (of a minimum of 8.9 Newtons) on antagonistic muscles during motion testing, and produced repeatable active wrist motion. Optical trackers inserted into the radius, ulna, and third metacarpal provide closed-loop feedback to the system in real-time.



Figure 1.20. Active motion wrist simulator by Iglesias et al. This active motion simulator utilized closed-loop optical control and tests in several gravity-loaded positions. (Reprinted with permission from: Iglesias et al. Thesis Dissertation 2015: Development of an in-vitro passive and active motion simulator for the investigation of wrist function and kinematics).

1.3 CLINICAL DISORDERS OF THE WRIST: SCAPHOID FRACTURES

1.3.1 Scaphoid fractures

Scaphoid fractures account for 90% of carpal bone fractures(25) and occur second in frequency of fractures to the hand and wrist. Scaphoid fractures occur most commonly at the level of the waist (up to 80%), followed by the proximal pole (10-20%), and distal pole (5%). High velocity injuries may be associated with scapholunate ligament (SL) tears and transscaphoid perilunate fracture dislocations(26).

Gelberman and Botte described the blood supply to the scaphoid in detail(27) (**Figure 1.21**). The majority (70-80%) of blood flow originates dorsally, and the remainder from a volar blood supply. Notably, the proximal pole of the scaphoid is reliant on endosteal blood flow. In 1938, Oblatz and Halbstein (28) studied 297 scaphoids, and identified that 13% lack an arterial foramen proximal to the waist, 20% had one small foramen and 67% had two or more foramina; consequently vascularity of the proximal pole is often a concern in fractures between the proximal pole and scaphoid waist.

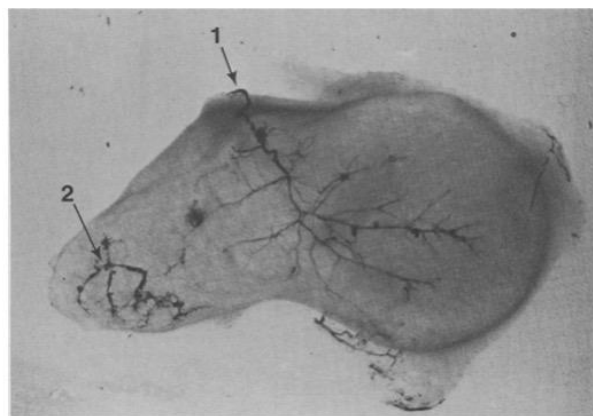


Figure 1.21. Cleared specimen showing internal vascularity of scaphoid. 1- dorsal scaphoid branch of radial artery, 2- volar scaphoid branch of radial artery. (Reprinted with permission from: Gelberman, R. H., & Menon, J. (1980). The vascularity of the scaphoid bone. *The Journal of Hand Surgery*, 5(5), 508–513)

1.3.2 Scaphoid fracture classification

Scaphoid fractures can be classified according to location and orientation. The Herbert classification stratifies fractures based on stability, while Mayo and Russe classifications are based on anatomic planes of the scaphoid.

1.3.2.1 Herbert fracture classification

The Herbert classification system divides scaphoid fractures into stable and unstable patterns(29) (**Figure 1.22**). Type A fractures are stable acute fractures, which can be divided into A1 (fractures of the scaphoid tubercle), and A2 (incomplete waist fracture). On the other hand, type B fractures are acute and unstable, and again can be divided into subtypes: B1 (oblique distal 1/3 fracture), B2 (displaced waist fracture), and B3 (proximal pole), B4 (fracture dislocations), and B5 (comminuted). Type C fractures indicate delayed union, after at least 6 weeks of immobilization in a cast. Type D fractures identify fibrous (D1) or sclerotic (D2) scaphoid nonunions.

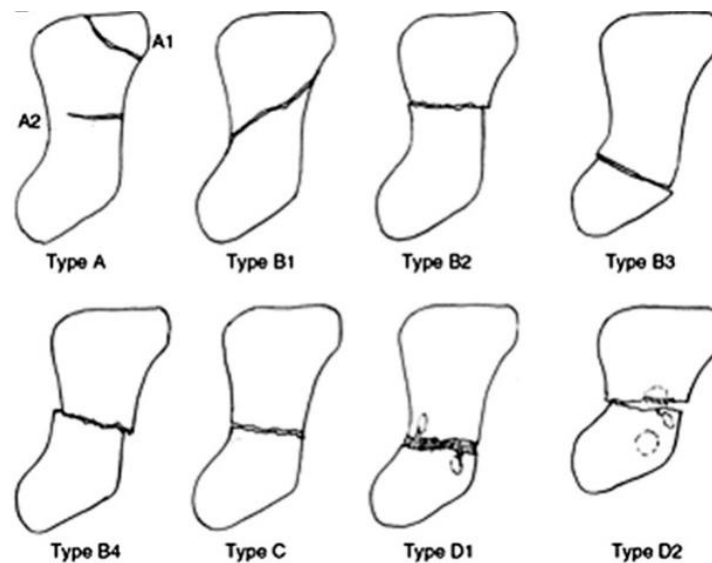


Figure 1.22. Illustration of Herbert Classification of scaphoid fractures. (Reprinted with permission from: Sendher, R., & Ladd, A. L. (2013). The Scaphoid. Orthopedic Clinics of North America, 44(1), 107–120)

1.3.2.2 Mayo fracture classification

The Mayo classification system was coined by Cooney et al. in 1980 (30), and identified scaphoid fractures based on stability and anatomic location (**Figure 1.23**). Stable, undisplaced fractures featured intact periosteum, whereas a displaced, unstable fracture was defined as >1mm fracture offset, or unstable collapse pattern (dorsal lunate rotation) on lateral x-ray. These fractures could then be further classified based on location: distal tubercle, distal intraarticular surface, distal 1/3 of scaphoid, waist, and proximal pole.

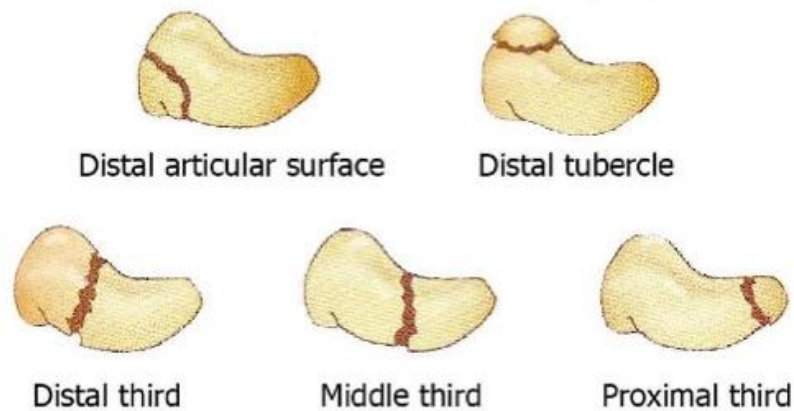


Figure 1.23. Illustration of Mayo Classification of scaphoid fractures. (Reprinted with permission from: Rhemrev, S.J., Ootes, D., Beeres, F.J. et al. (2011) Current methods of diagnosis and treatment of scaphoid fractures. Int J Emerg Med 4(4))

1.3.2.3 Russe fracture classification

Russe classification(31) is based on fracture line orientation and can be categorized as vertical oblique, transverse, or horizontal oblique (**Figure 1.24**). He demonstrated that the chance of successful conservative treatment is highly dependent on fracture orientation, with vertical oblique fractures having the most difficulty healing compared to the others.

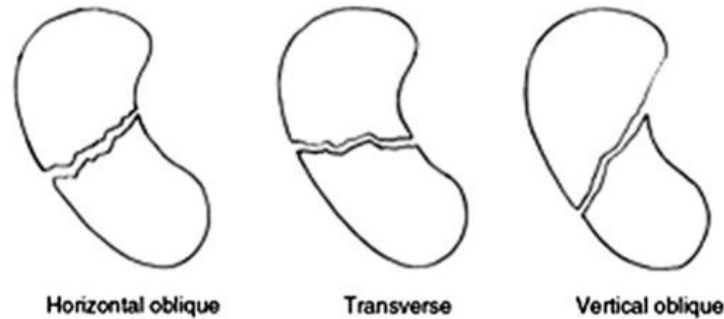


Figure 1.24. Illustration of Russe classification of scaphoid fractures. (Reprinted with permission from: Rhemrev, S.J., Ootes, D., Beeres, F.J. et al. (2011) Current methods of diagnosis and treatment of scaphoid fractures. Int J Emerg Med 4(4))

1.3.3 Epidemiology of scaphoid fractures

The epidemiology of scaphoid fractures is inconsistently reported; however, a group using a prospective database from the United States identified an annual incidence of 29 per 100,000 individuals(32). Another study estimated the incidence to be 1.47 fractures per 100,000 person-years(33).

Similar to other orthopedic injuries, such as shoulder dislocations, the frequency of scaphoid fractures occurs in a bimodal distribution with peaks in the younger population (10-29 years old) and in the elderly population (50-60 years old) (34). Although the most common inciting event is a fall on outstretched hand (FOOSH) overall, the younger population is injured more frequently from higher velocity mechanisms (including sports-related injury or motor vehicle collisions) while the older population tends to experience low velocity mechanisms (such as a fall from standing height).

1.3.4 Clinical diagnosis

The diagnosis of scaphoid fractures relies on a combination of the clinical history, physical exam, and radiographic investigations.

1.3.4.1 History

Patients suffering from a scaphoid fracture often report a history of trauma, and subsequent pain on the radial aspect of the wrist. Typically, scaphoid fractures occur secondary to a FOOSH with the wrist in hyperextension and radial deviation(25). A thorough history including patient age, handedness, occupation, recreational activities, past medical history, past surgical history, past traumatic history, medications, allergies, and smoking habits should be taken to assist in decision making. For instance, a young, active laborer may prefer operative intervention to allow for earlier recovery and return to work.

1.3.4.2 Physical Exam

Depending on the location of the fracture, different physical exam findings may be elicited. On physical exam, patients with proximal pole fractures may report more pain at the dorsal scaphoid within the anatomic snuffbox, while fractures of the scaphoid tubercle would be more painful volarly.

Classically, scaphoid fractures present with anatomic snuffbox tenderness; however, while this test is highly sensitive, it has low specificity(35). Tenderness at the scaphoid tubercle is also quite sensitive and is more specific(35), making it a better test to heighten clinical suspicion for scaphoid fractures. Patients typically have soft tissue swelling, but this is common to many hand and wrist injuries. They also often present with decreased grip strength and ROM secondary to pain and swelling.

Parivizi et al. compared the use of individual tests versus combining them in the diagnosis of scaphoid fractures (**Table 1.4**) (36). Overall, the use of multiple clinical exam maneuvers increases the sensitivity and specificity to more accurately detect scaphoid fractures.

Additionally, Bergh et al. (37) developed the Clinical Scaphoid Score with the following scoring system: snuffbox tenderness with wrist in ulnar deviation (3 points), scaphoid tubercle tenderness (2 points), and pain with thumb axial loading (1 point). They found a score of <4 has a negative predictive value of 96%, making a scaphoid fracture very unlikely.

| Physical Exam Finding | Sensitivity (95% CI) | Specificity (95% CI) |
|----------------------------------|----------------------|----------------------|
| 1. Anatomic snuffbox tenderness | 1.0 (0.94, 1.0) | 0.19 (0.13, 0.26) |
| 2. Tender at scaphoid tubercle | 1.0 (0.94, 1.0) | 0.30 (0.23, 0.38) |
| 3. Pain with thumb axial loading | 1.0 (0.94, 1.0) | 0.48 (0.40, 0.60) |
| 4. Decreased thumb motion | 0.66 (0.52, 0.78) | 0.66 (0.58, 0.73) |
| 1 + 3 | 1.0 (0.94, 1.0) | 0.54 (0.46, 0.62) |
| 1 + 2 + 3 | 1.0 (0.94, 1.0) | 0.74 (0.67, 0.81) |

Table 1.4. Specificity and sensitivity of physical exam findings to diagnose scaphoid fractures. Table modified from Parvizi et al. (36)

1.3.4.3 Investigations

Investigations begin with posteroanterior (PA), oblique, and lateral x-rays (XR) of the wrist(38) (**Figure 1.25**). Additionally, scaphoid views (PA with wrist in ulnar deviation) are helpful; when combined with traditional radiographs, the majority of scaphoid fractures can be visualized. Only 3% of patients with a suspected scaphoid fracture on clinical exam have normal XRs(39).



Figure 1.25. Radiographs of right wrist and scaphoid tubercle fracture. A) Posteroanterior B) Lateral, C) Oblique, D) Scaphoid views.

Additional imaging techniques including bone scans, computed tomography (CT) scans, and magnetic resonance imaging (MRI) can be utilized. According to a systematic review and meta-analysis in 2009 by Yin et al., pooled sensitivity of detecting acute scaphoid fractures is highest in bone scintigraphy (97%), followed by MRI (96%) then CT (93%). Pooled specificity was equivalent between MRI and CT at 99%, while bone scan was lower at 89%.

Bone scintigraphy has been used to diagnose scaphoid fractures. False positives may occur in arthritis, synovitis, and SL instability(40). A negative bone scan is able to rule out a scaphoid fracture, but a positive scan cannot reliably diagnose it. With a positive bone scan, a CT scan is warranted.

CT scan of the scaphoid provides high resolution detail about fracture orientation and displacement. CT scaphoid should be used to in patients with negative plain XRs and a high index of clinical suspicion of a fracture, to assess fracture morphology, for confirmation of union prior to cast discontinuation, pre-operatively for surgical planning, and in cases of suspected non-union(41). These images should be taken in the sagittal plane of the scaphoid as it allows for assessment of fracture displacement and angulation, such as with humpback deformities(42) (**Figure 1.26**).

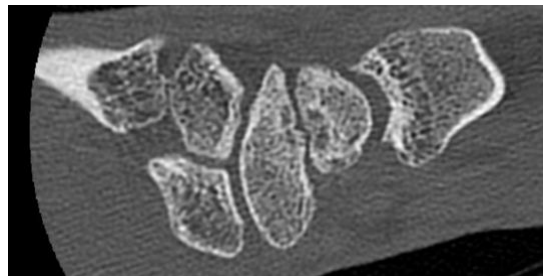


Figure 1.26. Sagittal CT of scaphoid with humpback deformity.

MRI has 100% sensitivity and 95-100% specificity in identifying acute scaphoid fractures(43, 44). Additionally, it has good interobserver reliability with kappa values of 0.8-0.96(43, 44). Unenhanced MRI may also be useful if there is a strong suspicion for scaphoid fracture but initial XRs are negative, as they are capable of identifying osseous and soft tissue injuries. Additionally, gadolinium (Gd)-enhanced MRI is the gold standard for assessing for avascular necrosis (AVN) of the proximal pole(45, 46). Gd-enhanced MRI has 85% sensitivity, 95% specificity and reliability coefficient of 0.85 for detecting AVN. As such, these enhanced scans are recommended when AVN is suspected in proximal pole fractures or when there is sclerosis of the proximal pole on XR.

1.3.5 Treatment

Treatment of scaphoid fractures depends on multiple factors including location, comminution, displacement, and angulation.

Undisplaced scaphoid waist or distal pole fractures may be treated with cast immobilization. Two prospective, randomized control trials have compared the use of short-arm casting and short-arm thumb spica casting in the treatment of undisplaced scaphoid fractures(47, 48). Both studies concluded that union rates were similar regardless of cast type. Given these results, short-arm casting may be preferred to avoid additional thumb stiffness. Mean time to union has been reported at 53 days and 65 days, respectively, although factors such as degree of comminution, sclerosis and displacement are associated with longer time to union(49). A significant limitation to these studies, however, is that assessment of union was performed with plain radiographs which is not as reliable as CT imaging (41).

Indications for operative fixation include proximal pole fractures, displacement ≥ 1 mm, humpback deformity (intra-scaphoid angle $\geq 35^\circ$), significant bone loss or comminution, or perilunate fracture-dislocation(50). In selected patients, undisplaced scaphoid waist fractures may be treated operatively.

1.4 CLINICAL DISORDERS OF THE WRIST: SCAPHOID NONUNION ADVANCED COLLAPSE

Scaphoid nonunion is defined as a failure of fracture healing (with evidence of bony cysts, sclerosis, resorption) or failure of union by 6 months from time of injury(51).

1.4.1 Epidemiology of scaphoid nonunion

Similar to how the incidence of scaphoid fractures is inconsistently documented, the incidence of scaphoid nonunion is also poorly documented. In an epidemiologic study by Sward et al.(52), the authors reported a rate of scaphoid nonunion at 2% (males at 3% and females 0.6%) over a 9-year period. Risk factors for nonunion include proximal pole fractures, comminution, fracture displacement >1mm(53), dorsal intercalated segment instability (DISI) deformity(54), and delayed medical treatment. Occasionally, scaphoid fractures that are appropriately treated with immobilization or surgical intervention can still progress to nonunion.

In a retrospective cohort study, Vender et al.(55) observed that in 64 patients with symptomatic scaphoid nonunion, approximately 40% of patients had developed radioscapoid arthritis at 1-year post-injury and at this increased to 75% by 4-years.

1.4.2 Pathophysiology of scaphoid nonunion advanced collapse

As mentioned earlier, the scaphoid spans and links the proximal and distal carpal rows. This link is disrupted in scaphoid nonunion resulting in abnormal carpal kinematics, particularly rotary subluxation of the distal scaphoid fragment(55). If left untreated, scaphoid nonunion can develop into a predictable pattern of progressive wrist arthritis known as scaphoid nonunion advanced collapse (SNAC) (55).

The classification system by Vender et al. (55) is widely accepted and is used to delineate treatment options and prognosis (**Table 1.5**). In stage I SNAC, arthritis develops between the scaphoid fossa of the radius and the distal fragment of the non-united scaphoid. Radiographically, this presents as radial styloid beaking and joint space narrowing. This progresses to arthritis between the capitate and proximal scaphoid fragment in stage II. In stage III, arthrosis develops between the capitate and lunate. Finally, pancarpal arthritis is seen in end-stage disease. Notably, the radiolunate joint and radius-proximal scaphoid fragment interface are spared in SNAC(55, 56).

| Stage of SNAC | Radiographic findings |
|----------------------|--|
| Stage I | Arthrosis to fractured distal scaphoid and radial styloid, with radial styloid beaking |
| Stage II | Stage I + arthrosis between proximal scaphoid and capitate |
| Stage III | Stage II + arthrosis between capitate and lunate |
| Stage IV | Pancarpal arthrosis (radiolunate and proximal radioscapoid joint spared) |

Table 1.5. Vender et al. classification of scaphoid nonunion advanced collapse.

1.4.3 Clinical presentation of SNAC

Patients with scaphoid nonunion may present with similar symptoms to an acute scaphoid fracture including snuffbox tenderness, general wrist pain, weakness, and stiffness(57). As scaphoid nonunion progresses to SNAC, patients may develop joint effusions, dorsal/radial wrist swelling, and tenderness at the radioscapoid or midcarpal joint.

Interestingly, symptomatology varies considerably in those with radiographic signs of SNAC. Although wrist pain is reported in the majority of cases, it can occasionally be discovered incidentally in asymptomatic patients. Other causes of radial-sided wrist pain, such as 1st carpometacarpal (CMC) joint osteoarthritis (OA), STT arthritis, trigger finger, DeQuervain's tenosynovitis, and carpal tunnel syndrome should be ruled out.

1.5 CLINICAL DISORDERS OF THE WRIST: SCAPHOLUNATE LIGAMENT INJURY

1.5.1 Scapholunate ligament disruption

The scapholunate (SL) ligament is a C-shaped structure and can be divided into 3 components: volar, membranous and dorsal(58). The volar segment has a tensile strength of 150 Newtons (N) and due to its oblique fibers, is responsible for rotational motion. The avascular intermediate section, comprised of fibrocartilaginous tissue, is the weakest withstanding forces of only 25-50 N. Consequently, the majority of degenerative tears and ligament avulsions occur at this junction. Finally, the dorsal SL acts as the primary stabilizer of the SL joint and can withstand forces up to 300 N.

When the SL ligament is disrupted, the scaphoid rotates volarly, while the lunate is forced into dorsiflexion due to its attachment with the triquetrum via the lunotriquetral ligament. This results into the radiographic finding of dorsal intercalated segment instability (DISI).

Damage to the SL ligament can be categorized as traumatic or atraumatic. Acute traumatic SL injury is commonly associated with intra-articular distal radius fractures, and occurs in 10-30% of cases(59). Degenerative weakening of the SL also occurs in 50% of individuals older than 80 years of age(60). Ligament attenuation can occur secondary to inflammatory conditions such as rheumatoid arthritis, calcium pyrophosphate dehydrate crystal deposition, and amyloid deposition diseases(61, 62).

1.5.2 Epidemiology of scapholunate ligament disruption

The natural history of SL injuries is not accurately documented since many injuries are not identified in the acute setting. Oftentimes patients believe they suffered from a sprain, rather than a partial or complete ligamentous tear and do not seek medical attention. Others with partial ligamentous injury may present with normal radiographs, and are only diagnosed arthroscopically or with open surgery(63). As a result, the true rate of symptomatic instability and progression to arthritis after SL disruption is not completely known.

1.5.3 Clinical diagnosis

1.5.3.1 History

In acute traumatic SL injuries, patients can generally recall an inciting event prior to becoming symptomatic. Patients with SL ligament injury report a degree of pain, decreased ROM, and weakness in grip strength.

1.5.3.2 Physical exam

On physical exam, patients may present with dorsal wrist swelling and have localized pain over the dorsal wrist where the SL ligament is situated.

They may also have a positive Watson's test(64). The Watson scaphoid shift test is performed with the examiner applying pressure to the scaphoid tubercle. The examiner then uses his or her other hand to passively move from an ulnar deviated position into radial deviation with slight flexion. Constant pressure is applied to the scaphoid throughout. A positive test occurs when the scaphoid is unstable and subluxates dorsally. The patient typically experiences dorsal wrist pain and an audible 'clunk' may be appreciated. Importantly, a positive Watson's test occurs in 20% of the population normally so this should be tested bilaterally. In addition, the test is relatively insensitive in acute SL tears.

1.5.3.3 Investigations

Patients complaining of wrist pain are typically worked up with plain radiographs. However, diagnosis of SL ligament injury in the acute setting may be difficult as it often takes 3-12 months before signs of instability are visualized on XR (including PA, lateral, oblique and clenched-fist views in ulnar deviation) (65). The scapholunate angle is an important parameter to assess. It is measured between the longitudinal axis of the lunate and the volar aspect of the scaphoid. Normal scapholunate angle is between 30-60°(66). An angle between 61-80° should heighten clinical suspicion for osseous or ligamentous injury, while an angle >80° is certainly abnormal. Signs of instability include a scapholunate gap greater than 3mm (also known as the Terry Thomas sign) and an SL angle >60°. Formally, a DISI deformity is defined as having an SL angle >60°, and

capitolunate angle $>30^\circ$ on the lateral view. On the PA view, the ‘scaphoid ring sign’ may be visualized whereby the normal morphology of the scaphoid is lost and instead appears triangular in shape(67). It may be helpful to obtain bilateral wrist XRs for comparison.

MRI or MR arthrography (MRI with contrast injected into the joint) can also be useful in the diagnosis of SL ligament injury, although studies have shown that a negative result cannot rule out ligamentous injury with certainty(68). Signs of complete SL ligament disruption include increased signal intensity or complete absence of the ligament. Signs of partial injury include thinning, fraying or overall distortion in the ligament.

Due to the variability in radiographic findings with SL ligament injury, the gold standard method for diagnosis is wrist arthroscopy. Geissler et al. developed a classification system to stratify the degree of injury visualized on arthroscopy to direct treatment options(69).

1.5.4 Treatment

Garcia-Elias et al.(70) developed the following 5 questions to help guide treatment of SL tears:

1. Is the integrity of the dorsal SL ligament maintained?
2. What is the healing potential of disrupted ligaments?
3. Is scaphoid positioning normal?
4. Is carpal malalignment reducible?
5. Is cartilage present at the radiocarpal and midcarpal joints.

These questions provide important information. For example, direct ligamentous tears often heal poorly, whereas osseous avulsions are more likely to heal with direct fixation. Additionally, if scaphoid positioning is altered, this may suggest disruption of secondary scaphoid stabilizers including the STT, SC and volar STT capsule. Irreducible carpal malalignment may suggest that the deformity may not be correctable with a soft tissue procedure alone. And finally, the presence of cartilage at the radiocarpal and midcarpal joints are important when considering salvage procedures for wrist arthritis. Generally, treatment of SL ligament injury ranges on a spectrum including arthroscopic debridement, direct or arthroscopic ligament repair, capsulodesis, ligament reconstruction and salvage procedures(65).

1.6 CLINICAL DISORDERS OF THE WRIST:

SCAPHOLUNATE ADVANCED COLLAPSE

1.6.1 Epidemiology of scapholunate advanced collapse

Scapholunate advanced collapse (SLAC) is the most common pattern of wrist arthritis (71). A recent study characterized the sociodemographic features of patients with SLAC and noted the average age of onset was 53 years, 80% affected males, 69.5% had a previous history of trauma, and 49% of patients were physical laborers (60).

1.6.2 Pathophysiology of scapholunate advanced collapse

The scapholunate ligament functions as an important wrist stabilizer, particularly maintaining the scaphoid and lunate in the appropriate positions. As the SL is injured, the lunate shifts into an extended position while the scaphoid deviates into a flexed position. Eventually this leads to the characteristic dorsal intercalated segment instability (DISI) deformity(72), whereby the scapholunate angle increases to greater than 60°, and the radiolunate angle is greater than 15°. These changes in carpal bone position alter the force distribution across the midcarpal and radiocarpal joints. Arthritic changes begin at the radioscaphoid joint and progress ulnarly (71) (Table 1.6). As the distance between the proximal pole of the scaphoid and the lunate progressively increases, eventual capitate proximal migration occurs(59, 71). Classically, the radiolunate joint is spared from developing arthritis because the proximal side of the lunate and the radius remain concentric in a DISI deformity.

| Stage of SLAC | Radiographic findings |
|---------------|--|
| Stage I | Arthrosis to radial side of scaphoid and radial styloid |
| Stage II | Arthrosis of entire radioscaphoid joint |
| Stage III | Stage II + capitoulunate arthrosis |
| Stage IV | Pancarpal arthrosis (with preservation of radiolunate joint) |

Table 1.6. Watson & Ballet classification of scapholunate advanced collapse.

1.6.3 Clinical presentation of SLAC

Similar to those with SNAC, as patients progress to SLAC arthritis, they may complain of wrist pain and stiffness. Again, it is critical to differentiate other causes of arthritic pain (STT, 1st CMC OA), and soft tissue causes of radial-sided wrist pain (DeQuervain's tenosynovitis, carpal tunnel syndrome).

1.7 TREATMENT OF SCAPHOID NONUNION

ADVANCED COLLAPSE AND SCAPHOLUNATE

ADVANCED COLLAPSE

The primary goals of treatment in SLAC and SNAC arthritis include managing pain while optimizing wrist function (grip strength and ROM). A conservative approach should be used in early disease(73). Patients should be offered non-steroidal anti-inflammatory drugs (NSAIDs) with gastrointestinal prophylaxis, wrist immobilization with splinting, and some may benefit from corticosteroid injections.

Operative intervention is typically considered once conservative measures have failed, although there is no consensus on the timeframe that nonsurgical treatment should be trialed for before offering surgical options(73). Early surgical options include radial styloidectomy, wrist denervation (anterior interosseous nerve (AIN), posterior interosseous nerve (PIN), or combined neurectomies), and distal scaphoid pole excision. These procedures are only indicated in early disease with involvement of the scaphoid and distal radius. As the condition progresses to stage II/III disease, salvage procedures including scaphoidectomy and four corner fusion (4CF), proximal row carpectomy (PRC), total wrist arthrodesis or wrist arthroplasty may be offered. Typically, radiographic signs of advanced arthritis are associated with more severe symptoms, although occasionally pain symptoms do not correlate with the stage of disease.

1.7.1 Radial styloidectomy

Radial styloidectomy is recommended in patients with arthritis between the scaphoid and radial styloid, and consequently is only indicated in early symptomatic patients with stage I/II SLAC or stage I SNAC.

Three styloidectomy patterns have been described including horizontal, vertical, and short oblique. Although all three options involve partial disruption of the radiocarpal ligaments, the short oblique osteotomy removed the least amount of bone and preserved the most extrinsic wrist ligaments(74). Nakamura et al. recommends removing less than 3-4mm of the distal styloid with the short oblique osteotomy(75). Larger radial styloidectomies may disinsert the origin of the RSC ligament and result in ulnar translation of the carpus.

1.7.2 Wrist denervation

The terminal branches of the AIN and PIN innervate the wrist joint and are thought to contribute to proprioception and pain(76, 77). Wrist denervation involves neurectomy of terminal sensory fibers innervating the wrist capsule and may be performed in isolation or in combination with other procedures. Complete wrist denervation involves transection of all wrist articular branches, whereas partial denervation involves transection of the AIN or PIN in isolation.

Combined AIN and PIN neurectomy was first described by Berger through a single dorsal incision(78). The PIN lies over the interosseous membrane between extensor indicis proprius and extensor digitorum communis within the 4th extensor compartment. The AIN can then be identified after incising of the interosseous membrane between the radius and ulna. In a cadaveric study by Lin et al., the authors report that this approach risks damaging branches to pronator quadratus (PQ). Consequently, it is recommended that AIN neurectomy should be performed carefully at the distal border of PQ(79).

In a retrospective cohort study of 70 patients who underwent complete denervation with a mean follow-up of 9.6 years, 39 reported considerable improvement, 8 little improvement, 10 temporary improvement, 7 with no change, and 6 with worsened symptoms(80). The majority (48/70) of

patients reported they would repeat the procedure. Patients with SLAC/SNAC had lower Disabilities of the Arm, Shoulder, and Hand (DASH) scores.

Advantages to denervation techniques include pain relief without any major complications and are relatively simple procedures to perform. Patients do not need to be immobilized post-operatively and are still candidates for other operative interventions discussed.

1.7.3 Distal scaphoid excision

Distal scaphoid pole excision can be performed with or without radial styloidectomy. This procedure is indicated in early symptomatic patients with stage I SNAC (i.e. with preservation of the capitolunate joint). Notably, greater than 50% of the proximal scaphoid must remain *in situ* (i.e. scaphoid nonunion must occur at the distal waist or distal pole), to avoid destabilization of the wrist(81). Excision of the proximal scaphoid pole results in similar carpal destabilization as total scaphoidectomy due to the removal of proximal supports like the RSC (82).

Malerich et al. reported on outcomes of 19 patients with SNAC arthritis treated with distal scaphoid pole excision with mean follow-up of 49 months(81). Thirteen patients experienced complete pain resolution. One patient had persistent wrist pain after this procedure and elected to have a total wrist arthrodesis. The authors emphasize that capitolunate arthritis is a contraindication to this procedure, as this procedure only addresses arthritis between the scaphoid and radial styloid. They report that 2 of 4 patients with CL arthritis experienced persistent wrist pain, and 3 patients continued to have degenerative change.

More recently, Malerich et al. updated the outcomes of this same cohort, with a mean follow-up period of 15 years(83). Since then, one additional patient underwent proximal row carpectomy. Overall pre-operative motion arc was improved from 72° preoperatively to 139° at final follow up ($p<0.001$). Additionally, grip strength improved from 36% of the contralateral side preoperatively to 83% at the latest follow up ($p<0.001$). Midcarpal arthritis developed in 13 of 18 patients (1 patient deceased). Proximal radioscaphoid and radiolunate articulations were spared in all patients. The authors also comment that this procedure may be performed in patients with CL arthrosis

radiographically as additional patients who developed this finding since the last study remained asymptomatic.

1.7.4 Scaphoidectomy and four corner fusion

Scaphoidectomy and four corner fusion (4CF) is recommended for patients with arthritic involvement of the midcarpal joint. The scaphoid is excised during this operation to address the radial-sided wrist pain secondary to arthritis between the scaphoid and radial styloid. Contraindications for 4CF include radiolunate degeneration and ulnar carpal translation. It was first described by Watson and Ballet, whereby the scaphoid was excised and fusion performed between the capitate, lunate, hamate, and triquetrum using K-wires and a distal radius bone graft(71). In the original description, the excised scaphoid was replaced with a silicone implant, however, this practice has since been abandoned due to high rates of implant dislocation and particulate synovitis. Patients were immobilized and K-wires were removed at 6 weeks post-operatively.

Since then multiple methods of fixation have been tried including headless compression screws, circular plates, wires, and staples. A limited number of retrospective cohort studies and case series have compared the different methods of fixation in 4CF (**Table 1.7**). To date, no randomized control trials have been conducted comparing fixation techniques. Overall, it appears that complication rates and functional outcomes are similar between the different fixation methods, although a few studies noted higher rates of nonunion and impingement in staple and plate fixation (84-86).

Two biomechanical studies have been conducted to investigate the importance of correcting lunate extension (DISI) in 4CF. In a study by De Carli et al., they compared 3 positions of 4CF without scaphoidectomy with neutral (0°), extended (30°), and flexed (20°) capitollunate angles(87). They found that fusion in the flexed position resulted in significantly reduced wrist flexion and increased extension. Similarly, fusion in extension resulted in significantly reduced wrist extension and increased flexion. Additionally, there were no statistically significant differences in radial-ulnar deviation between the 3 conditions. In the second study by Dvinskikh et al., a biomechanical computational model was developed to compare 4CF with “scaphoidectomy” performed with the

same capitulum angles as noted above(88). They found that fusion with the lunate in flexion did not improve extension, but rather favoured ulnar deviation. Fusion with the lunate in extension restricted wrist motion, only allowing flexion and radial deviation.

While these studies emphasize the importance of correcting the DISI deformity when performing 4CF, the impact of altering the relationship between the proximal and distal rows in the coronal plane is poorly understood. Only one biomechanical study has been conducted comparing fusion in an anatomic position (with no alteration in position in a native wrist) and a radial-aligned position with alignment of the radial border of the capitate and lunate in the coronal plane(89). The major finding was that radial 4CF results in a radially-deviated resting wrist position and that radial deviation was greater in comparison to the native state and anatomic 4CF. This study was limited as the authors utilized a passive motion simulator, did not compare flexion-extension motion, and did not assess for multiplanar wrist motion.

Although 4CF is more technically demanding and time consuming compared to proximal row carpectomy (PRC), advantages include the preservation of the anatomic radiolunate joint and maintenance of carpal height(90). By maintaining carpal height, tendons maintain proper length and tension, reducing the risk of weakness and accounting for greater grip strength compared to PRC. Some disadvantages to 4CF include risk of nonunion, hardware complications, and the requirement for bone grafting (although cancellous bone from the excised scaphoid is often used).

| Author (Year) | Group 1 | | Group 2 | Conclusion |
|---------------------------------|---|------------------------|---------------------------------------|---|
| Vance (2005) (84) | 27 plate | | 31 traditional (wire/staple/screw) | <ul style="list-style-type: none"> - Plate has higher nonunion and impingement - ROM and GS similar |
| Backer (2007) (85) | 36 K-wire | | 18 spider plate | <ul style="list-style-type: none"> - Spider plate associated with more complications (nonunion, infection, hardware failure) |
| Rodgers (2008) (91) | 12 K-wire | | 12 circular plates | <ul style="list-style-type: none"> - Pain relief, GS, pinch and ROM similar - Similar complications |
| De Smet (2009) (92) | 11 circular plate | | 17 traditional (K-wire or screw) | <ul style="list-style-type: none"> - Similar pain, PRWE, DASH - Similar complications |
| Pauchard (2014) (86) | 31 plate | | 35 staples | <ul style="list-style-type: none"> - Similar ROM, GS, pain, disability - Staples had higher nonunion - Staples had higher dorsal impingement |
| Le Corre (2015) (93) | 37 shape memory quadripodal staples | | 15 dorsal locking circular plates | <ul style="list-style-type: none"> - Similar pain and ROM - Functional scores and patient satisfaction comparable |
| Hernekamp (2016) (94) | 11 locking plates | | 10 K-wire | <ul style="list-style-type: none"> - Similar active ROM, pain, functional scores - No implant complications noted |
| Erne (2019) (95) | 21 K-wire | 26 locking plate | 17 headless compression screw | <ul style="list-style-type: none"> - Similar complication rates and non-union rates - Screw fixation better wrist extension and DASH scores |

Table 1.7. Summary of studies comparing fixation methods in 4CF.

1.7.5 Proximal row carpectomy

Proximal row carpectomy was first described by Stamm and involves excision of the scaphoid, lunate, and triquetrum(96). Importantly, the radioscaphocapitate (RSC) ligament must be kept intact when performing this procedure to prevent ulnar translocation of the wrist.

Indications for PRC include stage II-III SLAC/SNAC arthritis with sparing of the capitulunate and radiolunate joints. The articular surfaces of the head of the capitate and the lunate facet must be intact as this procedure creates a new articulation between the capitate and distal radius.

Advantages to PRC include the lack of fixation and risk of nonunion, simplicity of the procedure, and some have argued for immediate post-operative mobilization(97). Although PRC reliably reduces pain and improves function, removal of the proximal carpal row significantly alters biomechanics of the wrist joint. The capitate head is incongruent with the lunate fossa(98), suggesting that this non-anatomic articulation may be a new source of late arthritis(99). Biomechanical studies have reported a decreased contact area and increased pressure between the capitate and radius after PRC(100, 101). Consequently, this procedure may be more suitable for older patients (>40 years old) who are low demand. Additionally, the reduction in carpal height reduces tension on muscles and tendons, perhaps accounting for reduced ROM and grip strength.

1.7.6 Total wrist arthrodesis

Total wrist arthrodesis is a dependable method of treating wrist pain but comes with the cost of eliminating all wrist motion. It was first described by Ely in the 1900s(102). It is critical to rule out any distal radioulnar joint (DRUJ) arthritis or ulnocarpal impaction prior to performing total wrist fusions as the procedure is ineffective at addressing pain arising from alternate etiologies.

The most common method of performing total wrist arthrodesis is with dorsal plate fixation with the wrist in 10-15° of extension. Union rates ranging from 93-100% have been reported when autologous bone grafting is performed in conjunction with dorsal plating(103, 104). Other techniques include intramedullary fixation, screw fixation, and pinning(105).

Total wrist fusion is preferred in patients who are heavy labourers as they likely cannot comply with the activity restrictions associated with arthroplasty or partial wrist fusion procedures.

Disadvantages to total wrist arthrodesis include elimination of motion at the radiocarpal and midcarpal joints. Patients who undergo total wrist fusion express the following concerns: 80% report difficulty with personal hygiene, 50% have trouble pushing open a heavy door, and 70% of patients “feel less capable”(106).

Complications with total wrist fusion are mainly secondary to hardware (such as prominence and hardware failure necessitating removal), but also include delayed union, nonunion, and impingement(105). Overall, complication rates are fewer than with total wrist arthroplasty(105).

1.7.7 Total wrist arthroplasty

Total wrist arthroplasty (TWA) was first introduced by Themistocles Gluck in 1890 using an ivory ball-and-socket type implant(107, 108). This was followed by Swanson who developed the first silicone implant for the radiocarpal joint in 1967(109). Short-term data suggested that patients experienced good pain relief after surgery(105). However, long term data has identified complications such as reactive synovitis, secondary osteolysis and implant failure. Since then multiple generations of implants have been manufactured(105, 110-112).

This procedure is typically reserved for low demand individuals with pancarpal arthritis who agree to comply with strict activity restrictions including avoidance of loading the wrist and lifting objects heavier than 10 lb(113).

According to a systematic review comparing outcomes of TWA to total wrist fusion, complication rates were higher in the arthroplasty group although this difference was not statistically significant(105). Complications included prominent hardware (2.3%), hardware removal (6.1%), carpal and metacarpal osteolysis (3.7%), and implant dislocation. Implant revision rates ranged from 3.5-52.6% and conversion to fusion ranged from 0-42.1%.

1.8 FOUR CORNER FUSION VERSUS PROXIMAL ROW CARPECTOMY

There is ongoing debate regarding which motion-sparing salvage procedure is better in terms of wrist ROM, grip strength, and patient-reported outcomes.

1.8.1 Clinical outcomes of 4CF versus PRC

In one of the largest case series reporting on outcomes of scaphoidectomy and 4CF published by Ashmead et al.(114), wrist flexion-extension was reduced to 53% of the contralateral side (average arc 72°), wrist radial-ulnar deviation was reduced to 59% of the contralateral side (average arc 37°) and patients were left with an average of 80% grip strength of the contralateral side. Patients were followed on average for 4-years, and 91% of cases experienced significant improvement in pain symptoms. This group experienced a 13% revision rate secondary to dorsal impingement between the capitate and the radius, supporting the importance of coaxial alignment of the capitate and lunate. They also reported a 3% non-union rate, and 2% of patients experienced degeneration of the radiolunate joint associated with ulnar translation of the carpus.

Two systematic reviews have been conducted comparing outcomes of scaphoidectomy and 4CF versus PRC. In a systematic review and meta-analysis by Mulford et al. (115), they reported a weighted average grip strength of 70% of contralateral (33kg) for PRC and 75% of contralateral (31kg) for scaphoidectomy and 4CF. The weighted average of post-operative flexion, extension, radial and ulnar deviation were: 38°, 41°, 17°, 22° for PRC and 33°, 33°, 19° and 30° for 4CF. Meta-analysis was performed comparing secondary conversion to fusion and was similar between groups (relative risk 1.02), while post-operative osteoarthritis was significantly higher in PRC (relative risk 4.35). They conclude that PRC may provide more motion and be associated with a lower risk complication profile (i.e. no risk of bony complications, hardware complications), although patients are at risk for developing osteoarthritis later.

In Saltzman et al.'s(116) systematic review, they found that the percentage change in flexion, extension, radial and ulnar deviation from pre- to post-op were: -14%, +1%, -20%, -4.8% for PRC

and -13%, +1%, +55%, +1% for 4CF. Grip strength was relatively improved from pre-op, but compared to the contralateral unaffected side were $67\pm 16\%$ (PRC) and $74\pm 13\%$ (4CF) ($p<0.05$). Overall complication rate was 29% in 4CF compared to 14% in PRC ($p=0.01$). They concluded that absolute flexion and extension after PRC are greater, while radial deviation was higher in 4CF.

Additionally, two prospective randomized control trials (RCT) have compared outcomes of 4CF vs. PRC. In an earlier study by Bisneto et al.(117), 23 patients with grade I/II SLAC or SNAC were randomized to undergo 4CF or PRC. Three patients were lost to follow up and excluded from analysis. They found that grip strength of the operated wrist was consistently reduced compared to the contralateral side across all time points (preoperative, 3 months, 6 months, 12 months), and cited a 53% reduction in PRC and 27% reduction in 4CF ($p<0.05$). Overall, ROM was higher in PRC ($p<0.05$), except in radial deviation which was higher in 4CF ($p<0.05$). Consistent with the literature, both groups experienced an improvement in pain scales and DASH scores. Notably, the authors failed to describe the operative technique (so it is unclear if 4CF was performed with scaphoidectomy), and to indicate the number of participants within each group, follow up period, and method of fixation in 4CF.

Later, Aita et al. (118) performed a small RCT comparing outcomes of these two procedures in patients with stage II SNAC. Thirteen patients underwent PRC and 14 underwent scaphoidectomy and 4CF. Proximal row carpectomy was performed concurrently with radial styloidectomy and 4CF fixation was achieved with a special plate (blocked carpal button). Patients were followed for an average of 74 months. They noted that ROM in PRC was 69% and grip strength was 79% of the contralateral unaffected side, while the ROM in 4CF was lower at 58% and grip strength at 65%. Complications rates were similar at 7.7% (PRC) and 7.1% (4CF). One patient from the PRC group experienced radiocarpal arthritis within 1 year post-operatively and underwent a total wrist arthrodesis. One patient from the 4CF group experienced hardware complications but declined revision surgery. Pre- and post-operative pain, DASH scores, strength and ROM measurements were similar between groups.

In 2017, Brinkhorst et al.(119) compared ADLs using the modified timed Sollerman hand function test (120) in 48 patients who have been followed for greater than 6 months after 4CF and PRC (24

in each group). The original Sollerman hand function test consisted of 20 ADLs using 7 of 8 handgrips (121). Results were normalized to the contralateral, unaffected limb. They found that patients took longer to complete the tasks after 4CF compared to PRC (241 seconds vs. 221 seconds). Patients in the PRC group were also faster in tasks associated with better pulp pinch, transverse volar grip, combination pulp and lateral pinch, combination tripod and five-finger pinch, combination tripod pinch and diagonal volar grip. Patients in the 4CF group were only faster in one task, corresponding to better spherical volar grip (i.e. unscrewing lids). Additionally, patient reported outcomes were reported using the Michigan Hand Questionnaire, and the PRC group reported higher function with better ADL function, less pain, and higher satisfaction.

1.8.2 Cost-analysis of 4CF versus PRC

Kazmers et al. conducted a comparison of direct surgical costs between 4CF and PRC(122). They identified 19 patients who underwent 4CF and 23 who underwent PRC over a 6-year period at a single tertiary care centre in the United States. They found the cost of 4CF was 425% higher than PRC, with longer operative time (121 vs. 57 minutes) and equipment expenses (10-fold). The majority of the cost (55%) was attributed to hardware expenses. They also report that plating and staple fixation were more costly than compression screws (by 70% and 240%, respectively). They did not include costs associated with any post-operative complications. Additionally, costs were normalized with individual cost over the average cost.

Although this study may have limited generalizability to other centres, as surgical costs and equipment expenses are typically priced according to agreements between institutions and suppliers, similar principles apply worldwide; scaphoidectomy and four corner fusion has the additional cost of hardware, and operations are longer compared to PRC.

1.9 RATIONALE FOR THESIS

The goal of the two main salvage procedures, 4CF and PRC, in wrist arthritis is to reduce pain while preserving some wrist motion. Many studies have reported patient outcomes in terms of ROM, grip strength, and pain relief(115, 116). Currently there is a lack of consensus as to which of the two procedures is clinically superior. There are limited biomechanical studies comparing these procedures or evaluating alterations in their surgical technique to improve outcomes. Further, the studies that have been done are limited since they use passive motion simulators and only report on either uniplanar or multiplanar wrist motion(87-89).

There is ongoing debate regarding the optimal position of fusion in scaphoidectomy and 4CF. The importance of maintaining linear alignment of the capitate and lunate in the sagittal plane to correct the DISI deformity is well-established (87, 88). However, the significance of altering the capitulunate relationship in the coronal plane in 4CF is not clear. Some surgeons routinely perform scaphoidectomy and 4CF in a radial-aligned position(95, 123-130), while others tend to fuse in an anatomic position(131-134).

1.9.1 Objective

The primary objectives of this work are:

1. To understand and characterize how anatomic 4CF and radial 4CF influence uniplanar wrist motion (flexion-extension, radial-ulnar deviation) and multiplanar motion (circumduction).
2. To understand and characterize how anatomic 4CF and PRC compare in uniplanar wrist motion (flexion-extension, radial-ulnar deviation) and multiplanar motion (circumduction).

1.9.2 Hypothesis

The following hypotheses have been generated:

1. Anatomic and radial-aligned positions of 4CF will result in similar reductions in wrist flexion and extension,
2. The radial-aligned fusion position will result in increased ulnar deviation compared to anatomic fusion,
3. Anatomic and radial-aligned positions of 4CF will result in reduced circumduction motion compared to native state.
4. PRC and 4CF will result in similar reductions in wrist flexion and extension,
5. PRC will result in reduced radial deviation compared to 4CF,
6. PRC will result in a greater circumduction area than 4CF.

1.9.3 Thesis overview

Chapter 2: This study compares wrist kinematics for scaphoidectomy and 4CF in two fusion positions (anatomic and radial-aligned in the coronal plane) using a cadaveric biomechanical model.

Chapter 3: This study compares wrist kinematics for scaphoidectomy and anatomic 4CF, and PRC using a cadaveric biomechanical model.

Chapter 4: This chapter includes a summary of the work completed, discussion, and possible future studies.

References

1. Berger R, Garcia-Elias M. General anatomy of the wrist. New York: Springer; 1991.
2. Cooney W, 0.0px ppmppp, Helvetica} fp. The Wrist: Diagnosis and Operative Treatment. 2 ed: Lippincott Williams & Wilkins; 2010.
3. Gray H. Anatomy of the human body. Philidelphia: Lea & Febiger; 1918.
4. Hirt B, Seyhan H, Wagner M, Zumhasch R. Hand and wrist anatomy and biomechanics: a comprehensive guide: Thieme; 2016.
5. Berger RA. The anatomy and basic biomechanics of the wrist joint. J Hand Ther. 1996;9(2):84-93.
6. Lichtman D. The wrist and its disorders. Philidelphia: Saunders; 1988.
7. Watson H, Ottoni L, Pitts EC, Handal AG. Rotary subluxation of the scaphoid: a spectrum of instability. J Hand Surg Br. 1993;18(1):62-4.
8. Taleisnik J. The ligaments of the wrist. J Hand Surg Am. 1976;1(2):110-8.
9. Berger RA, Kauer JM, Landsmeer JM. Radioscapholunate ligament: a gross anatomic and histologic study of fetal and adult wrists. J Hand Surg Am. 1991;16(2):350-5.
10. Bajuri M, Kadir M. Computational biomechanics of the wrist joint. 1 ed: Springer-Verlag Berlin Heidelberg; 2012.
11. Wu G, van der Helm FC, Veeger HE, Makhsous M, Van Roy P, Anglin C, et al. ISB recommendation on definitions of joint coordinate systems of various joints for the reporting of human joint motion--Part II: shoulder, elbow, wrist and hand. J Biomech. 2005;38(5):981-92.
12. Hardy DC, Totty WG, Reinus WR, Gilula LA. Posteroanterior wrist radiography: importance of arm positioning. J Hand Surg Am. 1987;12(4):504-8.
13. Palmer AK, Werner FW, Murphy D, Glisson R. Functional wrist motion: a biomechanical study. J Hand Surg Am. 1985;10(1):39-46.
14. Ryu JY, Cooney WP, Askew LJ, An KN, Chao EY. Functional ranges of motion of the wrist joint. J Hand Surg Am. 1991;16(3):409-19.
15. Li ZM, Kuxhaus L, Fisk JA, Christophel TH. Coupling between wrist flexion-extension and radial-ulnar deviation. Clin Biomech (Bristol, Avon). 2005;20(2):177-83.
16. Crisco JJ, Heard WM, Rich RR, Paller DJ, Wolfe SW. The mechanical axes of the wrist are oriented obliquely to the anatomical axes. J Bone Joint Surg Am. 2011;93(2):169-77.

17. Bryce TH. Certain Points in the Anatomy and Mechanism of the Wrist-Joint Reviewed in the Light of a Series of Röntgen Ray Photographs of the Living Hand. *J Anat Physiol.* 1896;31(Pt 1):59-79.
18. Navarro A. Anatomy and physiology of the carpus Imprenta Artist Dornaleche Hnos. 1935:166-89.
19. Gilford W, Boltan R, Lambrinudi C. The mechanism of the wrist joint with special reference to fractures of the scaphoid. *Guy Hospital Rep.* 1943;92:52-9.
20. Stoesser H, Padmore CE, Nishiwaki M, Gammon B, Langohr GDG, Johnson JA. Biomechanical Evaluation of Carpal Kinematics during Simulated Wrist Motion. *J Wrist Surg.* 2017;6(2):113-9.
21. Werner FW, Palmer AK, Somerset JH, Tong JJ, Gillison DB, Fortino MD, et al. Wrist joint motion simulator. *J Orthop Res.* 1996;14(4):639-46.
22. Dunning CE, Lindsay CS, Bicknell RT, Patterson SD, Johnson JA, King GJ. Supplemental pinning improves the stability of external fixation in distal radius fractures during simulated finger and forearm motion. *J Hand Surg Am.* 1999;24(5):992-1000.
23. Igleisias D. Development of an in-vitro passive and active motion simulator for the investigation of wrist function and kinematics. London, Ontario: University of Western Ontario; 2016.
24. Patterson RM, Williams L, Andersen CR, Koh S, Viegas SF. Carpal kinematics during simulated active and passive motion of the wrist. *J Hand Surg Am.* 2007;32(7):1013-9.
25. Leslie IJ, Dickson RA. The fractured carpal scaphoid. Natural history and factors influencing outcome. *J Bone Joint Surg Br.* 1981;63-B(2):225-30.
26. Elzinga K, Chung K. The University of Michigan's Upper Extremity Fracture Surgery. In: Chung K, Lawton J, editors.: Lippincott Williams & Wilkins; 2019.
27. Gelberman RH, MJ. B. Vascularity of the carpus. . *The Wrist and its Disorders.* 21988. p. 34-47.
28. Oblatz BE, BM H. Nonunion of fractures of the carpal navicular. *Journal of Bone and Joint Surgery.* 1938;20A:424-8.
29. Herbert T, Fisher W. Management of the fractured scaphoid using a new bone screw. *Journal of Bone and Joint Surgery Britain.* 1984;66(1):114-23.

30. Cooney WP, Dobyns JH, Linscheid RL. Fractures of the scaphoid: a rational approach to management. *Clin Orthop Relat Res.* 1980(149):90-7.
31. Russe O. Fracture of the carpal navicular. Diagnosis, non-operative treatment, and operative treatment. *J Bone Joint Surg Am.* 1960;42-A:759-68.
32. Duckworth AD, Jenkins PJ, Aitken SA, Clement ND, Court-Brown CM, McQueen MM. Scaphoid fracture epidemiology. *J Trauma Acute Care Surg.* 2012;72(2):E41-5.
33. Van Tassel DC, Owens BD, Wolf JM. Incidence estimates and demographics of scaphoid fracture in the U.S. population. *J Hand Surg Am.* 2010;35(8):1242-5.
34. Brøndum V, Larsen CF, Skov O. Fracture of the carpal scaphoid: frequency and distribution in a well-defined population. *Eur J Radiol.* 1992;15(2):118-22.
35. Freeland P. Scaphoid tubercle tenderness: a better indicator of scaphoid fractures? *Arch Emerg Med.* 1989;6(1):46-50.
36. Parvizi J, Wayman J, Kelly P, Moran CG. Combining the clinical signs improves diagnosis of scaphoid fractures. A prospective study with follow-up. *J Hand Surg Br.* 1998;23(3):324-7.
37. Bergh TH, Lindau T, Soldal LA, Bernardshaw SV, Behzadi M, Steen K, et al. Clinical scaphoid score (CSS) to identify scaphoid fracture with MRI in patients with normal x-ray after a wrist trauma. *Emerg Med J.* 2014;31(8):659-64.
38. Adams JE, Steinmann SP. Acute scaphoid fractures. *Orthop Clin North Am.* 2007;38(2):229-35, vi.
39. Young MR. Clinical carpal scaphoid injuries. *Br Med J (Clin Res Ed).* 1988;296(6639):1799-800.
40. Rolfe EB, Garvie NW, Khan MA, Ackery DM. Isotope bone imaging in suspected scaphoid trauma. *Br J Radiol.* 1981;54(645):762-7.
41. Temple CL, Ross DC, Bennett JD, Garvin GJ, King GJ, Faber KJ. Comparison of sagittal computed tomography and plain film radiography in a scaphoid fracture model. *J Hand Surg Am.* 2005;30(3):534-42.
42. Bain GI, Bennett JD, Richards RS, Slethaug GP, Roth JH. Longitudinal computed tomography of the scaphoid: a new technique. *Skeletal Radiol.* 1995;24(4):271-3.
43. Hunter JC, Escobedo EM, Wilson AJ, Hanel DP, Zink-Brody GC, Mann FA. MR imaging of clinically suspected scaphoid fractures. *AJR Am J Roentgenol.* 1997;168(5):1287-93.

44. Gaebler C, Kukla C, Breitenseher M, Trattnig S, Mittlboeck M, Vécsei V. Magnetic resonance imaging of occult scaphoid fractures. *J Trauma*. 1996;41(1):73-6.
45. Smith M, Bain GI, Turner PC, Watts AC. Review of imaging of scaphoid fractures. *ANZ J Surg*. 2010;80(1-2):82-90.
46. Cerezal L, Abascal F, Canga A, García-Valtuille R, Bustamante M, del Piñal F. Usefulness of gadolinium-enhanced MR imaging in the evaluation of the vascularity of scaphoid nonunions. *AJR Am J Roentgenol*. 2000;174(1):141-9.
47. Clay NR, Dias JJ, Costigan PS, Gregg PJ, Barton NJ. Need the thumb be immobilised in scaphoid fractures? A randomised prospective trial. *J Bone Joint Surg Br*. 1991;73(5):828-32.
48. Buijze GA, Goslings JC, Rhemrev SJ, Weening AA, Van Dijkman B, Doornberg JN, et al. Cast immobilization with and without immobilization of the thumb for nondisplaced and minimally displaced scaphoid waist fractures: a multicenter, randomized, controlled trial. *J Hand Surg Am*. 2014;39(4):621-7.
49. Grewal R, Suh N, Macdermid JC. Use of computed tomography to predict union and time to union in acute scaphoid fractures treated nonoperatively. *J Hand Surg Am*. 2013;38(5):872-7.
50. Tait MA, Bracey JW, Gaston RG. Acute Scaphoid Fractures: A Critical Analysis Review. *JBJS Rev*. 2016;4(9).
51. Simonian PT, Trumble TE. Scaphoid Nonunion. *J Am Acad Orthop Surg*. 1994;2(4):185-91.
52. Swärd EM, Schriever TU, Franko MA, Björkman AC, Wilcke MK. The epidemiology of scaphoid fractures in Sweden: a nationwide registry study. *J Hand Surg Eur Vol*. 2019;44(7):697-701.
53. Osterman AL, Mikulics M. Scaphoid nonunion. *Hand Clin*. 1988;4(3):437-55.
54. Weber ER. Biomechanical implications of scaphoid waist fractures. *Clin Orthop Relat Res*. 1980(149):83-9.
55. Vender MI, Watson HK, Wiener BD, Black DM. Degenerative change in symptomatic scaphoid nonunion. *J Hand Surg Am*. 1987;12(4):514-9.
56. Hammert WC, Bozentka DJ, Boyer MI. *ASSH Manual of Hand Surgery*: Wolters Kluwer Health/Lippincott Williams & Wilkins; 2010.
57. Ruby LK, Stinson J, Belsky MR. The natural history of scaphoid non-union. A review of fifty-five cases. *J Bone Joint Surg Am*. 1985;67(3):428-32.

58. Sokolow C, Saffar P. Anatomy and histology of the scapholunate ligament. *Hand Clin.* 2001;17(1):77-81.
59. Watson HK, Ryu J. Evolution of arthritis of the wrist. *Clin Orthop Relat Res.* 1986(202):57-67.
60. Murphy BD, Nagarajan M, Novak CB, Roy M, McCabe SJ. The Epidemiology of Scapholunate Advanced Collapse. *Hand (N Y).* 2018;1558944718788672.
61. Doherty W, Lovallo JL. Scapholunate advanced collapse pattern of arthritis in calcium pyrophosphate deposition disease of the wrist. *J Hand Surg Am.* 1993;18(6):1095-8.
62. Stäbler A, Heuck A, Reiser M. Imaging of the hand: degeneration, impingement and overuse. *Eur J Radiol.* 1997;25(2):118-28.
63. Adolfsson L, Povlsen B. Arthroscopic findings in wrists with severe post-traumatic pain despite normal standard radiographs. *J Hand Surg Br.* 2004;29(3):208-13.
64. M G-E. Carpal Instability. In: Livingstone EC, editor. *Green's operative hand surgery.* 1. 6 ed. New York 2011. p. 465-522.
65. Pappou IP, Basel J, Deal DN. Scapholunate ligament injuries: a review of current concepts. *Hand (N Y).* 2013;8(2):146-56.
66. Smith DK, Gilula LA, Amadio PC. Dorsal lunate tilt (DISI configuration): sign of scaphoid fracture displacement. *Radiology.* 1990;176(2):497-9.
67. Cautilli GP, Wehbé MA. Scapho-lunate distance and cortical ring sign. *J Hand Surg Am.* 1991;16(3):501-3.
68. Andersson JK, Andernord D, Karlsson J, Fridén J. Efficacy of Magnetic Resonance Imaging and Clinical Tests in Diagnostics of Wrist Ligament Injuries: A Systematic Review. *Arthroscopy.* 2015;31(10):2014-20.e2.
69. Geissler WB. Arthroscopic management of scapholunate instability. *J Wrist Surg.* 2013;2(2):129-35.
70. Garcia-Elias M, Lluch AL, Stanley JK. Three-ligament tenodesis for the treatment of scapholunate dissociation: indications and surgical technique. *J Hand Surg Am.* 2006;31(1):125-34.
71. Watson HK, Ballet FL. The SLAC wrist: scapholunate advanced collapse pattern of degenerative arthritis. *J Hand Surg Am.* 1984;9(3):358-65.

72. Linscheid RL, Dobyns JH, Beabout JW, Bryan RS. Traumatic instability of the wrist. Diagnosis, classification, and pathomechanics. *J Bone Joint Surg Am.* 1972;54(8):1612-32.
73. McCarthy C. Scaphoid nonunion advanced collapse: A review. *Medical Research Archives.* 2015.
74. Siegel DB, Gelberman RH. Radial styloidectomy: an anatomical study with special reference to radiocarpal intracapsular ligamentous morphology. *J Hand Surg Am.* 1991;16(1):40-4.
75. Nakamura T, Cooney WP, Lui WH, Haugstvedt JR, Zhao KD, Berglund L, et al. Radial styloidectomy: a biomechanical study on stability of the wrist joint. *J Hand Surg Am.* 2001;26(1):85-93.
76. Dellon AL, Mackinnon SE, . DA. Terminal branch of anterior interosseous nerve as source of wrist pain. *Journal of Hand Surgery (British).* 1984;9(3):316-22.
77. Dellon AL, Seif SS. Anatomic dissections relating the posterior interosseous nerve to the carpus, and the etiology of dorsal wrist ganglion pain. *J Hand Surg Am.* 1978;3(4):326-32.
78. Berger RA. Partial denervation of the wrist: a new approach. *Tech Hand Up Extrem Surg.* 1998;2(1):25-35.
79. Lin DL, Lenhart MK, Farber GL. Anatomy of the anterior interosseous innervation of the pronator quadratus: evaluation of structures at risk in the single dorsal incision wrist denervation technique. *J Hand Surg Am.* 2006;31(6):904-7.
80. Schweizer A, von Känel O, Kammer E, Meuli-Simmen C. Long-term follow-up evaluation of denervation of the wrist. *J Hand Surg Am.* 2006;31(4):559-64.
81. Malerich MM, Clifford J, Eaton B, Eaton R, Littler JW. Distal scaphoid resection arthroplasty for the treatment of degenerative arthritis secondary to scaphoid nonunion. *J Hand Surg Am.* 1999;24(6):1196-205.
82. Garcia-Elias M, Lluch A. Partial excision of scaphoid: is it ever indicated? *Hand Clin.* 2001;17(4):687-95, x.
83. Malerich MM, Catalano LW, Weidner ZD, Vance MC, Eden CM, Eaton RG. Distal scaphoid resection for degenerative arthritis secondary to scaphoid nonunion: a 20-year experience. *J Hand Surg Am.* 2014;39(9):1669-76.

84. Vance MC, Hernandez JD, Didonna ML, Stern PJ. Complications and outcome of four-corner arthrodesis: circular plate fixation versus traditional techniques. *J Hand Surg Am.* 2005;30(6):1122-7.
85. Backer K, Englert A, Lukas B. Results of four-corner-fusion – spider plate fixation compared with k-wires. *J Hand Surg Eur Vol.* 2007;32(Supplement 1):71.
86. Pauchard N, Lecoanet-Strugarek C, Segret J, De Gasperi M, Dap F, Dautel G. Dorsal locking plates versus staples in four-corner fusion: a comparative clinical and radiological study. *Orthop Traumatol Surg Res.* 2014;100(6):593-7.
87. De Carli P, Donndorff AG, Alfie VA, Boretto JG, López Ovenza JM, Gallucci GL. Four-corner arthrodesis: influence of the position of the lunate on postoperative wrist motion: a cadaveric study. *J Hand Surg Am.* 2007;32(9):1356-62.
88. Dvinskikh NA, Blankevoort L, Strackee SD, Grimbergen CA, Streekstra GJ. The effect of lunate position on range of motion after a four-corner arthrodesis: a biomechanical simulation study. *J Biomech.* 2011;44(7):1387-92.
89. Hernandez-Soria A, Das De S, Model Z, Lee SK, Wolfe SW. The Effect of Capitate Position on Coronal Plane Wrist Motion After Simulated 4-Corner Arthrodesis. *J Hand Surg Am.* 2016;41(11):1049-55.
90. Debottis DP, Werner FW, Sutton LG, Harley BJ. 4-corner arthrodesis and proximal row carpectomy: a biomechanical comparison of wrist motion and tendon forces. *J Hand Surg Am.* 2013;38(5):893-8.
91. Rodgers JA, Holt G, Finnerty EP, Miller B. Scaphoid excision and limited wrist fusion: a comparison of K-wire and circular plate fixation. *Hand (N Y).* 2008;3(3):276-81.
92. De Smet L, Deprez P, Duerinckx J, Degreef I. Outcome of four-corner arthrodesis for advanced carpal collapse: circular plate versus traditional techniques. *Acta Orthop Belg.* 2009;75(3):323-7.
93. Le Corre A, Ardouin L, Loubersac T, Gaisne E, Bellemère P. Retrospective study of two fixation methods for 4-corner fusion: Shape-memory staple vs. dorsal circular plate. *Chir Main.* 2015;34(6):300-6.
94. Hernekamp JF, Reinecke A, Neubrech F, Bickert B, Kneser U, Kremer T. Four-corner fusion: comparison of patient satisfaction and functional outcome of conventional K-wire technique vs. a new locking plate. *Arch Orthop Trauma Surg.* 2016;136(4):571-8.

95. Erne HC, Broer PN, Weiss F, Loew S, Cerny MK, Schmauss D, et al. Four-corner fusion: Comparing outcomes of conventional K-wire-, locking plate-, and retrograde headless compression screw fixations. *J Plast Reconstr Aesthet Surg.* 2019;72(6):909-17.
96. Stamm TT. Excision of the Proximal Row of the Carpus. *Proc R Soc Med.* 1944;38(2):74-5.
97. Jacobs R, Degreef I, De Smet L. Proximal row carpectomy with or without postoperative immobilisation. *J Hand Surg Eur Vol.* 2008;33(6):768-70.
98. Hawkins-Rivers S, Budoff JE, Ismaily SK, Noble PC, Haddad J. MRI study of the capitate, lunate, and lunate fossa with relevance to proximal row carpectomy. *J Hand Surg Am.* 2008;33(6):841-9.
99. Chim H, Moran SL. Long-term outcomes of proximal row carpectomy: a systematic review of the literature. *J Wrist Surg.* 2012;1(2):141-8.
100. Zhu YL, Xu YQ, Ding J, Li J, Chen B, Ouyang YF. Biomechanics of the wrist after proximal row carpectomy in cadavers. *J Hand Surg Eur Vol.* 2010;35(1):43-5.
101. Tang P, Gauvin J, Muriuki M, Pfaeffle JH, Imbriglia JE, Goitz RJ. Comparison of the "contact biomechanics" of the intact and proximal row carpectomy wrist. *J Hand Surg Am.* 2009;34(4):660-70.
102. LW E. An operation for tuberculosis of the wrist. *J Am Med Assoc.* 1920;75:1707-9.
103. Wright CS, McMurtry RY. AO arthrodesis in the hand. *J Hand Surg Am.* 1983;8(6):932-5.
104. Weiss AP, Hastings H. Wrist arthrodesis for traumatic conditions: a study of plate and local bone graft application. *J Hand Surg Am.* 1995;20(1):50-6.
105. Berber O, Garagnani L, Gidwani S. Systematic Review of Total Wrist Arthroplasty and Arthrodesis in Wrist Arthritis. *J Wrist Surg.* 2018;7(5):424-40.
106. Sauerbier M , Kluge S , Bickert B , G G. Subjective and objective outcomes after total wrist arthrodesis in patients with radiocarpal arthrosis or Kienböck's disease . *Chirurgie de la Main.* 2000;19(4):223-31.
107. Ritt MJ, Stuart PR, Naggar L, Beckenbaugh RD. The early history of arthroplasty of the wrist. From amputation to total wrist implant. *J Hand Surg Br.* 1994;19(6):778-82.
108. Carlson JR, Simmons BP. Total Wrist Arthroplasty. *JAAOS - Journal of the American Academy of Orthopaedic Surgeons.* 1998;6(5):308-15.

109. Swanson AB, de Groot Swanson G, Maupin BK. Flexible implant arthroplasty of the radiocarpal joint. Surgical technique and long-term study. *Clin Orthop Relat Res.* 1984(187):94-106.
110. Meuli HC. Meuli total wrist arthroplasty. *Clin Orthop Relat Res.* 1984(187):107-11.
111. Volz RG. Total wrist arthroplasty. A clinical review. *Clin Orthop Relat Res.* 1984(187):112-20.
112. Figgie HE, Ranawat CS, Inglis AE, Straub LR, Mow C. Preliminary results of total wrist arthroplasty in rheumatoid arthritis using the Trispherical total wrist arthroplasty. *J Arthroplasty.* 1988;3(1):9-15.
113. Anderson MC, Adams BD. Total wrist arthroplasty. *Hand Clin.* 2005;21(4):621-30.
114. Ashmead D, Watson HK, Damon C, Herber S, Paly W. Scapholunate advanced collapse wrist salvage. *J Hand Surg Am.* 1994;19(5):741-50.
115. Mulford JS, Ceulemans LJ, Nam D, Axelrod TS. Proximal row carpectomy vs four corner fusion for scapholunate (Slac) or scaphoid nonunion advanced collapse (Snac) wrists: a systematic review of outcomes. *J Hand Surg Eur Vol.* 2009;34(2):256-63.
116. Saltzman BM, Frank JM, Slikker W, Fernandez JJ, Cohen MS, Wysocki RW. Clinical outcomes of proximal row carpectomy versus four-corner arthrodesis for post-traumatic wrist arthropathy: a systematic review. *J Hand Surg Eur Vol.* 2015;40(5):450-7.
117. Bisneto EN, Freitas MC, Paula EJ, Mattar R, Zumiotti AV. Comparison between proximal row carpectomy and four-corner fusion for treating osteoarthritis following carpal trauma: a prospective randomized study. *Clinics (Sao Paulo).* 2011;66(1):51-5.
118. Aita MA, Nakano EK, Schaffhausser HL, Fukushima WY, Fujiki EN. Randomized clinical trial between proximal row carpectomy and the four-corner fusion for patients with stage II SNAC. *Rev Bras Ortop.* 2016;51(5):574-82.
119. Brinkhorst ME, Singh HP, Dias JJ, Feitz R, Hovius SER. Comparison of activities of daily living after proximal row carpectomy or wrist four-corner fusion. *J Hand Surg Eur Vol.* 2017;42(1):57-62.
120. Singh HP, Dias JJ, Thompson JR. Timed Sollerman hand function test for analysis of hand function in normal volunteers. *J Hand Surg Eur Vol.* 2015;40(3):298-309.
121. Sollerman C, Ejeskär A. Sollerman hand function test. A standardised method and its use in tetraplegic patients. *Scand J Plast Reconstr Surg Hand Surg.* 1995;29(2):167-76.

122. Kazmers NH, Stephens AR, Presson AP, Xu Y, Feller RJ, Tyser AR. Comparison of Direct Surgical Costs for Proximal Row Carpectomy and Four-Corner Arthrodesis. *J Wrist Surg.* 2019;8(1):66-71.
123. Bain GI, Watts AC. The outcome of scaphoid excision and four-corner arthrodesis for advanced carpal collapse at a minimum of ten years. *J Hand Surg Am.* 2010;35(5):719-25.
124. Ball B, Bergman JW. Scaphoid excision and 4-corner fusion using retrograde headless compression screws. *Tech Hand Up Extrem Surg.* 2012;16(4):204-9.
125. Cha SM, Shin HD, Kim KC. Clinical and radiological outcomes of scaphoidectomy and 4-corner fusion in scapholunate advanced collapse at 5 and 10 years. *Ann Plast Surg.* 2013;71(2):166-9.
126. Stanley J. Arthroplasty and arthrodesis of the wrist. *Green's Operative Hand Surgery.* 6 ed. Philadelphia: Elsevier; 2010. p. 429-63.
127. Dacho AK, Baumeister S, Germann G, Sauerbier M. Comparison of proximal row carpectomy and midcarpal arthrodesis for the treatment of scaphoid nonunion advanced collapse (SNAC-wrist) and scapholunate advanced collapse (SLAC-wrist) in stage II. *J Plast Reconstr Aesthet Surg.* 2008;61(10):1210-8.
128. Traverso P, Wong A, Wollstein R, Carlson L, Ashmead D, Watson HK. Ten-Year Minimum Follow-Up of 4-Corner Fusion for SLAC and SNAC Wrist. *Hand (N Y).* 2017;12(6):568-72.
129. Cohen MS, Kozin SH. Degenerative arthritis of the wrist: proximal row carpectomy versus scaphoid excision and four-corner arthrodesis. *J Hand Surg Am.* 2001;26(1):94-104.
130. Chaudhry T, Spiteri M, Power D, Brewster M. Four corner fusion using a multidirectional angular stable locking plate. *World J Orthop.* 2016;7(8):501-6.
131. Mamede J, Castro Adeodato S, Aquino Leal R. Four-Corner Arthrodesis: Description of Surgical Technique Using Headless Retrograde Crossed Screws. *Hand (N Y).* 2018;13(2):156-63.
132. Ozyurekoglu T, Turker T. Results of a method of 4-corner arthrodesis using headless compression screws. *J Hand Surg Am.* 2012;37(3):486-92.
133. Trail IA, Murali R, Stanley JK, Hayton MJ, Talwalkar S, Sreekumar R, et al. The long-term outcome of four-corner fusion. *J Wrist Surg.* 2015;4(2):128-33.

134. Richards AA, Afifi AM, Moneim MS. Four-corner fusion and scaphoid excision using headless compression screws for SLAC and SNAC wrist deformities. Tech Hand Up Extrem Surg. 2011;15(2):99-103.

CHAPTER 2

2 A BIOMECHANICAL STUDY COMPARING UNIPLANAR AND MULTIPLANAR WRIST MOTION IN TWO POSITIONS OF FOUR CORNER FUSION

2.1 INTRODUCTION

A predictable and progressive pattern of radiographic changes occurs in scapholunate advanced collapse (SLAC) and scaphoid non-union advanced collapse (SNAC) arthritis. Arthrosis begins between the radial styloid and scaphoid in both conditions. As the disease progresses to stage II, arthrosis occurs at the scaphocapitate articulation in SNAC, while the disease involves the scaphoid and entire scaphoid fossa of the distal radius in SLAC. Finally, the capitolunate articulation is affected in stage III of both conditions. Treatment options for advanced carpal arthritis secondary to SLAC and SNAC include wrist denervation, partial wrist arthrodesis (scaphoidectomy and four corner fusion, 4CF, most commonly), proximal row carpectomy, total wrist arthroplasty and total wrist fusion.

Four corner fusion involves arthrodesis of the capitate, hamate, lunate and triquetrum. This procedure is routinely performed in conjunction with scaphoidectomy to address the radial-sided arthritis in SLAC and SNAC. Contraindications to the procedure include radiolunate joint degeneration and ulnar carpal translation. With regards to the fixation itself, multiple methods have been described including the use of Kirshner wires, staples, plates, wires and screws. Overall the complication rates between these options are similar(1-4), although staple and plate fixation have been shown to be associated with higher rates of nonunion and impingement(5-7).

Although multiple studies have illustrated the importance of re-establishing colinear alignment of the wrist in the sagittal plane when performing 4CF(8, 9), the impact of adjusting the relationship

between the proximal and distal carpal rows in the coronal plane is not well understood. Two positions of capitulate alignment in the coronal plane in 4CF have been described. When looking at radiographic images of a native wrist, one will notice variable degrees of “capitate overhang”, whereby the radial border of the capitate sits more radially than the radial border of the lunate(10) (**Figure 2.1A**). This anatomic relationship between the capitate and lunate corresponds to one of the alternative positions for 4CF referred to as “anatomic 4CF”. Many groups strongly recommend fusion in the anatomic position to maintain this overhang with the belief that doing so retains more physiologic anatomy of the carpus(10-13).

Four corner fusion can be also be performed with alignment of the radial capitulate border in the coronal plane to improve osseous contact between the capitate and lunate, although this alters the relationship between the hamate and triquetrum (1, 14-21) (**Figure 2.1B**). Additionally, arthrodesis in this radial-aligned position may be required in advanced SLAC with significant capitate proximal migration, as the capitate must be reduced into the distal carpal row to restore its position distal to the lunate. The practice of aligning the radial capitulate border is endorsed by many, with reports of acceptable long-term outcomes (15). However, a recent biomechanical study questioned the practice of radial capitulate alignment in 4CF, reporting that this fusion pattern with non-anatomic alignment of the proximal and distal carpal rows results in a radially-deviated resting wrist position, altering normal wrist kinematics(22). However, this study was limited, as it only investigated the influence on uniplanar wrist motion (specifically only radial-ulnar deviation), which does not mimic wrist function as well as multiplanar motion(23).

The purpose of this *in vitro* biomechanical study was to quantify changes in wrist kinematics during wrist flexion-extension, radial-ulnar deviation, and circumduction in “anatomic 4CF”, and “radial 4CF” conditions using an active motion simulator. We hypothesized that anatomic and radial-aligned positions of 4CF will result in similar reductions in wrist flexion and extension, radial-aligned fusion position will result in increased ulnar deviation compared to anatomic fusion, and both positions of 4CF will result in reduced circumduction motion compared to native state.

A



B



Figure 2.1. Plain radiographs of right wrist. (A) Pre-operative with native "capitate overhang" (B) Post-operative after scaphoidectomy and radial-aligned 4CF. (Right image reprinted with permission from: Ozyurekoglu T, Turker T. Results of a method of 4-corner arthrodesis using headless compression screws. The Journal of hand surgery. 2012 Mar 1;37(3):486-92)

2.2 METHODS

2.2.1 Specimen preparation

2.2.1.1 Pretesting validation

Six (6) fresh-frozen cadaveric upper extremity specimens, which were amputated at the upper humerus, were included in this study. A computed tomography (CT) scan of each specimen was performed to ensure there was no osseous or soft tissue pathology. All specimens were thawed 18 hours prior to biomechanical testing. Passive range of motion (ROM) was assessed under fluoroscopy to confirm full wrist ROM. All included specimens were free of osseous or soft tissue disease. The absence of osseous abnormalities, arthritis or pre-existing ligament injuries was also confirmed during testing when performing the partial wrist fusion procedure.

2.2.1.2 Optical tracker placement

A dorsal midline approach to the wrist was used. Full thickness subcutaneous skin flaps were raised, and the extensor retinaculum was incised along the third extensor compartment. The septum between the third and fourth extensor compartments was incised. Tendons of the fourth compartment were visualized and retracted radially, and the septum between the fourth and fifth extensor compartments was then released. The fourth compartment tendons were then taken ulnarly and this process was repeated to release the second compartment. Subsequently, a capsulotomy was performed using the Berger ligament-sparing approach to expose the carpal bones (24). Under fluoroscopic guidance, two 2.7 mm bone screws with an attached optical tracker were inserted into the dorsal lip of the lunate angled proximally at 60° from the long axis of the lunate. The screws were inserted parallel and adjacent to one another, just ulnar to the scapholunate (SL) ligament. The wrist was then passively ranged under fluoroscopic guidance to confirm that the trackers did not result in restricted ROM. Optical trackers were inserted into the radius, ulna, and third metacarpal head.

2.2.1.3 Four corner fusion

For the purposes of 4CF simulation, K-wires were positioned under fluoroscopic guidance. Five 0.062” K-wires were driven in a retrograde fashion, from distal to proximal (**Figure 2.2**). Two wires were inserted across the capitolunate joint, two across the triquetrohamate joint, and one across the luno-triquetral joint. The wrist was then passively ranged and lack of motion of the midcarpal joint was noted to confirm successful “fusion”. A mark was made on each K-wire at the level of the skin to indicate the distance each K-wire had to be advanced for successful fusion. K-wires were then partially withdrawn to reverse the midcarpal joint fusion but left in situ to maintain trajectory.

During testing on the wrist simulator, K-wires were advanced to the level of the marker and midcarpal fusion was confirmed. Motion was maintained at the radiocarpal joint. This was repeated in both anatomic 4CF (where fusion was performed with maintenance of the native capitate and lunate relationship, i.e. no reduction maneuver was performed) and radial-aligned 4CF positions (with fusion performed after ulnar translation of the distal row relative to the proximal row, aligning the radial border of the capitate and lunate in the coronal plane).

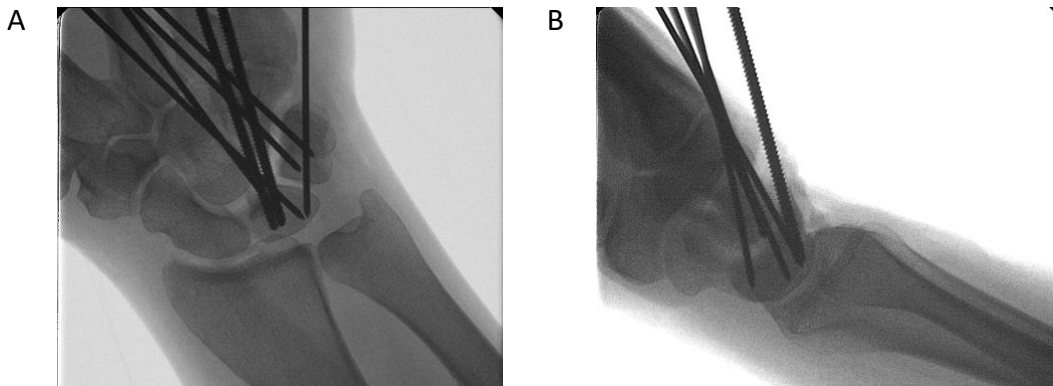


Figure 2.2. Fluoroscopic confirmation of midcarpal fusion. (A) Posteroanterior view (B) Lateral view.

2.2.1.4 Soft tissue preparation

The following tendons were identified to control flexion-extension and radial-ulnar deviation via the respective SmartMotors (SM2316D-PLS2, SMI Animatics Corp.) at the base of the wrist simulator: flexor carpi radialis (FCR), flexor carpi ulnaris (FCU), extensor carpi radialis brevis (ECRB), extensor carpi radialis longus (ECRL), and extensor carpi ulnaris (ECU) (**Figure 2.3**, **Figure 2.4**). For control of pronation-supination, pronator teres (PT) and biceps brachii (BB) were also identified. Musculotendinous junctions were tagged using 100 lb. load fishing line (PowerPro Fishing Line Braided Spectra Model 100-1500-W) in a running, locking Krakow fashion. Each tendon and its suture line were passed through independent subcutaneous tunnels in a direction of muscle origin-insertion to prevent overlap and to ensure targeted control of each tendon. Sutures were then passed through medial and lateral epicondyle blocks in a pre-determined fashion to maintain physiologic line of pull of each tendon (**Figure 2.5**).

Prior to any motion testing, the dorsal wrist capsule was repaired using 4'0-Vicryl using figure-of-eight sutures. The extensor retinaculum was also repaired in the same manner. Volar and dorsal skin incisions were reapproximated using 3'0-Prolene sutures in a running continuous fashion.

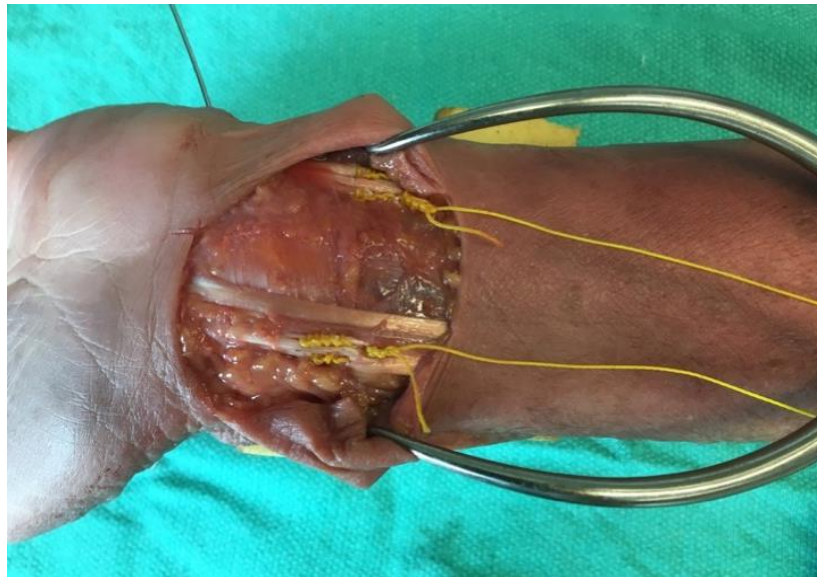


Figure 2.3. Flexor tendons with running locking Krakow stitches for motion actuation (from radial to ulnar: FCR, FCU).

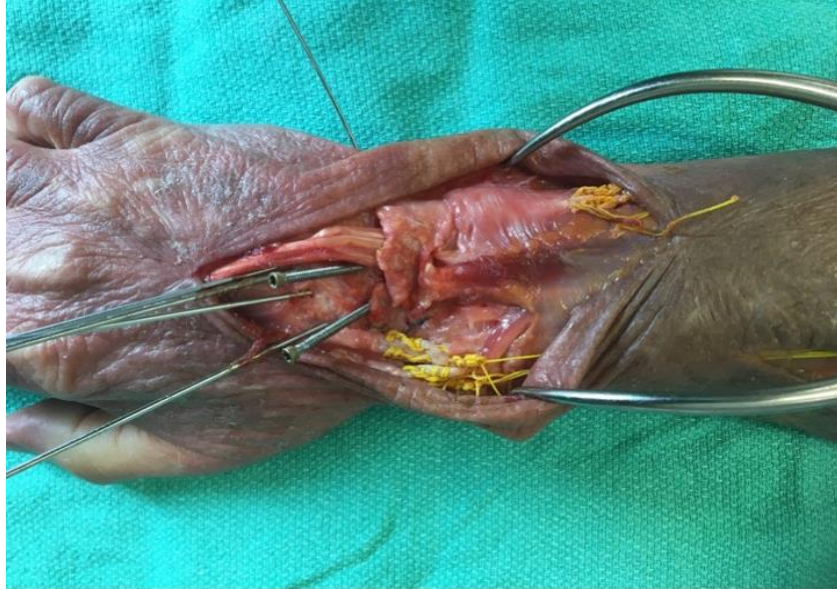


Figure 2.4. Extensor tendons with running locking Krakow stitches for motion actuation (from radial to ulnar: ECRL, ECRB, ECU).

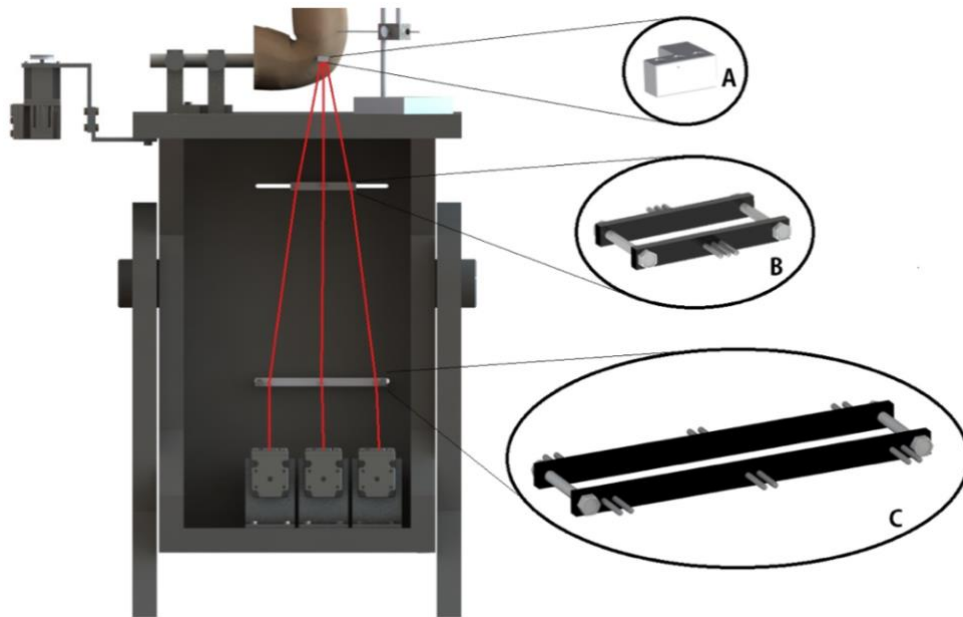


Figure 2.5. Schematic illustrating epicondyle block and cable stabilization guides. After tendons of interest are tagged, sutures are passed through epicondyle blocks to maintain physiologic line of pull.

2.2.1.5 Specimen set up

All specimens were positioned in the custom wrist simulator with the elbow flexed at 90° (**Figure 2.6**). Specimens were secured with a humeral clamp and 2 Steinmann pins were inserted along the length of the ulna for stabilization. Care was taken not to insert these too deep (i.e. beyond the second cortex of the ulna) as to restrict forearm rotation. Tagged tendons were then attached to their respective motors. Optical trackers (Optotrak Certus, Northern Digital, Waterloo, ON, Canada) were mounted on the tracker mounts and registered by the camera prior to testing.

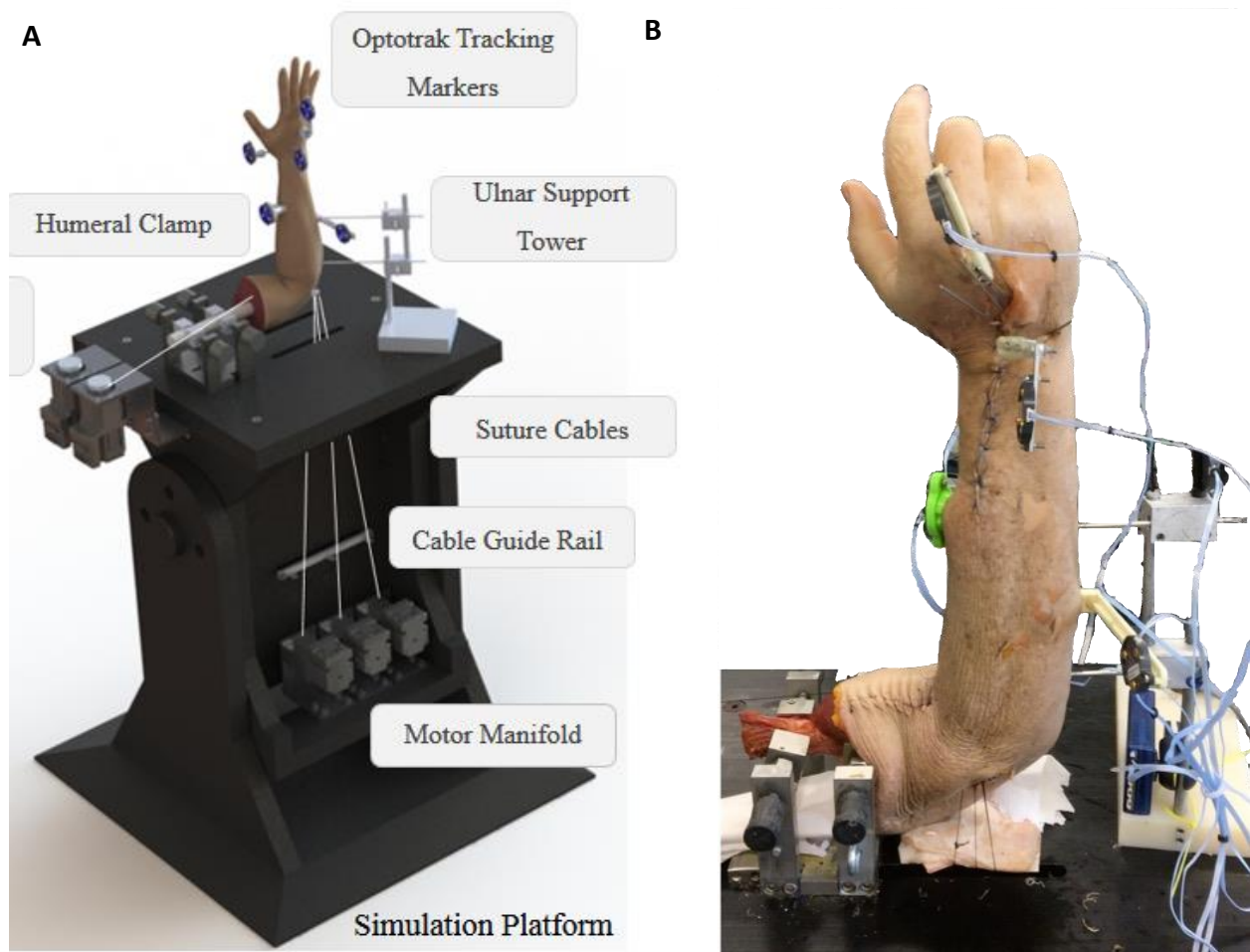


Figure 2.6. Active motion simulator. (A) Schematic of specimen mounted onto simulator using a humeral clamp and ulnar support tower. (B) Cadaveric specimen mounted onto simulator.

2.2.2 Testing protocol

Prior to testing, a coordinate system was generated by identifying anatomical landmarks on the radius, ulna and third metacarpal. The angles between the third metacarpal and long axis of the radius in the sagittal and coronal planes were used to define wrist position. All motion was measured with the wrist starting in neutral position (i.e. angle between the third metacarpal and long axis of the radius in the sagittal and coronal planes set to 0°). A constant 45 N tone load was applied on PT and BB to maintain neutral forearm rotation.

Baseline measurements for simulated active flexion (50°), extension (50°), radial (15°) and ulnar deviation (20°), and circumduction were taken in the native state without any interventions for all specimens. Circumduction motion was achieved by sequentially activating wrist flexion and ulnar deviation (FCU), followed by flexion and radial deviation (FCR), wrist extension and radial deviation (ECRL/ECRB), and extension and ulnar deviation (ECU), all while maintaining a minimum baseline tone of 8.9 N on other tendons. Each motion arc was repeated 3 times with the final simulation being recorded. Motion trials were performed at 5° per second following each stage of the protocol.

After obtaining baseline motion data in the native state, the scaphoid was excised utilizing the previous dorsal incision, with care taken to preserve the volar radiocarpal ligaments. All measurements were repeated in the following positions of fusion (**Figure 2.7**):

1. Four corner fusion with carpus in anatomic position,
2. Four corner fusion with radial border of lunate and capitate aligned.

Care was taken to position the lunate colinear to the capitate (in a sagittal plane), avoiding any dorsal intercalated segment instability (DISI) or volar intercalated segment instability (VISI) deformity during fusion. This was confirmed visually by assessing the amount of dorsal lunate relative to the dorsal rim of the radius, and by restoring the lunate trackers to their original position relative to the capitate. Additionally, under direct visualization, it was confirmed that the radiocarpal joint was not fused by protruding K-wires. Successful fusion was verified by observing the capitate, lunate, hamate and triquetrum move as a single unit, and through motion data obtained

from the lunate trackers (i.e. the relationship between the third metacarpal and lunate trackers remained constant throughout testing). The dorsal wrist capsule, extensor retinaculum and skin were repaired after each intervention.

The final recorded measurement of 3 motion trials was used to compare flexion-extension, radial-ulnar deviation, and circumduction area between native state, anatomic 4CF, and radial 4CF. The area of the maximum 2-dimensional circumduction pattern (through tracking of the third metacarpal) that was generated after each condition was measured using MATLAB (MATLAB version 7.10.0 (R2010a). Natick, Massachusetts: The MathWorks Inc.; 2010) and reported in mm².

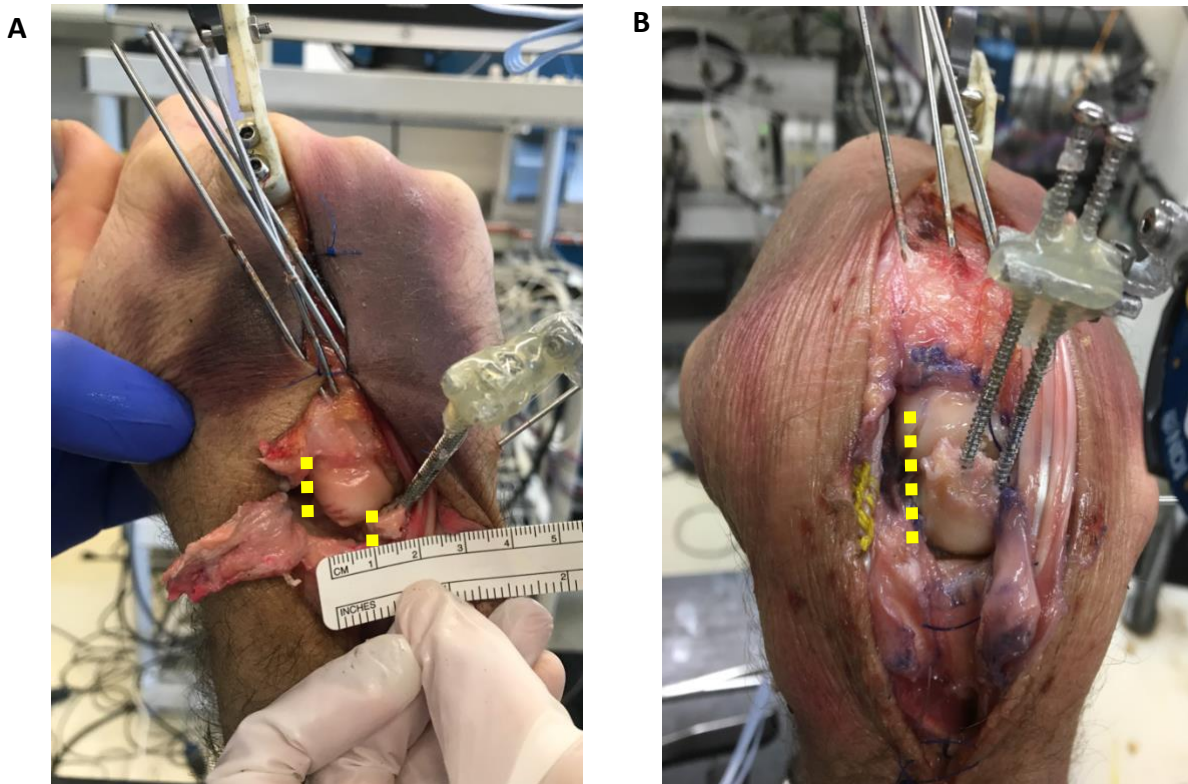


Figure 2.7. Cadaveric specimen illustrating scaphoidectomy and four corner fusion. (A) Anatomic 4CF position with capitulate overhang (B) Radial-aligned 4CF position.

2.2.3 Statistical analysis

A one-way repeated measures ANOVA was used to compare mean values in native state, anatomic 4CF and radial 4CF. A post-hoc power analysis confirmed that a sample size of 6 specimens was adequate to detect a difference of 6.7° while maintaining 80% power and 95% confidence interval, with significance set at $p < 0.05$.

2.3 RESULTS

2.3.1 Specimen demographics

Six (6) fresh-frozen cadaveric upper extremity specimens that were amputated at the upper humerus were included in the study. Five specimens were of the right side. All specimens were male. The average age of specimens was 58 years (range 39 to 71 years old).

2.3.2 Uniplanar wrist motion

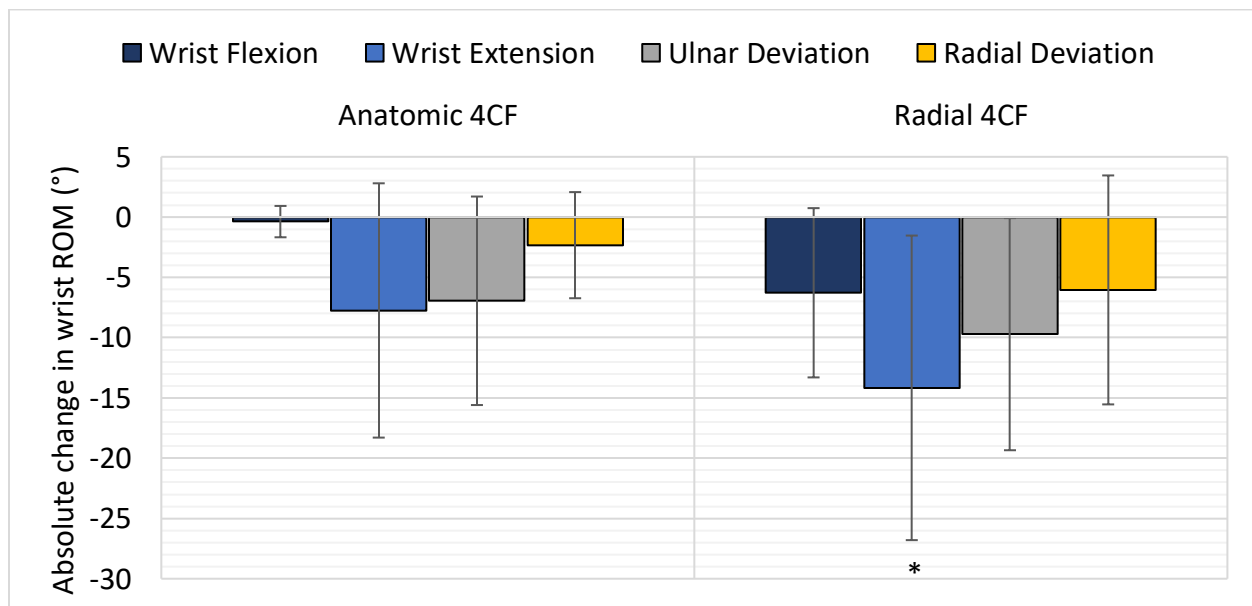


Figure 2.8. Absolute change (°) in wrist flexion, extension, ulnar and radial deviation compared to native state. Asterisk indicates statistical significance ($p < 0.05$). Asterisk at base illustrates significance compared to native state.

Four corner fusion performed in the anatomic position was found to have a $0.4 \pm 1.3^\circ$ reduction in wrist flexion and $7.7 \pm 10.5^\circ$ reduction in wrist extension compared to native ($p=0.48$ and $p=0.10$, respectively) (**Figure 2.8**). Fusion performed in a radial-aligned position demonstrated a $6.3 \pm 7.0^\circ$ reduction in wrist flexion and $14.2 \pm 12.6^\circ$ reduction in wrist extension compared to native ($p=0.07$ and $p=0.04$). These differences in wrist flexion and extension were not statistically different between fusion groups ($p=0.10$ and $p=0.40$).

Four corner fusion performed in the anatomic position was found to have a $6.9 \pm 8.6^\circ$ reduction in ulnar deviation and $2.3 \pm 4.4^\circ$ reduction in radial deviation compared to native ($p=0.13$ and $p=0.29$, respectively). Fusion performed in the radial-aligned position resulted in $9.7 \pm 9.6^\circ$ and $6.0 \pm 9.5^\circ$ reductions, respectively ($p=0.07$ and $p=0.21$). These reductions in ulnar and radial deviation were not statistically different between the two fusion groups ($p=0.12$ and $p=0.42$).

2.3.3 Circumduction

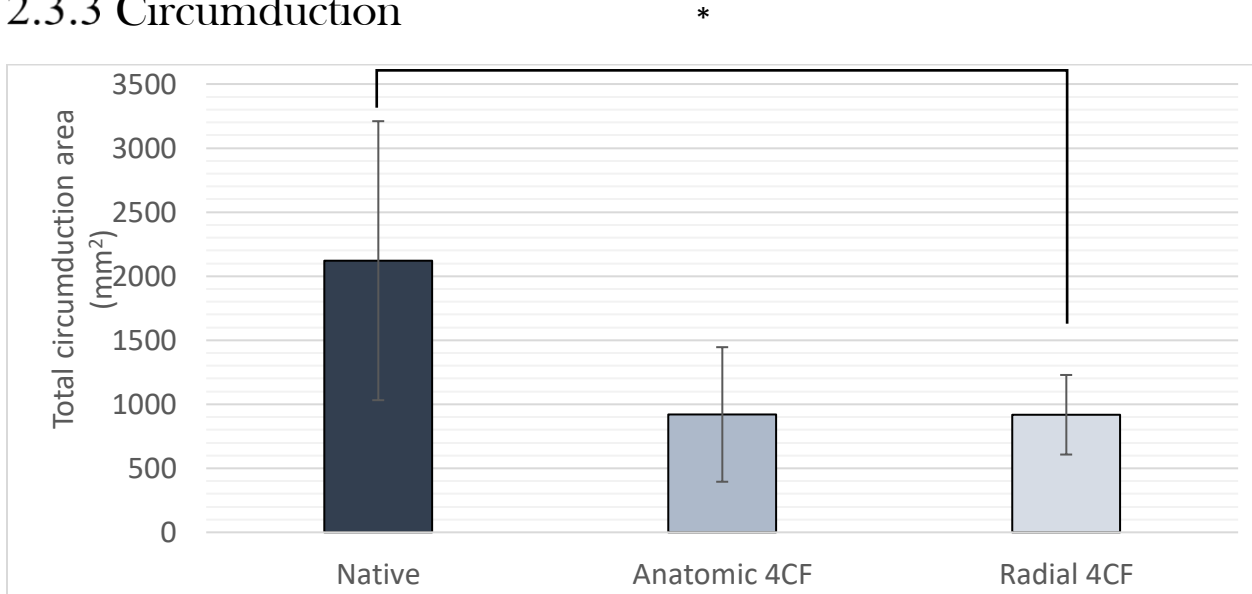


Figure 2.9 Total circumduction area (mm²) in native, anatomic 4CF and radial 4CF conditions. Significant differences ($p<0.05$) are noted with an asterisk.

Total circumduction area (mm²) was highest in native state (**Figure 2.9**). This was significantly reduced in radial-aligned 4CF ($p=0.048$) but not in anatomic 4CF ($p=0.11$). Total circumduction area was similar between the two fusion positions ($p=0.99$).

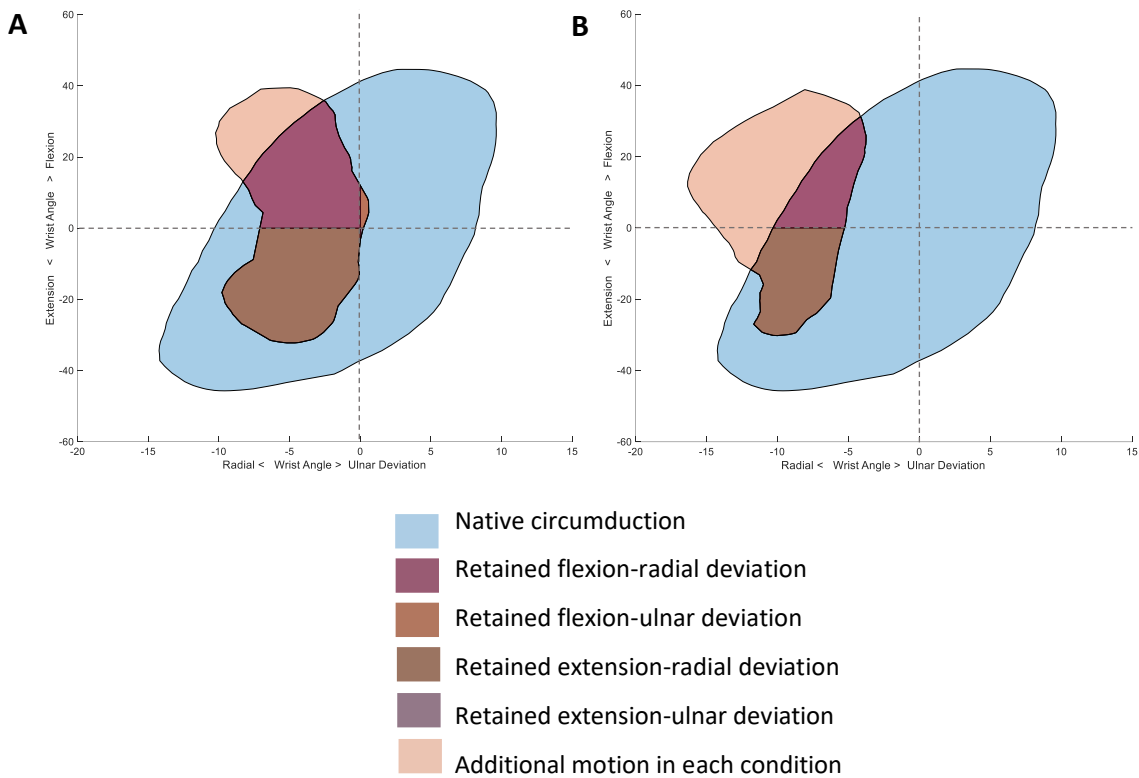


Figure 2.10. Circumduction pattern superimposed on native circumduction pattern. (A) Anatomic 4CF (B) Radial 4CF.

Circumduction pathways were recorded for both groups and compared to the circumduction pattern generated by the native state (**Figure 2.10**). The percentages of overlap between both conditions and the native circumduction pattern were noted. Anatomic 4CF maintained a closer circumduction pattern to native, with 41% overlap, while radial 4CF maintained 32%, although statistically no significant difference was detected between the two groups ($p=0.24$). Additionally, the majority of the radial 4CF circumduction pattern lay outside the native pattern, while the opposite was true of anatomic 4CF.

2.4 DISCUSSION

While the importance of correcting the DISI deformity by maintaining linear alignment of the capitate and lunate in the sagittal plane in 4CF is well-established (8, 9), the significance of altering the capitulunate relationship in the coronal plane during 4CF is less clear. There is no consensus on the optimal fusion position in the coronal plane, and some authors routinely perform this procedure in a radial-aligned position(1, 14-21), while others tend to fuse in an anatomic position(10-13). The objective of this biomechanical study was to delineate the motion pathways of the wrist after scaphoidectomy and 4CF in an anatomic position versus radial-aligned position. The results of this work can be summarized into two key findings. Firstly, ROM was reduced in both fusion positions compared to native state although only the reduction in wrist extension in radial 4CF reached statistical significance. Secondly, total circumduction was reduced in both fusion positions, but reached statistical significance only with radial-aligned fusion ($p=0.048$).

Only one reported biomechanical study has investigated the influence of adjusting capitulunate alignment in the coronal plane during 4CF. Hernandez-Soria et al.(22) compared 2 different positions of fusion in 6 fresh frozen human cadaveric upper limbs, with a “pre-operative” native wrist which had no fusion, the “anatomic position” being unchanged from the native carpal bone position, and the “lunate-covered” condition where the capitate was translated ulnarly to cover the lunate. Fixation was achieved with 2 K-wires between the capitate/lunate and hamate/triquetrum. The authors utilized a passive motion simulator and analyzed wrist resting position, radial deviation, and ulnar deviation. The native and anatomic 4CF wrists sat in slight ulnar deviation at rest, whereas the lunate-covered group rested in radial deviation ($p<0.01$). They noted increased radial deviation in the lunate-covered group compared to the native wrist (23° vs. 7° , $p=0.01$) and anatomic 4CF (23° vs. 10° , $p=0.03$). Ulnar deviation was increased in anatomic 4CF, and more restricted in native and lunate-covered conditions, though not statistically significant. This may be the outcome of tightening of the radioscapocapitate ligament after ulnar translation of the capitate. The authors did not report on any changes in flexion-extension.

Our findings demonstrate reduced ROM and circumduction in both 4CF conditions compared to native state. However, radially-aligned 4CF was more limited in wrist extension than native state,

although no statistical difference was found when compared to anatomic fusion. Further, the reduction in wrist flexion and ulnar deviation in radial 4CF compared to native approached statistical significance ($p=0.07$). In the biomechanical study by Hernandez-Soria et al., the authors noted the wrist assumed a radially-deviated position after 4CF in a radially-aligned position(22). These results are consistent with our finding of reduced ulnar deviation. We hypothesize that these changes may be secondary to tensioning of the radioscaphocapitate (RSC) ligament when the capitate is translated ulnarly. Increased tension on this strong ligament may tether the wrist into radial deviation and ultimately limit ulnar deviation(22).

Clinically, some surgeons advocate for radially-aligned 4CF and report good outcomes for this procedure(1, 14-21). Bain et al.'s retrospective cohort study looking at long term (10-year minimum follow-up) outcomes after radial 4CF in 31 patients found that grip strength was maintained post-operatively, but wrist flexion was reduced by 22%. They report mean radial deviation of 10° and ulnar deviation of 20° . Average patient satisfaction rating was 8/10, and patient reported outcomes regarding pain, wrist function and satisfaction were stable at 1 year compared to 10 years. Only 2 patients proceeded to total wrist fusion for persistent pain. The increased reduction in flexion and extension in radial 4CF compared to anatomic 4CF may be due to additional alteration in the relationship between the proximal and distal carpal rows, which is not adjusted in the latter. In another retrospective cohort study with a minimum follow up of 10 years, Traverso et al. reported a mean flexion-extension arc of 69° , and radial-ulnar deviation arc of 33° (19). Despite the fact that the majority of patients (73%) were noted to have radiographic changes in the radiolunate joint, patients were highly satisfied with the procedure and reported low functional impairment.

The wrist ROM results of our biomechanical study are consistent with the clinical literature. Although scaphoidectomy and 4CF in both anatomic and radial positions results in a reduction of uniplanar motion in all directions (wrist flexion, wrist extension, radial and ulnar deviation), the retained motion is well within the functional range in both biomechanical and clinical studies(25, 26).

Between the two fusion positions, total circumduction area was significantly reduced in radial 4CF but not anatomic 4CF, although both fusion positions were not statistically significantly different when compared. Additionally, the percent overlap of circumduction when compared to native state was 41% in anatomic 4CF and 32% in radial 4CF. These results were not statistically significant when compared with one another nor with native state. With these biomechanical findings in mind, anatomic 4CF appears to produce more favourable motion outcomes. Anatomic 4CF is suitable if there is sufficient pre-existing osseous contact between the proximal capitate and distal lunate to achieve fusion, to maximize circumduction area and to minimize restriction in wrist flexion, extension and ulnar deviation. In other circumstances, radial 4CF may be appropriate. For instance, in cases of SLAC with significant capitate proximal migration or minimal bone stock between the capitate and lunate, the fusion in the radial-aligned position may be required to optimize bony apposition to obtain adequate fixation. Increasing contact between the capitate and lunate may reduce rates of non-union(10). Clinical studies comparing the outcomes of anatomic and radial 4CF are required. Outcomes that should be measured include union rates, complication rates, pain relief, grip strength, ROM, and patient reported outcomes.

Limitations to this *in-vitro* biomechanical study includes the use of healthy, non-arthritis cadaveric wrists rather than those with SLAC or SNAC pathology. This was due to the lack of availability of arthritic cadaveric wrists. This cadaveric model also lacked the potential for ligament adaptation during healing, which would occur in clinical scenarios. Additionally, despite the fact that simulation was performed in a single position, a high-fidelity active motion simulator was used, which more closely resembles a physiologic state by applying forces on flexor and extensor tendons to generate motion(27-29). Although K-wire fixation is less rigid compared to screw or plate fixation, we attempted to improve construct rigidity with multiple large caliber K-wires (five 0.062"). K-wires were used in our study to allow for a repeated-measures study design. As the capitate is shifted ulnarly relative to the lunate, the bony defect created from a headless compression screw in anatomic fusion gets shifted proportionally, leaving a very limited amount of bone stock radially for radial-aligned fusion. As such, fixation may not have been maintained in the second (radial-aligned) procedure had we used screw fixation. Further, as there was a lack of access to fluoroscopy in the laboratory, we were unable to confirm correction of any DISI/VISI deformity radiographically, but this was confirmed visually. Finally, although the study was

sufficiently powered, there was high variance in the results (standard deviation) which is expected due to the variable size and shape of normal wrists.

Clinical studies are required to corroborate these biomechanical results. This may include a retrospective or prospective cohort study comparing wrist ROM outcomes, union rates, grip strength and patient-reported outcome measures, including pain relief. Ideally a randomized control trial comparing these two fusion positions would be conducted.

2.5 CONCLUSION

This *in-vitro* biomechanical model of scaphoidectomy and four corner fusion resulted in a reduction in overall uniplanar motion compared to native state, although only the reduction in wrist extension after radial 4CF reached statistical significance. Additionally, total circumduction area was reduced in both anatomic and radial-aligned fusion positions, although only the reduction in the radial 4CF group reached statistical significance. Total retained native circumduction area was 41% in anatomic 4CF and 32% in radial 4CF. Anatomic 4CF produces more favourable motion outcomes compared to radial 4CF. Future clinical studies comparing union rates, ROM, grip strength, functional and patient-reported outcomes in anatomic 4CF and radial 4CF are required to validate these results in a clinical context.

References

1. Erne HC, Broer PN, Weiss F, Loew S, Cerny MK, Schmauss D, et al. Four-corner fusion: Comparing outcomes of conventional K-wire-, locking plate-, and retrograde headless compression screw fixations. *J Plast Reconstr Aesthet Surg*. 2019;72(6):909-17.
2. Rodgers JA, Holt G, Finnerty EP, Miller B. Scaphoid excision and limited wrist fusion: a comparison of K-wire and circular plate fixation. *Hand (N Y)*. 2008;3(3):276-81.
3. De Smet L, Deprez P, Duerinckx J, Degreef I. Outcome of four-corner arthrodesis for advanced carpal collapse: circular plate versus traditional techniques. *Acta Orthop Belg*. 2009;75(3):323-7.
4. Le Corre A, Ardouin L, Loubersac T, Gaisne E, Bellemère P. Retrospective study of two fixation methods for 4-corner fusion: Shape-memory staple vs. dorsal circular plate. *Chir Main*. 2015;34(6):300-6.
5. Vance MC, Hernandez JD, Didonna ML, Stern PJ. Complications and outcome of four-corner arthrodesis: circular plate fixation versus traditional techniques. *J Hand Surg Am*. 2005;30(6):1122-7.
6. Backer K, Englert A, Lukas B. Results of four-corner-fusion – spider plate fixation compared with k-wires. *J Hand Surg Eur Vol*. 2007;32(Supplement 1):71.
7. Pauchard N, Lecoanet-Strugarek C, Segret J, De Gasperi M, Dap F, Dautel G. Dorsal locking plates versus staples in four-corner fusion: a comparative clinical and radiological study. *Orthop Traumatol Surg Res*. 2014;100(6):593-7.
8. De Carli P, Donndorff AG, Alfie VA, Boretto JG, López Ovenza JM, Gallucci GL. Four-corner arthrodesis: influence of the position of the lunate on postoperative wrist motion: a cadaveric study. *J Hand Surg Am*. 2007;32(9):1356-62.
9. Dvinskikh NA, Blankevoort L, Strackee SD, Grimbergen CA, Streekstra GJ. The effect of lunate position on range of motion after a four-corner arthrodesis: a biomechanical simulation study. *J Biomech*. 2011;44(7):1387-92.
10. Ozyurekoglu T, Turker T. Results of a method of 4-corner arthrodesis using headless compression screws. *J Hand Surg Am*. 2012;37(3):486-92.
11. Mamede J, Castro Adeodato S, Aquino Leal R. Four-Corner Arthrodesis: Description of Surgical Technique Using Headless Retrograde Crossed Screws. *Hand (N Y)*. 2018;13(2):156-63.

12. Trail IA, Murali R, Stanley JK, Hayton MJ, Talwalkar S, Sreekumar R, et al. The long-term outcome of four-corner fusion. *J Wrist Surg.* 2015;4(2):128-33.
13. Richards AA, Afifi AM, Moneim MS. Four-corner fusion and scaphoid excision using headless compression screws for SLAC and SNAC wrist deformities. *Tech Hand Up Extrem Surg.* 2011;15(2):99-103.
14. Stanley J. Arthroplasty and arthrodesis of the wrist. *Green's Operative Hand Surgery.* 6 ed. Philadelphia: Elsevier; 2010. p. 429-63.
15. Bain GI, Watts AC. The outcome of scaphoid excision and four-corner arthrodesis for advanced carpal collapse at a minimum of ten years. *J Hand Surg Am.* 2010;35(5):719-25.
16. Ball B, Bergman JW. Scaphoid excision and 4-corner fusion using retrograde headless compression screws. *Tech Hand Up Extrem Surg.* 2012;16(4):204-9.
17. Cha SM, Shin HD, Kim KC. Clinical and radiological outcomes of scaphoidectomy and 4-corner fusion in scapholunate advanced collapse at 5 and 10 years. *Ann Plast Surg.* 2013;71(2):166-9.
18. Dacho AK, Baumeister S, Germann G, Sauerbier M. Comparison of proximal row carpectomy and midcarpal arthrodesis for the treatment of scaphoid nonunion advanced collapse (SNAC-wrist) and scapholunate advanced collapse (SLAC-wrist) in stage II. *J Plast Reconstr Aesthet Surg.* 2008;61(10):1210-8.
19. Traverso P, Wong A, Wollstein R, Carlson L, Ashmead D, Watson HK. Ten-Year Minimum Follow-Up of 4-Corner Fusion for SLAC and SNAC Wrist. *Hand (N Y).* 2017;12(6):568-72.
20. Cohen MS, Kozin SH. Degenerative arthritis of the wrist: proximal row carpectomy versus scaphoid excision and four-corner arthrodesis. *J Hand Surg Am.* 2001;26(1):94-104.
21. Chaudhry T, Spiteri M, Power D, Brewster M. Four corner fusion using a multidirectional angular stable locking plate. *World J Orthop.* 2016;7(8):501-6.
22. Hernandez-Soria A, Das De S, Model Z, Lee SK, Wolfe SW. The Effect of Capitate Position on Coronal Plane Wrist Motion After Simulated 4-Corner Arthrodesis. *J Hand Surg Am.* 2016;41(11):1049-55.
23. Li ZM, Kuxhaus L, Fisk JA, Christophel TH. Coupling between wrist flexion-extension and radial-ulnar deviation. *Clin Biomech (Bristol, Avon).* 2005;20(2):177-83.

24. Berger RA, Bishop AT, Bettinger PC. New dorsal capsulotomy for the surgical exposure of the wrist. *Ann Plast Surg.* 1995;35(1):54-9.
25. Mulford JS, Ceulemans LJ, Nam D, Axelrod TS. Proximal row carpectomy vs four corner fusion for scapholunate (Slac) or scaphoid nonunion advanced collapse (Snac) wrists: a systematic review of outcomes. *J Hand Surg Eur Vol.* 2009;34(2):256-63.
26. Saltzman BM, Frank JM, Slikker W, Fernandez JJ, Cohen MS, Wysocki RW. Clinical outcomes of proximal row carpectomy versus four-corner arthrodesis for post-traumatic wrist arthropathy: a systematic review. *J Hand Surg Eur Vol.* 2015;40(5):450-7.
27. Werner FW, Palmer AK, Somerset JH, Tong JJ, Gillison DB, Fortino MD, et al. Wrist joint motion simulator. *J Orthop Res.* 1996;14(4):639-46.
28. Dunning CE, Lindsay CS, Bicknell RT, Patterson SD, Johnson JA, King GJ. Supplemental pinning improves the stability of external fixation in distal radius fractures during simulated finger and forearm motion. *J Hand Surg Am.* 1999;24(5):992-1000.
29. Iglesias D. Development of an in-vitro passive and active motion simulator for the investigation of wrist function and kinematics. London, Ontario: University of Western Ontario; 2016.

CHAPTER 3

3 A BIOMECHANICAL STUDY COMPARING UNIPLANAR AND MULTIPLANAR WRIST MOTION AFTER FOUR CORNER FUSION AND PROXIMAL ROW CARPECTOMY

3.1 INTRODUCTION

The mainstay treatment of advanced arthritis, caused by scaphoid non-union advanced collapse (SNAC) or scapholunate advanced collapse (SLAC), are salvage procedures, including scaphoidectomy with four corner fusion (4CF) and proximal row carpectomy (PRC). Patients with stage II-III SLAC or SNAC arthritis may be candidates for both procedures. These procedures provide reliable pain relief while preserving a degree of wrist motion(1). However, there is currently no consensus as to which of the two operations is clinically superior. Many clinical studies have compared outcomes including range of motion (ROM), grip strength, and pain relief; however, few have investigated wrist biomechanics following these operations to account for these clinical findings. Those that have been conducted use a passive motion simulator and report on uniplanar motion (flexion-extension, radial-ulnar deviation)(2), or multiplanar motion(3) in isolation.

In **Chapter 2**, uniplanar wrist motion and circumduction were compared in two positions (anatomic and radial-aligned capitulate border in the coronal plane) of scaphoidectomy with 4CF. Our findings indicate that while both partial fusions resulted in reduced total circumduction area compared to native, only radial 4CF reached statistical significance. Additionally, fusion in a radial-aligned position resulted in a statistically significant reduction in wrist extension, while wrist flexion and ulnar deviation approached statistical significance when compared to native state. Motion was reduced in anatomic fusion relative to the native wrist, however, this did not reach statistical significance. Collectively, the data from this study supports that scaphoidectomy and

anatomic 4CF may provide favourable motion outcomes. Consequently, the decision was made to compare “anatomic 4CF” and PRC conditions in this study.

The purpose of this *in vitro* biomechanical study was to quantify changes in wrist kinematics during wrist flexion-extension, radial-ulnar deviation, and circumduction in “anatomic 4CF”, and PRC conditions using an active motion simulator. We hypothesized that PRC and 4CF would result in similar magnitudes of wrist flexion and extension, that PRC would result in reduced radial deviation compared to 4CF, and that wrist circumduction motion would be greater after PRC compared to 4CF.

3.2 METHODS

3.2.1 Specimen preparation

Pretesting validation, optical tracker placement, scaphoidectomy and 4CF, soft tissue preparation, and specimen set up were performed as described in **Chapter 2**. The same 6 cadaveric specimens were used for this study.

3.2.2 Proximal row carpectomy

The previous dorsal cutaneous incision and Berger ligament-sparing approach to the wrist was used(4). The PRC stage was the final condition in the testing protocol. As scaphoidectomy had already been performed for the 4CF stage, only the lunate and triquetrum remained to be excised. This was done sharply with a No. 15 blade with both carpal bones excised *en-bloc*. Care was taken not to disrupt the volar ulnocarpal and radioscaphocapitate ligaments. The dorsal wrist capsule was then plicated to help maintain the position of the capitate within the lunate fossa of the radius. The extensor retinaculum and skin were reapproximated.

3.2.3 Testing protocol

Prior to testing, a coordinate system was generated by identifying anatomical landmarks on the radius, ulna and third metacarpal. The angles between the third metacarpal and long axis of the

radius in the sagittal and coronal planes were used to define wrist position. All motion was measured with the wrist starting in neutral position (i.e. angle between the third metacarpal and long axis of the radius in the sagittal and coronal planes set to 0°). A constant 45 N tone load was applied on PT and BB to maintain neutral forearm rotation.

Baseline measurements for simulated active flexion (50°), extension (50°), radial (15°) and ulnar deviation (20°), and circumduction were taken in the native state without any interventions for all specimens. Circumduction motion was achieved by sequentially activating wrist flexion and ulnar deviation (FCU), followed by flexion and radial deviation (FCR), wrist extension and radial deviation (ECRL/ECRB), and extension and ulnar deviation (ECU), all while maintaining a minimum baseline tone of 8.9 N on other tendons. Each motion arc was repeated 3 times with the final simulation being recorded. Motion trials were performed at 5° per second following each stage of the protocol.

After obtaining baseline motion data in the native state, the scaphoid was excised utilizing the previous dorsal incisions, with care taken to preserve the integrity of the volar radiocarpal ligaments. All measurements were repeated in the following conditions:

1. Four corner fusion and scaphoidectomy with the lunate and capitate aligned in the anatomic position (data obtained from the previous study in Chapter 2),
2. Proximal row carpectomy.

Care was taken to position the lunate colinear to the capitate in the sagittal plane, avoiding any dorsal intercalated segment instability (DISI) or volar intercalated segment instability (VISI) deformity during fusion. This was confirmed visually by assessing the amount of dorsal lunate relative to the dorsal rim of the radius, and by restoring the lunate trackers to their original position relative to the capitate. Additionally, under direct visualization, it was confirmed that the fixation did not cross the radiocarpal joint. Successful fusion was verified by observing the capitate, lunate, hamate, and triquetrum move as a single unit, and through motion data obtained from the lunate trackers (i.e. the relationship between the third metacarpal and lunate trackers remained constant

throughout testing). The dorsal wrist capsule, extensor retinaculum, and skin were repaired after each intervention.

The final recorded measurement of 3 motion trials was used to compare flexion-extension, radial-ulnar deviation, and circumduction area between native state, 4CF, and PRC. The area of the maximum 2-dimensional circumduction pattern (through tracking of the third metacarpal) that was generated after each condition was measured using MATLAB (MATLAB version 7.10.0 (R2010a). Natick, Massachusetts: The MathWorks Inc.; 2010) and reported in mm².

3.2.4 Statistical analysis

A repeated measures ANOVA was used to compare mean values in native state, 4CF and PRC. Once again, post-hoc power analysis confirmed that our sample size of 6 specimens could detect a difference of 6.7° while maintaining 80% power and 95% confidence interval, with significance set at $p < 0.05$.

3.3 RESULTS

3.3.1 Specimen demographics

Six (6) human cadaveric specimens were used in this study, of which 5 were the right upper extremity. All specimens were male. The average age of specimens was 58 years (range 39 to 71 years old).

3.3.2 Uniplanar wrist motion

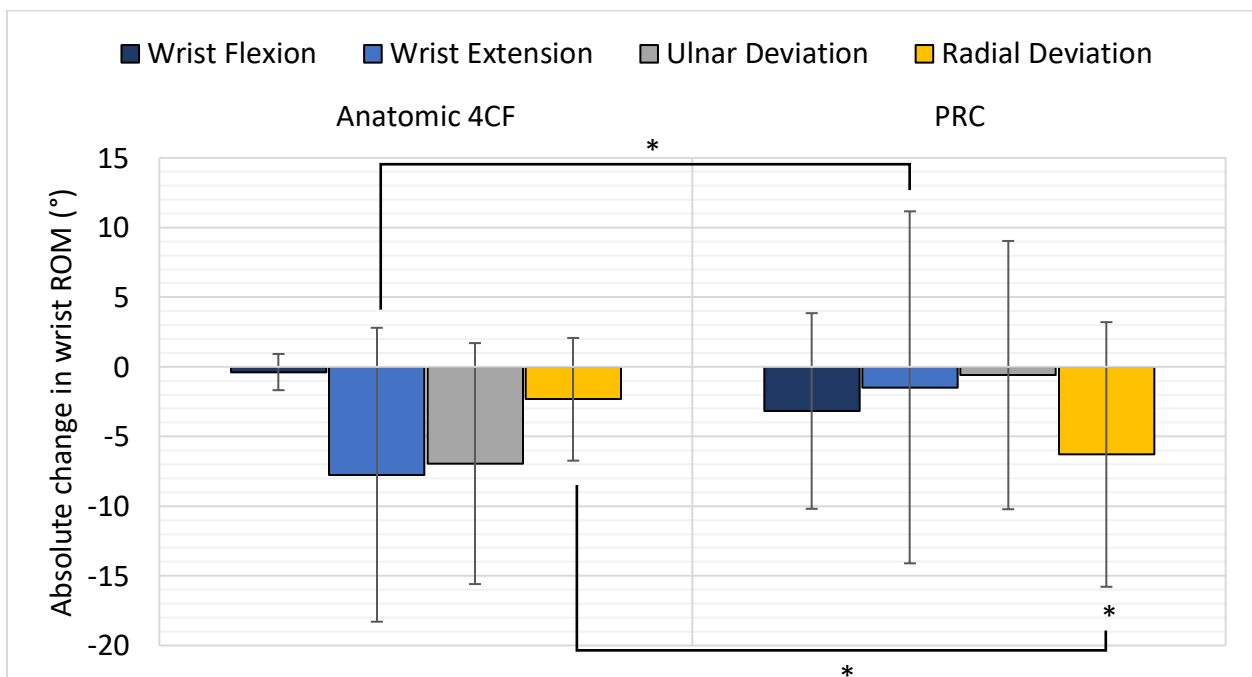


Figure 3.1. Absolute change (°) in wrist flexion, extension, ulnar and radial deviation compared to native state. Asterisk indicates statistical significance ($p < 0.05$). Asterisk at base illustrates significance compared to native state.

PRC demonstrated a $3.2 \pm 7.0^\circ$ reduction in wrist flexion ($p=0.30$), and $1.5 \pm 7.3^\circ$ reduction in wrist extension ($p=0.64$), while 4CF had a $0.4 \pm 1.3^\circ$ reduction in wrist flexion and $7.7 \pm 10.5^\circ$ reduction in wrist extension compared to native ($p=0.48$ and $p=0.10$, respectively) (**Figure 3.1**).

The reduction in wrist flexion was similar between groups ($p=0.38$), while the reduction in wrist extension was significantly less in PRC than 4CF ($p=0.04$).

PRC demonstrated a $0.6 \pm 1.0^\circ$ reduction in ulnar deviation ($p=0.25$), and $6.3 \pm 4.4^\circ$ reduction in radial deviation ($p=0.02$) compared to native. Four corner fusion was found to have a $6.9 \pm 8.6^\circ$ reduction in ulnar deviation and $2.3 \pm 4.4^\circ$ reduction in radial deviation compared to native ($p=0.13$ and $p=0.29$, respectively). The reduction in radial deviation was significantly greater after PRC compared to 4CF ($p=0.03$).

3.3.3 Circumduction

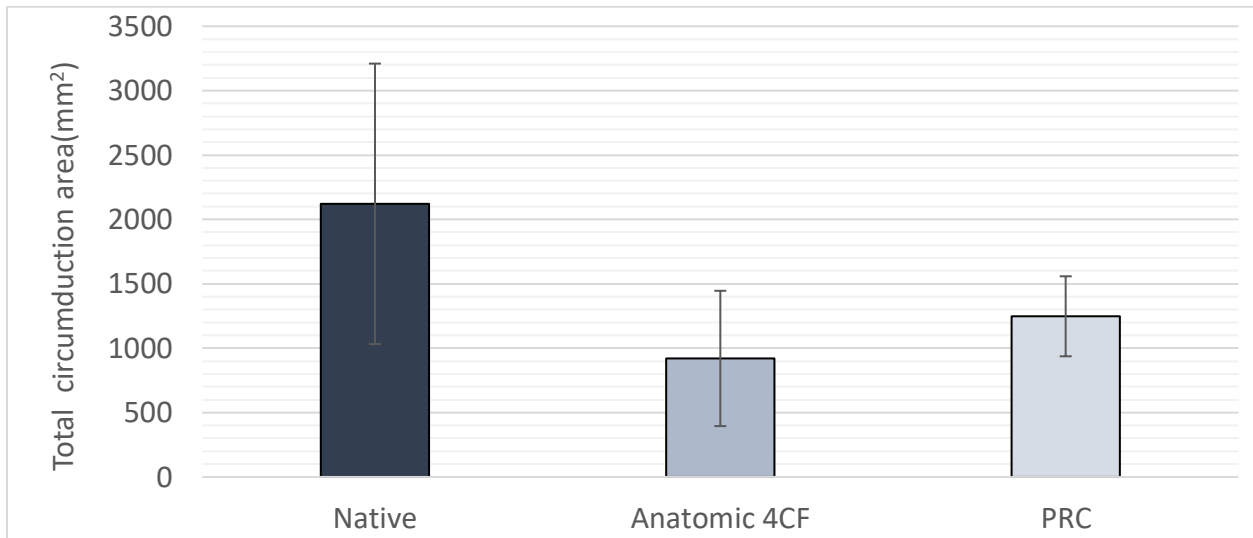


Figure 3.2 Total circumduction area (mm²) in native, anatomic 4CF and radial 4CF conditions.

Total circumduction area (mm²) was highest in native state (**Figure 3.2**) at 2121 mm², followed by PRC at 1248 mm², and finally 4CF at 920 mm². Total circumduction area was similar when comparing 4CF and PRC to native state ($p=0.11$ and $p=0.071$, respectively), and also between conditions ($p=0.56$).

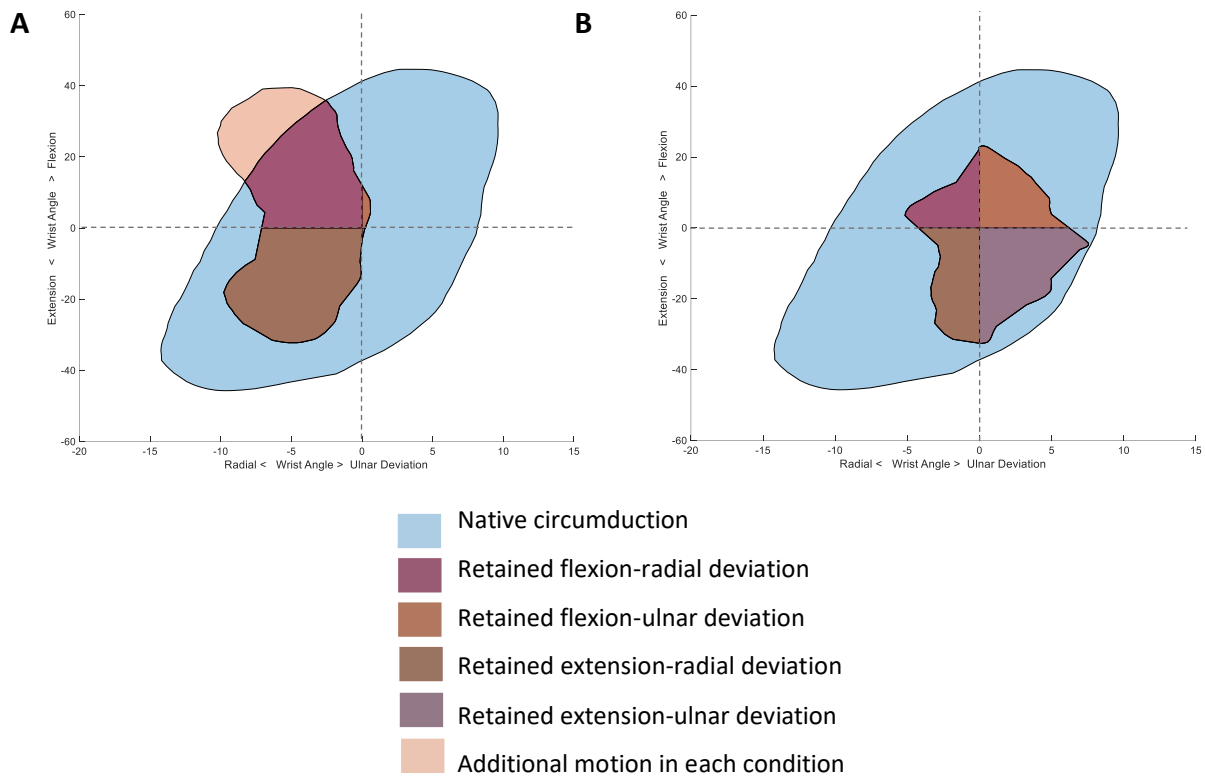


Figure 3.3. Circumduction pattern superimposed on native circumduction pattern. (A) 4CF (B) PRC.

Circumduction pathways were recorded for both groups and compared to the circumduction pattern generated by the native state (**Figure 3.3**). The percentages of overlap between both conditions and the native circumduction pattern were noted. PRC maintained a closer circumduction pattern to native, with 44% overlap, while 4CF maintained 41%, although no significant difference was detected ($p=0.86$). Additionally, the entire circumduction pattern for PRC lay within the native circumduction pathway, while a portion of 4CF extended beyond this.

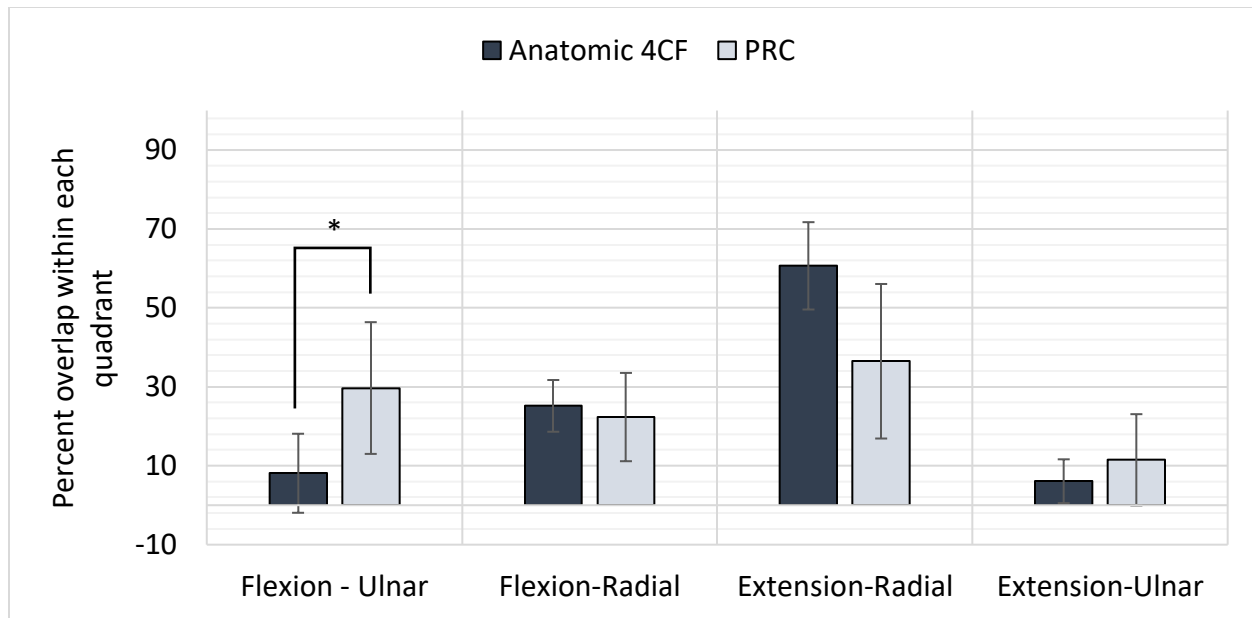


Figure 3.4. Percent of maintained motion within each quadrant compared to native state.

The area of overlap between both conditions and native circumduction was then further analyzed and split into 4 quadrants: flexion-ulnar deviation, flexion-radial deviation, extension-radial deviation and extension-ulnar deviation (**Figure 3.4**). A significantly greater area was maintained in the flexion-ulnar deviation quadrant in PRC compared to 4CF ($29 \pm 17\%$ and $8 \pm 10\%$, respectively, $p=0.02$). While both groups maintained the greatest area in the extension-radial deviation quadrant, the PRC group retained less motion than 4CF ($36 \pm 20\%$ and $60 \pm 11\%$, respectively, $p=0.076$). The degree of overlap in the flexion-radial deviation and extension-ulnar deviation quadrants was similar between groups.

3.4 DISCUSSION

As previously mentioned, there is currently no consensus on whether scaphoidectomy with 4CF or PRC has superior results. This biomechanical study sought to elucidate the changes in uniplanar and multiplanar wrist motion after scaphoidectomy and anatomic 4CF compared to PRC. The results of this work can be summarized into 2 key findings. Firstly, overall uniplanar and multiplanar ROM were reduced in 4CF and PRC conditions compared to the native state but did not reach statistical significance. This may be due to the small sample size and large variance among specimens. Four corner fusion resulted in a more significant reduction in wrist extension compared to PRC, while PRC resulted in a more significant reduction in radial deviation in comparison to 4CF. Additionally, total circumduction area was less compromised after PRC, with a higher percent retention of the native circumduction pattern (although this was not statistically significant).

Mean uniplanar flexion, extension, radial and ulnar deviation in 4CF and PRC compared to the native state was reduced, although only the reduction in radial deviation after PRC reached statistical significance. This reduction in motion may be explained by elimination of the midcarpal joint in the fusion condition leaving a single articulation. The loss of both the radiocarpal and midcarpal joints, and replacement with a single new articulation of the capitate on the radius likely explains the reduction in motion with PRC(2). The lack of statistical significance in our results may have been secondary to the large variance in our sample and the small number of specimens. When comparing the results of 4CF and PRC, the former demonstrated increased restriction in wrist extension, while the latter was more restricted in radial deviation. Restricted radial deviation in PRC is reported consistently in clinical studies(5, 6), and biomechanical studies have demonstrated that it may be secondary to impingement of the trapezium on the distal radius(7). Additionally, the ROM values we report are consistent with clinical studies after 4CF and PRC(8-11), all of which are reduced but lie within an acceptable range of functional motion. Of note, currently there is no consensus on functional ROM parameters. According to Ryu et al.(12), 40° flexion and extension, 10° radial deviation and 30° ulnar deviation are required, while Palmer et al.(13), who evaluated 52 tasks, identified that minimal functional ROM involves 5° flexion, 30° extension, 10° radial deviation, and 15° ulnar deviation.

A significant strength of this study relative to prior investigations was the evaluation of multiplanar motion. Circumduction has been shown to be a more clinically relevant outcome in the translation of *in vitro* results to *in vivo*(14). Our results suggest a 56.6% reduction in circumduction in 4CF compared to a 41.2% reduction in PRC relative to the native state. Additionally, we provide further insight that 44% and 41% of the native circumduction area is maintained with PRC and 4CF, respectively. Although we were unable to identify any biomechanical studies comparing circumduction after 4CF or PRC, a prospective cohort study by Singh et al. compared circumduction patterns in these groups(15). They found the mean circumduction area was similar after both procedures but was overall 30% reduced compared to the non-operative side. They also report that the centre of the PRC circumduction ellipse was closer to that of the non-operative wrist. The greater reduction in circumduction area noted in our study may be secondary to the intervention being performed on healthy specimens. Clinically, patients have months to years after surgery to compensate for the loss in midcarpal motion, when these outcomes are usually reported. Consistent with these results, we found that PRC exhibits a circumduction pattern more congruent with the native state in comparison to 4CF. Our results are further supported by a clinical study by Wolff et al. who report that PRC circumduction was closer than 4CF to normal conditions(16). Additionally, the circumduction exhibited by 4CF was more restricted and did not demonstrate the same elliptical pattern as non-operated wrists.

Clinical studies comparing function after 4CF and PRC have also been conducted. A study by Brinkhorst et al. compared the functional abilities in 48 patients who underwent 4CF or PRC at greater than 6 months post-operatively and found that patients who underwent PRC completed tasks more expeditiously than those who underwent 4CF(17). The only task that the 4CF group excelled at was improved spherical volar grip, corresponding to tasks such as unscrewing lids. Another functional study by Wolff et al. compared kinematics of dart throw and hammering in those who underwent PRC and 4CF(16). Similarly, this group found that patients performed better after PRC on kinematic and performance variables.

Two systematic reviews have been conducted to compare outcomes of both operations. Mulford et al. (6) reported a weighted average grip strength of 70% of contralateral (33kg) for PRC and 75% of contralateral (31kg) for scaphoidectomy and 4CF. The weighted average of post-operative

flexion, extension, radial and ulnar deviation were: 38°, 41°, 17°, 22° for PRC and 33°, 33°, 19° and 30° for 4CF, respectively. Meta-analysis was performed and both groups had similar rates of secondary fusion, while post-operative osteoarthritis was significantly higher in PRC (relative risk 4.35). They concluded that PRC may provide more motion and be associated with a lower, early risk complication profile (i.e. no risk of osseous or hardware complications), although patients are at risk for late development of osteoarthritis. In Saltzman et al.'s(5) systematic review, they found that the percentage change in flexion, extension, radial and ulnar deviation from pre- to post-op were: -14%, +1%, -20%, -4.8% for PRC and -13%, +1%, +55%, +1% for 4CF, respectively. Grip strength was relatively improved from pre-op, but decreased compared to the contralateral unaffected side (67±16% (PRC) and 74±13% (4CF) (p<0.05), respectively). The overall complication rate was 29% in 4CF compared to 14% in PRC (p=0.01). They concluded that absolute flexion and extension after PRC are greater, while radial deviation was higher in 4CF.

Limitations to this study include the use of healthy, non-arthritic cadaveric wrists rather than those with SLAC or SNAC pathology. This was due to the lack of availability of arthritic cadaveric wrists and a repeated measures experimental study design improves the statistical power by comparing procedures within specimens. This cadaveric model also lacked the potential for ligament adaptation during healing, which would occur in clinical scenarios. Additionally, despite the fact that simulation was performed in a single position, a high-fidelity active motion simulator was used, which more closely resembles a physiologic state by applying forces on flexor and extensor tendons to generate motion(18-20). Although K-wire fixation is less rigid compared to screw or plate fixation, we attempted to improve construct rigidity with multiple large caliber K-wires (five 0.062"). K-wires were used in our study to allow for a repeated-measures study design. As the capitate is shifted ulnarly relative to the lunate, the bony defect created from a headless compression screw in anatomic fusion gets shifted proportionally, leaving a very limited amount of bone stock radially for radial-aligned fusion. As such, fixation may not have been maintained in the second (radial-aligned) procedure had we used screw fixation. Further, as there was a lack of access to fluoroscopy in the laboratory, we were unable to confirm correction of any DISI deformity radiographically, but this was confirmed visually. Finally, although the study was sufficiently powered, there was high variance in the results (standard deviation) which is expected due to the variable size and shape of normal wrists.

This study demonstrates that scaphoidectomy with 4CF as well as PRC both result in reduced uniplanar and multiplanar motion compared to native state although not to a statistically significant. Four corner fusion resulted in decreased wrist extension compared to PRC, while PRC resulted in reduced radial deviation compared to 4CF. Although the total circumduction area was similar between groups, the circumduction pattern after PRC was more congruent with native state compared to anatomic 4CF, with a higher percentage of motion retained (44%) than 4CF (41%), though this was not significant. Taken together, these results suggest that both procedures have comparable outcomes of wrist circumduction, with limitations in specific uniplanar motions in both: 4CF is more restricted in wrist extension and PRC more restricted in radial deviation.

With the results of this study in mind, the recommendation for individuals who are candidates for PRC or 4CF remains unclear. Proximal row carpectomy results in greater circumduction retention, although radial deviation is more restricted in comparison to 4CF. This procedure is less technically demanding and lacks the hardware and potential bony complications, such as non-union and delayed union, that are associated with 4CF(5, 6). However, the formation of a non-anatomical joint between the capitate and radius in PRC, has been shown to increase contact pressure(21) predisposing individuals to delayed arthritis. As a result, PRC may be more suitable in older patients(22). Furthermore, excision of the entire proximal carpal row results in reduced carpal height and tension on tendons, explaining the reduced grip strength in PRC (5, 6, 23). This procedure is contraindicated in those with arthritis involving the capitate head or lunate fossa of the distal radius, and in those cases, an alternative salvage procedure like 4CF may be indicated(1).

Scaphoidectomy and 4CF also results in a reasonable circumduction pattern with a comparable degree of motion retention compared to PRC. Notably, however, wrist extension is more compromised in 4CF than in PRC. Advantages to 4CF include the preservation of the anatomic radiolunate joint and maintenance of carpal height(2). By maintaining carpal height, tendons maintain proper length and tension, reducing the risk of weakness and accounting for increased grip strength compared to PRC. Disadvantages to 4CF include the fact that is a more technically challenging procedure and has associated hardware and osseous complications(5, 6, 23). Consequently, the decision to pursue PRC or scaphoidectomy and 4CF in patients who are

candidates for both should be made in conjunction with the patients after reviewing the risks and benefits of both procedures.

3.5 CONCLUSIONS

This *in-vitro* biomechanical model comparing anatomic 4CF with scaphoidectomy, and PRC resulted in reduced overall uniplanar motion compared to native state, although only the reduction in radial deviation after PRC reached statistical significance. Uniplanar wrist motion was similar between the two procedures, with the exception of wrist extension and radial deviation. Total circumduction area was similar between 4CF, PRC and native state. Additionally, the percentage overlap between circumduction patterns for 4CF and PRC retained 41% and 44%, respectively of the native circumduction pattern. Both scaphoidectomy with 4CF, and PRC appear to result in comparable motion profiles. To validate these results, clinical studies comparing functional and patient-reported outcomes in anatomic 4CF and PRC are required. Additional considerations that were not possible to assess in this study include complications rates, pain relief, functional ability, and grip strength.

References

1. Shah CM, Stern PJ. Scapholunate advanced collapse (SLAC) and scaphoid nonunion advanced collapse (SNAC) wrist arthritis. *Curr Rev Musculoskelet Med.* 2013;6(1):9-17.
2. Debottis DP, Werner FW, Sutton LG, Harley BJ. 4-corner arthrodesis and proximal row carpectomy: a biomechanical comparison of wrist motion and tendon forces. *J Hand Surg Am.* 2013;38(5):893-8.
3. Rust PA, Manojlovich LM, Wallace R. A comparison of dart thrower's range of motion following radioscapholunate fusion, four-corner fusion and proximal row carpectomy. *J Hand Surg Eur Vol.* 2018;43(7):718-22.
4. Berger RA, Bishop AT, Bettinger PC. New dorsal capsulotomy for the surgical exposure of the wrist. *Ann Plast Surg.* 1995;35(1):54-9.
5. Saltzman BM, Frank JM, Slikker W, Fernandez JJ, Cohen MS, Wysocki RW. Clinical outcomes of proximal row carpectomy versus four-corner arthrodesis for post-traumatic wrist arthropathy: a systematic review. *J Hand Surg Eur Vol.* 2015;40(5):450-7.
6. Mulford JS, Ceulemans LJ, Nam D, Axelrod TS. Proximal row carpectomy vs four corner fusion for scapholunate (Slac) or scaphoid nonunion advanced collapse (Snac) wrists: a systematic review of outcomes. *J Hand Surg Eur Vol.* 2009;34(2):256-63.
7. Blankenhorn BD, Pfaeffle HJ, Tang P, Robertson D, Imbriglia J, Goitz RJ. Carpal kinematics after proximal row carpectomy. *J Hand Surg Am.* 2007;32(1):37-46.
8. Sobczak S, Rotsaert P, Vancabeke M, Van Sint Jan S, Salvia P, Feipel V. Effects of proximal row carpectomy on wrist biomechanics: a cadaveric study. *Clin Biomech (Bristol, Avon).* 2011;26(7):718-24.
9. Hernandez-Soria A, Das De S, Model Z, Lee SK, Wolfe SW. The Effect of Capitate Position on Coronal Plane Wrist Motion After Simulated 4-Corner Arthrodesis. *J Hand Surg Am.* 2016;41(11):1049-55.
10. De Carli P, Donndorff AG, Alfie VA, Boretto JG, López Ovenza JM, Gallucci GL. Four-corner arthrodesis: influence of the position of the lunate on postoperative wrist motion: a cadaveric study. *J Hand Surg Am.* 2007;32(9):1356-62.
11. Dvinskikh NA, Blankevoort L, Strackee SD, Grimbergen CA, Streekstra GJ. The effect of lunate position on range of motion after a four-corner arthrodesis: a biomechanical simulation study. *J Biomech.* 2011;44(7):1387-92.

12. Ryu JY, Cooney WP, Askew LJ, An KN, Chao EY. Functional ranges of motion of the wrist joint. *J Hand Surg Am.* 1991;16(3):409-19.
13. Palmer AK, Werner FW, Murphy D, Glisson R. Functional wrist motion: a biomechanical study. *J Hand Surg Am.* 1985;10(1):39-46.
14. Li ZM, Kuxhaus L, Fisk JA, Christophel TH. Coupling between wrist flexion-extension and radial-ulnar deviation. *Clin Biomech (Bristol, Avon).* 2005;20(2):177-83.
15. Singh HP, Brinkhorst ME, Dias JJ, Moojen T, Hovius S, Bhowal B. Dynamic assessment of wrist after proximal row carpectomy and 4-corner fusion. *J Hand Surg Am.* 2014;39(12):2424-33.
16. Wolff AL, Garg R, Kraszewski AP, Hillstrom HJ, Hafer JF, Backus SI, et al. Surgical Treatments for Scapholunate Advanced Collapse Wrist: Kinematics and Functional Performance. *J Hand Surg Am.* 2015;40(8):1547-53.
17. Brinkhorst ME, Singh HP, Dias JJ, Feitz R, Hovius SER. Comparison of activities of daily living after proximal row carpectomy or wrist four-corner fusion. *J Hand Surg Eur Vol.* 2017;42(1):57-62.
18. Werner FW, Palmer AK, Somerset JH, Tong JJ, Gillison DB, Fortino MD, et al. Wrist joint motion simulator. *J Orthop Res.* 1996;14(4):639-46.
19. Dunning CE, Lindsay CS, Bicknell RT, Patterson SD, Johnson JA, King GJ. Supplemental pinning improves the stability of external fixation in distal radius fractures during simulated finger and forearm motion. *J Hand Surg Am.* 1999;24(5):992-1000.
20. Iglesias D. Development of an in-vitro passive and active motion simulator for the investigation of wrist function and kinematics. London, Ontario: University of Western Ontario; 2016.
21. Tang P, Gauvin J, Muriuki M, Pfaeffle JH, Imbriglia JE, Goitz RJ. Comparison of the "contact biomechanics" of the intact and proximal row carpectomy wrist. *J Hand Surg Am.* 2009;34(4):660-70.
22. Wall LB, Didonna ML, Kiefhaber TR, Stern PJ. Proximal row carpectomy: minimum 20-year follow-up. *J Hand Surg Am.* 2013;38(8):1498-504.
23. Ashmead D, Watson HK, Damon C, Herber S, Paly W. Scapholunate advanced collapse wrist salvage. *J Hand Surg Am.* 1994;19(5):741-50.

CHAPTER 4

4 GENERAL DISCUSSION AND CONCLUSIONS

4.1 SUMMARY

This work was conducted to expand the current knowledge on the biomechanics of treatment options for scapholunate advanced collapse (SLAC) and scaphoid nonunion advanced collapse (SNAC) patterns of wrist arthritis. This thesis includes two *in-vitro* biomechanical studies to compare the motion patterns of the normal wrist to those observed after proximal row carpectomy (PRC) and two techniques of four corner partial wrist fusions (4CF). The specific objectives outlined previously in this work have been achieved.

The objectives of this thesis were:

1. To understand and characterize how anatomic 4CF and radial 4CF influence uniplanar wrist motion (flexion-extension, radial-ulnar deviation) and multiplanar motion (circumduction).
2. To understand and characterize how anatomic 4CF and PRC compare in uniplanar wrist motion (flexion-extension, radial-ulnar deviation) and multiplanar motion (circumduction).

The outcomes, strengths and limitations of these studies detailed in **Chapter 2** and **Chapter 3** are summarized.

4.2 CHAPTER 2: A BIOMECHANICAL STUDY COMPARING UNIPLANAR AND MULTIPLANAR WRIST MOTION IN TWO POSITIONS OF FOUR CORNER FUSION

4.2.1 Overview

The impact of altering the relationship between the capitate and lunate in the coronal plane during scaphoidectomy and four corner fusion on wrist motion is poorly understood. There is controversy regarding the optimal fusion position. Some surgeons routinely align the radial border of the capitate and lunate to increase the contact area for fusion (1-9), while others tend to fuse the carpal bones with them aligned in an anatomic position(10-13). With the use of a high-fidelity active motion simulator(14), this *in-vitro* biomechanical study sought to elucidate the changes in wrist kinetics after anatomic 4CF and radial-aligned 4CF.

The hypotheses for this chapter were:

1. Anatomic and radial-aligned positions of 4CF will result in similar reductions in wrist flexion and extension,
2. The radial-aligned fusion position will result in increased ulnar deviation compared to anatomic fusion,
3. Anatomic and radial-aligned positions of 4CF will result in reduced circumduction motion compared to native state.

This study confirmed our hypothesis that anatomic and radial-aligned fusion positions in scaphoidectomy and 4CF would result in similar reductions in wrist flexion and extension, although wrist extension in radial 4CF was significantly reduced when compared to the native state. Our second hypothesis was rejected. No statistically significant differences were detected in the absolute reduction in radial and ulnar deviation between fusion groups. Despite this, when compared with the native state, the reduction in ulnar deviation in radial 4CF approached statistical significance and may be a result of radioscapocapitate ligament tensioning. Lastly, both fusion

positions resulted in reduced circumduction area compared to native state, though only radial 4CF reached statistical significance. Anatomic 4CF maintained a closer circumduction pattern to native, with 41% overlap, while radial 4CF maintained 32%.

With these biomechanical findings in mind, anatomic 4CF appears to better replicate the motion patterns of the normal wrist and may be suitable if there is sufficient osseous contact between the capitate and lunate. Anatomic 4CF may maximize circumduction area and minimize restriction in wrist extension. Whether these small differences in circumduction motion pathways are clinically important requires further study. Clinical studies comparing pain relief, motion outcomes, grip strength, patient-reported outcomes, complication rates and union rates are required to validate these findings.

4.3 CHAPTER 3: A BIOMECHANICAL STUDY COMPARING UNIPLANAR AND MULTIPLANAR WRIST MOTION AFTER FOUR CORNER FUSION AND PROXIMAL ROW CARPECTOMY

4.3.1 Overview

Salvage procedures for treatment of SLAC and SNAC patterns of wrist arthritis include scaphoidectomy and 4CF, and PRC. To date, there is controversy regarding which procedure provides better outcomes including wrist motion. Biomechanical studies suggest that uniplanar motion is greater after PRC; however, these studies utilize a passive motion simulator and report either uniplanar or multiplanar motion in isolation(15, 16). Using a high-fidelity active motion simulator(14), this *in-vitro* biomechanical study sought to elucidate the changes in wrist kinematics after anatomic 4CF and PRC.

In this study, overall uniplanar motion was reduced compared to native state, although only the reduction in radial deviation after PRC reached statistical significance. Wrist extension was significantly more limited in anatomic 4CF compared to PRC while the opposite was true for radial deviation. Total circumduction area was reduced in both conditions compared to native, although not statistically significant. The circumduction pattern after PRC was more congruent with native state compared to anatomic 4CF. The percentage overlap with the native circumduction pattern were 44% and 41%, respectively.

The hypotheses of this chapter were:

1. PRC and 4CF will result in similar reductions in wrist flexion and extension,
2. PRC will result in reduced radial deviation compared to 4CF,
3. PRC will result in a greater circumduction area than 4CF.

This study suggests that our first hypothesis was only partially correct. Although no statistically significant differences in wrist flexion was found between groups, wrist extension was more

restricted in 4CF. The second hypothesis was correct, as radial deviation was more restricted in PRC compared to 4CF. Ulnar deviation was similar between groups. Finally, our hypothesis that PRC would result in a greater circumduction area than 4CF was incorrect, as no statistically significant differences were noted upon analysis.

Both scaphoidectomy with 4CF and PRC appear to be reasonable options in the appropriate situations. Consequently, the decision to pursue PRC or scaphoidectomy and 4CF in patients who are candidates for both should be made in conjunction with the patients after reviewing the risks and benefits of both procedures.

4.4 STRENGTHS AND LIMITATIONS

These two studies utilized a high-fidelity active motion simulator(14) to mimic physiologic wrist motion as closely as possible. This allowed for investigation of overall multiplanar motion (circumduction) in conjunction to uniplanar motion. Circumduction has been shown to be a more clinically relevant compared to uniplanar motion (17). A repeated measures experimental study design also improved the statistical power by comparing procedures within specimens.

Limitations to these *in-vitro* biomechanical studies include the use of healthy, non-arthritis cadaveric wrists rather than those with SLAC or SNAC pathology. This was due to the lack of availability of arthritic cadaveric wrists and a repeated measures experimental study design improves the statistical power by comparing procedures within specimens. This cadaveric model also lacked the potential for ligament adaptation during healing, which would occur in clinical scenarios. Additionally, despite the fact that simulation was performed in a single position, a high-fidelity active motion simulator was used, which more closely resembles a physiologic state by applying forces on flexor and extensor tendons to generate motion(18-20). Although K-wire fixation is less rigid compared to screw or plate fixation, we attempted to improve construct rigidity with multiple large caliber K-wires (five 0.062”). K-wires were used in our study to allow for a repeated-measures study design. As the capitate is shifted ulnarly relative to the lunate, the bony defect created from a headless compression screw in anatomic fusion gets shifted proportionally, leaving a very limited amount of bone stock radially for radial-aligned fusion. As such, fixation may not have been maintained in the second (radial-aligned) procedure had we used screw fixation. Further, as there was a lack of access to fluoroscopy in the laboratory, we were unable to confirm correction of any DISI deformity radiographically, but this was confirmed visually. Finally, although the study was sufficiently powered, there was high variance in the results (standard deviation) which is expected due to the variable size and shape of normal wrists.

Some of our results may have achieved statistical significance if the sample size was increased, although the clinical significance of such results is questionable. For example, wrist flexion was reduced by $6.3 \pm 7.0^\circ$ in radial 4CF compared to the native state and approached statistical

significance at $p=0.07$. Whether or not a reduction of this magnitude is clinically relevant is debatable.

4.5 OVERALL CONCLUSION

The overarching goal of these studies was to identify which procedure (between two positions of scaphoidectomy and 4CF, and PRC) would result in better motion outcomes to assist clinicians with decision-making.

In the first study comparing anatomic 4CF and radial 4CF, we report that radial 4CF was associated with a significant reduction in wrist extension compared to the native state, while the reduction in wrist flexion and ulnar deviation approached significance. Overall, uniplanar motion was similar between anatomic and radial 4CF groups. Total circumduction area was significantly reduced in radial 4CF compared to the native state, but again was similar to anatomic 4CF. A greater percentage of the native circumduction pattern (41% vs. 32%) was retained in anatomic 4CF.

In the second study comparing anatomic 4CF and PRC, only the reduction in radial deviation after PRC reached statistical significance compared to native state. Four corner fusion resulted in decreased wrist extension compared to PRC, while PRC resulted in reduced radial deviation compared to 4CF. Although the total circumduction area was similar between all groups, the circumduction pattern after PRC was more similar to native state in comparison to anatomic 4CF.

Upon consideration of these results, the recommended procedure for individuals who are candidates for both still remains unclear. Proximal row carpectomy results in greater circumduction retention, although radial deviation is more restricted in comparison to 4CF. Advantages and disadvantages of each procedure must be considered and discussed with patients. In general, PRC is technically simpler and lacks hardware and bony complications, although a nonanatomic articulation is created between the capitate and radius predisposing patients to late arthritis and the loss of midcarpal height is associated with reduced grip strength (20-24). On the other hand, 4CF maintains carpal height and can be performed in patients with capitulate arthrosis, though possesses risk for bony (delayed union and non-union) and hardware complications(20, 21).

When the decision to perform 4CF has been made, the surgeon must decide between anatomic 4CF and radial 4CF positions. Our study suggests that anatomic 4CF may produce more favourable motion outcomes (by maximizing circumduction area and minimizing the reduction in wrist extension). Additional considerations include the degree of osseous contact between the capitate and lunate. Specifically, anatomic 4CF may be suitable if there is adequate bony apposition between the proximal capitate and distal lunate. In other circumstances, such as in cases of SLAC with significant capitate proximal migration or minimal bone stock between the capitate and lunate, radial 4CF may be required to obtain adequate fixation and bony contact. Increasing contact between the capitate and lunate to maximize bone purchase may reduce rates of non-union(11).

4.6 FUTURE DIRECTIONS

Additional biomechanical studies with a larger sample size could be performed to confirm these results and compensate for the high variance noted across specimens. Further, clinical studies comparing anatomic 4CF, radial-aligned 4CF, and PRC are required to validate these results in the clinical context. This may include retrospective or prospective cohort studies comparing wrist ROM outcomes (including uniplanar wrist motion and multiplanar motion like circumduction), grip strength, patient-reported outcome measures, pain relief, and complication rates. Specifically, additional considerations that were not possible to assess in this study include complication rates, pain relief, functional ability and grip strength. In an ideal situation, a randomized control trial could be conducted to compare these two fusion positions and PRC.

References

1. Bain GI, Watts AC. The outcome of scaphoid excision and four-corner arthrodesis for advanced carpal collapse at a minimum of ten years. *J Hand Surg Am.* 2010;35(5):719-25.
2. Ball B, Bergman JW. Scaphoid excision and 4-corner fusion using retrograde headless compression screws. *Tech Hand Up Extrem Surg.* 2012;16(4):204-9.
3. Erne HC, Broer PN, Weiss F, Loew S, Cerny MK, Schmauss D, et al. Four-corner fusion: Comparing outcomes of conventional K-wire-, locking plate-, and retrograde headless compression screw fixations. *J Plast Reconstr Aesthet Surg.* 2019;72(6):909-17.
4. Cha SM, Shin HD, Kim KC. Clinical and radiological outcomes of scaphoidectomy and 4-corner fusion in scapholunate advanced collapse at 5 and 10 years. *Ann Plast Surg.* 2013;71(2):166-9.
5. Stanley J. Arthroplasty and arthrodesis of the wrist. *Green's Operative Hand Surgery.* 6 ed. Philadelphia: Elsevier; 2010. p. 429-63.
6. Dacho AK, Baumeister S, Germann G, Sauerbier M. Comparison of proximal row carpectomy and midcarpal arthrodesis for the treatment of scaphoid nonunion advanced collapse (SNAC-wrist) and scapholunate advanced collapse (SLAC-wrist) in stage II. *J Plast Reconstr Aesthet Surg.* 2008;61(10):1210-8.
7. Traverso P, Wong A, Wollstein R, Carlson L, Ashmead D, Watson HK. Ten-Year Minimum Follow-Up of 4-Corner Fusion for SLAC and SNAC Wrist. *Hand (N Y).* 2017;12(6):568-72.
8. Cohen MS, Kozin SH. Degenerative arthritis of the wrist: proximal row carpectomy versus scaphoid excision and four-corner arthrodesis. *J Hand Surg Am.* 2001;26(1):94-104.
9. Chaudhry T, Spiteri M, Power D, Brewster M. Four corner fusion using a multidirectional angular stable locking plate. *World J Orthop.* 2016;7(8):501-6.
10. Mamede J, Castro Adeodato S, Aquino Leal R. Four-Corner Arthrodesis: Description of Surgical Technique Using Headless Retrograde Crossed Screws. *Hand (N Y).* 2018;13(2):156-63.
11. Ozyurekoglu T, Turker T. Results of a method of 4-corner arthrodesis using headless compression screws. *J Hand Surg Am.* 2012;37(3):486-92.
12. Trail IA, Murali R, Stanley JK, Hayton MJ, Talwalkar S, Sreekumar R, et al. The long-term outcome of four-corner fusion. *J Wrist Surg.* 2015;4(2):128-33.

13. Richards AA, Afifi AM, Moneim MS. Four-corner fusion and scaphoid excision using headless compression screws for SLAC and SNAC wrist deformities. *Tech Hand Up Extrem Surg.* 2011;15(2):99-103.
14. Iglesias D. Development of an in-vitro passive and active motion simulator for the investigation of wrist function and kinematics. London, Ontario: University of Western Ontario; 2016.
15. Rust PA, Manojlovich LM, Wallace R. A comparison of dart thrower's range of motion following radioscapolunate fusion, four-corner fusion and proximal row carpectomy. *J Hand Surg Eur Vol.* 2018;43(7):718-22.
16. Debottis DP, Werner FW, Sutton LG, Harley BJ. 4-corner arthrodesis and proximal row carpectomy: a biomechanical comparison of wrist motion and tendon forces. *J Hand Surg Am.* 2013;38(5):893-8.
17. Li ZM, Kuxhaus L, Fisk JA, Christophel TH. Coupling between wrist flexion-extension and radial-ulnar deviation. *Clin Biomech (Bristol, Avon).* 2005;20(2):177-83.
18. Werner FW, Palmer AK, Somerset JH, Tong JJ, Gillison DB, Fortino MD, et al. Wrist joint motion simulator. *J Orthop Res.* 1996;14(4):639-46.
19. Dunning CE, Lindsay CS, Bicknell RT, Patterson SD, Johnson JA, King GJ. Supplemental pinning improves the stability of external fixation in distal radius fractures during simulated finger and forearm motion. *J Hand Surg Am.* 1999;24(5):992-1000.
20. Mulford JS, Ceulemans LJ, Nam D, Axelrod TS. Proximal row carpectomy vs four corner fusion for scapholunate (Slac) or scaphoid nonunion advanced collapse (Snac) wrists: a systematic review of outcomes. *J Hand Surg Eur Vol.* 2009;34(2):256-63.
21. Saltzman BM, Frank JM, Slikker W, Fernandez JJ, Cohen MS, Wysocki RW. Clinical outcomes of proximal row carpectomy versus four-corner arthrodesis for post-traumatic wrist arthropathy: a systematic review. *J Hand Surg Eur Vol.* 2015;40(5):450-7.
22. Tang P, Gauvin J, Muriuki M, Pfaeffle JH, Imbriglia JE, Goitz RJ. Comparison of the "contact biomechanics" of the intact and proximal row carpectomy wrist. *J Hand Surg Am.* 2009;34(4):660-70.
23. Wall LB, Didonna ML, Kiefhaber TR, Stern PJ. Proximal row carpectomy: minimum 20-year follow-up. *J Hand Surg Am.* 2013;38(8):1498-504.

24. Ashmead D, Watson HK, Damon C, Herber S, Paly W. Scapholunate advanced collapse wrist salvage. J Hand Surg Am. 1994;19(5):741-50.

STACY FAN

BMSc (Honors), MD, MSc Candidate

EDUCATION

| | |
|--|--------------|
| Plastic and Reconstructive Surgery Residency (Projected graduation 2023) Schulich School of Medicine & Dentistry, Western University, London, ON | 2018-Present |
| Master of Science in Surgery (Projected graduation 2020) Schulich School of Medicine & Dentistry, Western University, London, ON | 2019-Present |
| Doctor of Medicine (MD) Schulich School of Medicine & Dentistry, Western University, London, ON | 2014-2018 |
| Bachelor of Medical Sciences (BMSc), Honors Schulich School of Medicine & Dentistry, Western University, London, ON | 2010-2014 |

PUBLICATIONS

Haddara M, **Fan S**, Matache B, Chinchalkar S, Ferreira, Suh N. Development of an in-vitro swan neck deformity biomechanical model. Accepted 2020 Jul 20 to *HAND*.

Fan S, Chen H, Grant A, DeLyzer T. Outcomes of immediate alloplastic breast reconstruction in patients receiving post-mastectomy radiotherapy. Accepted 2020 Jun 14 to *Plastic Surgery*.

Fan S, Suh N, Grewal R. Observation of bony resorption during scaphoid fracture healing: a case series. Accepted 2020 Apr 13 to *Journal of Hand Surgery European Volume*.

Clark R, **Fan S**, Navaratnam R, Punjani N, Power N. To clamp or not to clamp? Early venous and arterial vascular control improves blood loss in open radical prostatectomy. *University of Western Ontario Medical Journal*. 2020 Mar 26;88(2).

Fan S, Hackett J, Lutz K, Heaton G, Symonette C, Grant A. Regional wait times for patients with non-melanoma skin cancer in Southwestern Ontario. *Plastic Surgery* 2019 Oct 23;28(1):5-11.

Fan S, Cepek J, Symonette C, Ross D, Chinchalkar S, Grant A. Variation of Grip Strength and Wrist Range of Motion with Forearm Rotation in Healthy Young Volunteers Aged 23 to 30. *Journal of Hand and Microsurgery*. 2019 Aug;11(02):088-93.

Abbass M, **Fan S**, Barker K, Fenster A, Cepek J. Real-Time Mechanical-Encoding of Needle Shape for Image-Guided Medical and Surgical Interventions. *Journal of Medical Devices*. 2019 Mar 1;13(1):015001.

Fan S, Li B, Chen Q, Midia M. Impact of interventional oncology therapies on tumor microenvironment and strategies to enhance their efficacy. *American Journal of Roentgenology*. 2018 Mar;210(3):648-56.

Fan S. Two cases of plasmacytoid variant of bladder cancer. *University of Western Ontario Medical Journal*. 2018 Jan 20;86(S1):9-11.

Milosevic MF, Townsley CA, Chaudary N, Clarke B, Pintilie M, **Fan S**, et al. Sorafenib increases tumor hypoxia in cervical cancer patients treated with radiation therapy: results of a phase 1 clinical study. *International Journal of Radiation Oncology* Biology* Physics*. 2016 Jan 1;94(1):111-7.

PENDING SUBMISSIONS

Fan S, Suh N, MacDermid J, Ross D, Grewal R. Use of vascularized and non-vascularized bone grafting in scaphoid non-union: A prospective randomized control trial. Submitted to *Journal of Hand Surgery*. 2020

Kadar A, Padmore C, **Fan S**, Grewal R, Suh N. How much scaphoid can be safely resected?: A biomechanical analysis of distal scaphoid resection arthroplasty. Submitted to *Journal of Hand Surgery*. 2020

Chambers S, Padmore C, **Fan S**, Grewal R, Johnson J, Suh N. The impact of scaphoid malunion on carpal motion: A biomechanical analysis. Submitted to *Journal of Hand Surgery (European Volume)*. 2020

Kadar A, Haddara M, **Fan S**, Chinchalkar S, Ferreira L, Suh N. External thermoplastic rings restore near-normal flexor biomechanics following venting of the pulleys. Submitted to *Journal of Hand Surgery*. 2020

PRESENTATIONS

| | |
|---|------------------------------------|
| Fan S , Suh N, MacDermid J, Ross D, Grewal R. Use of vascularized and non-vascularized bone grafting in scaphoid non-union: A prospective randomized control trial. | AAHS 2020 COA 2020 CSSH 2020 |
| Awarded the Joint Outstanding Paper Award AAHS/ASPN/ASRM 2020 | ASSH 2020 |
| Fan S , Chen H, Grant A, DeLyzer T. Outcomes of immediate alloplastic breast reconstruction in patients receiving post-mastectomy radiotherapy. | CSPS 2020 |
| Chambers S, Padmore C, Fan S , Grewal R, Johnson J, Suh N. The impact of scaphoid malunion on carpal motion: A biomechanical analysis. | COA 2020 |
| Kadar A, Haddara M, Fan S , Chinchalkar S, Ferreira L, Suh N. External thermoplastic rings restore near-normal flexor biomechanics following venting of the pulleys. | COA 2020 ISL&T 2020 |
| Haddara M, Fan S , Matache B, Chinchalkar S, Ferreira, Suh N. Development of an in-vitro swan neck deformity biomechanical model | COA 2020 |
| Fan S , Hackett J, Lutz K, Heaton G, Symonette C, Grant A. Regional wait times for patients with non-melanoma skin cancer in Southwestern Ontario. | CSPS 2019 LHRD 2019 |
| Clark R, Fan S , Wong K, Punjani N, Power N, Chin J, Izawa, J. Does symptomatic recurrence predict survival post cystectomy? Results from a large Canadian cohort. | CUA 2017 |
| Fan S , Malvankar M, Stojanovic D, Hutnik C. Antiviral treatment of active herpes zoster ophthalmicus in immunocompetent adults: A systematic review and Canadian cost comparison. | COS 2016 LHRD 2016 |

EDUCATIONAL PROJECTS

| | |
|--|------|
| Scrotal Masses module (https://medskl.com/Module/Index/scrotal-masses) Supervisor: Dr. Nicholas Power | 2016 |
| Hyponatremia module (https://medskl.com/Module/Index/hyponatremia) Supervisor: Dr. Andrew House | 2016 |

PROFESSIONAL MEMBERSHIPS

| | |
|---|--------------|
| American Society of Plastic Surgeons (ASPS), <i>Resident Member</i> | 2020-Present |
| Canadian Society of Plastic Surgeons (CSPS), <i>Resident Member</i> | 2019-Present |
| Professional Association of Residents in Ontario (PARO) | 2018-Present |
| Canadian Medical Association (CMA) | 2014-Present |
| Ontario Medical Association (OMA) | 2014-Present |

ACHIEVEMENTS

| | |
|--|------------|
| Joint outstanding paper session at AAHS/ASPN/ASRM 2020 | AAHS 2020 |
| Canada Graduate Scholarship 2019/2020 <i>accepted</i> | 2019 |
| Ontario Graduate Scholarship 2019/2020 <i>declined</i> | 2019 |
| Elena B. Wolf Memorial Award | 2017 |
| Nomination for Award for OB/GYN Rotation | 2017 |
| Meds Class of '62 Bursary | 2016-2017 |
| John and Emily Kidd Continuing Scholarship (Based on academic achievement) | 2014-2017 |
| Undergraduate Student Supported OSOTF II Bursaries | 2016 |
| Radiation Medicine Program Summer Student (Summer research funding at Princess Margaret Hospital) | 2014, 2015 |
| Medical School Admission Bursary | 2014 |
| Deans Honor List (Average 80%+) | 2011-2014 |